STUDIES TOWARDS IMPROVED FOCUSING METHODS OF PHOTOELECTRON AUTORADIOGRAPHY

A

THESIS

submitted by

DAVID J. SHAPLAND

B.Sc., (St. Andrews)

for the degree of

DOCTOR OF PHILOSOPHY

University of Edinburgh

August, 1955.

TABLE OF CONTENTS.

Table of Contents (Contd).

Table of Contents (Contd)

Table of Contents (Contd)

PREFACE.

The work described in this thesis was carried out in the Department of Natural Philosophy of the University of Edinburgh under the supervision of Professor N. Feather, F.R.S. The focusing method was initiated by Professor Feather and the electron-optical lens system was designed by Professor H.O.W. Richardson. The construction of the instrument and preliminary investigations were carried out by Dr. A.N. Barker.

The problem was to make a thorough study of the properties of the lens system and to investigate the possibilities of improving the focusing method; also to study possible applications of the instrument and to investigate the factors affecting the usefulness of the method in the field of autoradiography.

INTRODUCTION.

Since the discovery of radioactivity, due to the photographic action of the emitted radiations, by Becquerel in 1896, the photographic plate has been an important tool in the detection of electrons. Although overshadowed by electronic counting devices, it still plays an important role, since the developed image gives a more detailed distribution of the radioisotope in the specimen under observation. The technique of autoradiography utilises the photographic action of all the emitted ionizing radiations for locating the radioactive material in a sample, and was first used by Lacassagne and Lattes [1] in 1925.

The general procedure is to introduce the active isotope into the system and to select the specimen to be studied, which is then placed in contact with a suitable photographic material and left for exposure. After processing, the location of the radioactive material can be deduced by studying the image, but the latter is not sharp since it is difficult to achieve intimate contact between the specimen and recording film. This method gives autoradiographs with a resolution of 50 to 100 microns [2]. An improved method was achieved by Evans [3], who floated

sections of his material on to a photographic plate which was then dried out and left for exposure. The resolving power of this method was estimated to be 5 to 6 microns. Belanger and Leblond[4] obtained similar resolution by coating sections with liquefied emulsion at 37° C.

These methods suffer from many disadvantages. The activity has to be firmly fixed in the emulsion so that subsequent treatment will not leach it out; also there is a danger of artifacts caused by diffusion and pressure, and the inactive substances in the specimen often render the emulsion grains developable. In the stripping plate technique described by Pelc[5] and others, the emulsion is mounted on a thin support (cellulose esters have been used) and the latter shields the emulsion from abrasion and chemical action, but this advantage is gained at the expense of resolution.

There have been many refinements of the method. Berriman, Herz, and Stevens[6] using a new, fine grain emulsion 4 microns thick on top of ordinary emulsion have obtained a resolution of 200 lines per mm. Gomberg[7] has developed a method called wet process autoradiography and claims a resolution down to 1 micron, but there is a corresponding loss in resolution when a protective coating is used to shield the one

micron thick sensitized layer, formed on the surface of the specimen, from direct interaction with the chemicals used in forming the film.

None of these methods employs direct magnification, although Fink[8] mechanically enlarged the specimen between lead sheets in a rolling mill, before the autoradiograph was taken. Optical magnification of the image is employed, but when this is greater than 10x, the silver grains appear as groups of hazy smudges, irregularly distributed, and no longer give a true picture. The only way to get direct magnification is to use a focusing method, in which the electrons emitted from the specimen pass through a suitable magnetic field and form an image on the photographic plate some distance from the specimen. In this method the whole system is in vacuo. Emission microscopes, in which the object constitutes the source of electrons, have been used for a long time, but these did not employ a radioisotope as a source of electrons. According to Lawrence[9], sections have been placed in magnetic fields in an attempt "to pull the β -rays straight out and get real cell definition" but magnetic fields are not intense enough for this.

In 1947, Marton and Abelson[10] described a method called tracer micography in which monoenergetic

internal conversion electrons from a radioactive source were focused by a magnetic lens, producing a magnification of 1.6x. With their apparatus, using a 1 milli curie per mm^2 source of Ga^{67} at a numerical aperture of 0.04 radians, satisfactory blackening of a plate was obtained after a 1 hour exposure. They obtained a best resolution of 30 microns, and proposed after-acceleration of the electrons to reduce exposure time, spherical aberration, and possibly chromatic aberration.

At the same time, a similar instrument was developed in Edinburgh[11], [12] with which a resolution of 5 to 10 microns was obtained at a magnification of 7x. An attempt has been made to improve this instrument, and to study the principles on which its operation depends; also to evaluate the potential of such an instrument in the field of autoradiography. The work involved is described in the following chapters.

CHAPTER I.

THE ELECTRON EMISSION MICROSCOPE.

1. General Principles of the Focusing Method.

Assuming that we have a certain distribution of radioactivity on a small surface, it is required to focus the electrons given off from this surface by means of an electron optical lens system. The resulting magnified image is picked up on a photographic plate, which, after development gives an electron-micrograph showing the distribution of radioactivity in the original specimen. The detail and fine structure visible in the image will depend on the resolving power of the lens system used.

In the usual type of transmission electron microscope, electrons of one energy only are used, in order to avoid chromatic aberration, but in the microscope under discussion, the electrons emitted by the source are not monokinetic, but contain all energies embraced by the continuous spectrum of the radioactive isotope. In addition, alpha- and gamma-rays might be present but these are not influenced by the field. Hence, the instrument suffers from an inherent chromatic aberration. This can be reduced, however, by selecting an isotope which has an internally converted

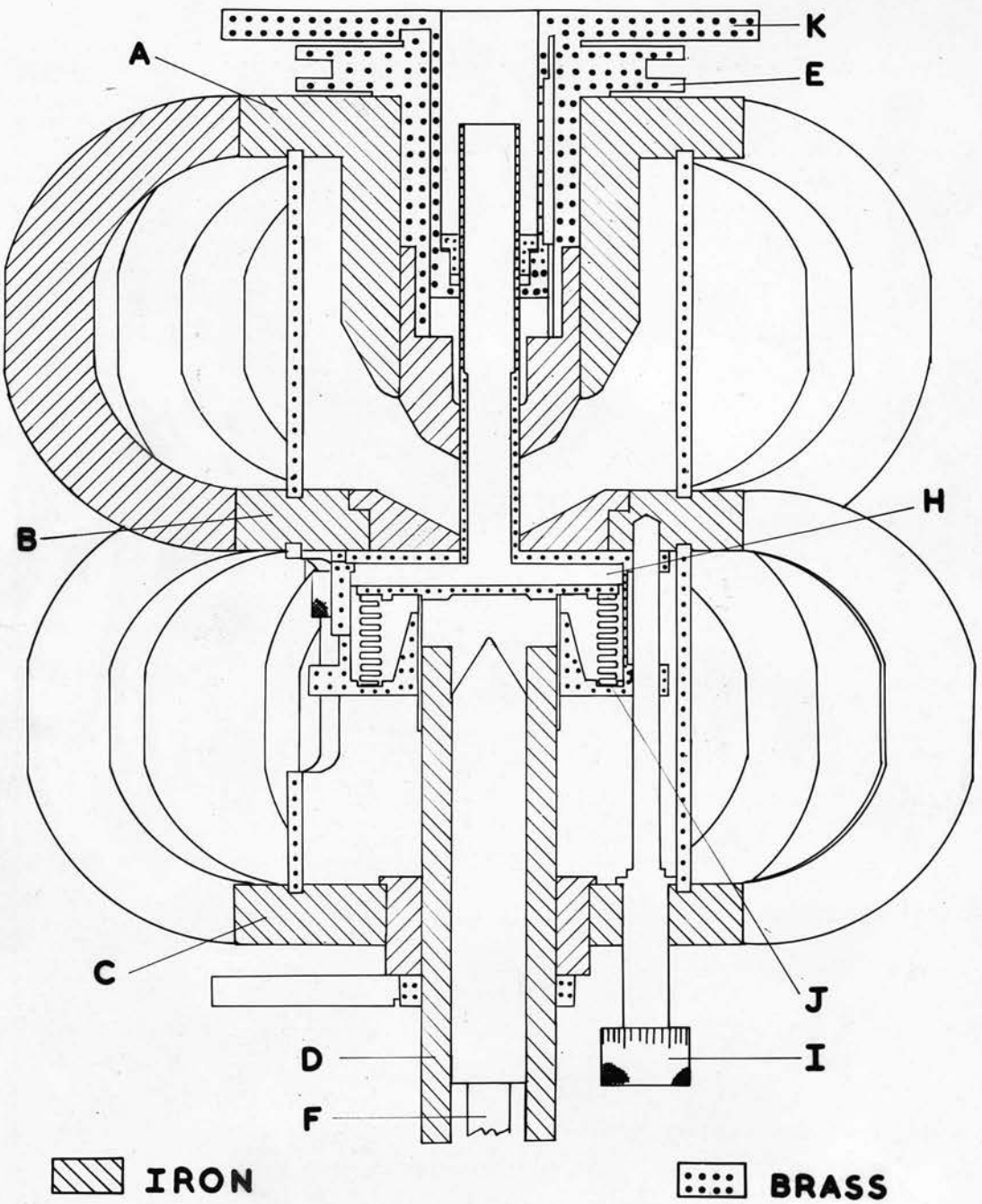

Fig. 1.

The Electron Optical Lens System.

gamma-ray, which gives rise to a strong line of internal conversion electrons, all of the same energy. When the lens system is set to focus these photo-electrons, the selectivity is greatly increased, and the image is well defined above the general background.

2. Description of the Instrument.

The electron emission microscope consists essentially of three main parts:

(a) The electron optical lens system.

(b) The object stage.

(c) The image stage.

Fig. (1) shows a cross section through the lens components, along the axis, and Fig. (2) is an elevation, with part of the lower clamping ring cut away, showing the magnetic system, specimen chamber, movement controls, and scales. In Fig. (2), the overall height from G to K is 21¾ in. A general view of the instrument is shown in Plate (I).

(a) The Electron Optical Lens System.

The lens is a permanent magnetic one. The main focusing field is maintained by 8 permanent horse-shoe magnets of Alnico steel, which are arranged symmetrically around two soft iron rings, which act as holders for the pole pieces. The upper ring (A)

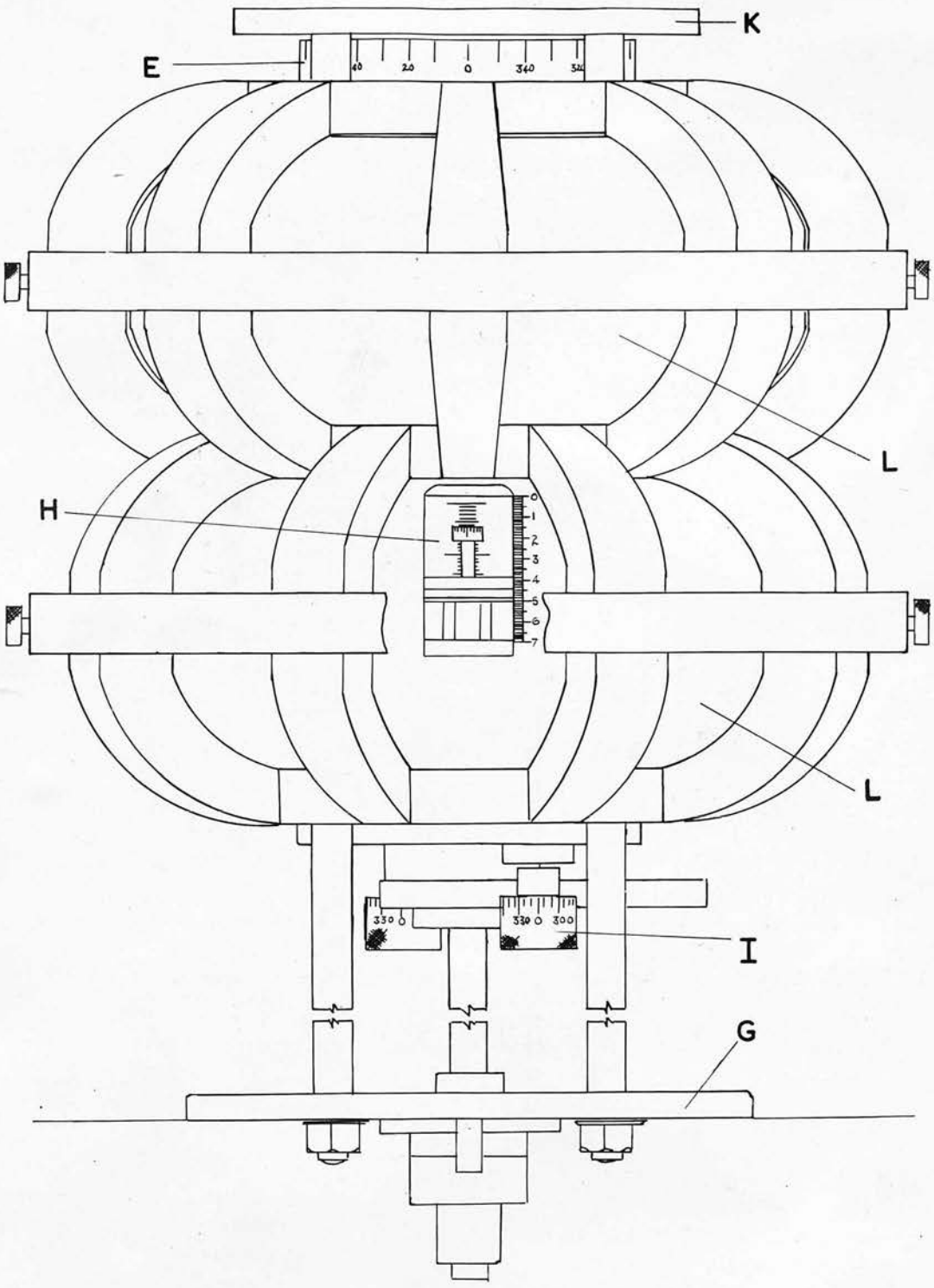

Fig. 2.

Diagram to show Magnets, Specimen Chamber and Controls.

ends in a hollow cylinder which projects downwards at right angles to the ring, and holds the upper pole piece, which has the shape shown. The lower ring (B) is connected to the middle pole piece, which is circular, and tapered on the inner side. Both these pole pieces are cylindrical in shape with 1 in. diameter holes through the centre.

A second bank of 8 similar magnets fits across the ring (B) and a lower ring (C). This ring (C) supports the lower pole piece which is in the form of a long solid cylinder, to the end of which variously shaped pole tips can be attached. The pole piece is surrounded by a soft iron sleeve (D).

The whole system is axially symmetric about the electron optical axis. The pole tips are carefully machined, and the system correctly aligned, to prevent any asymmetries in the lens field. Each magnet has an end area of 1 x 1 sq. in., a magnetic length of 10 in., and is thicker near the centre to give minimum flux leakage.

The middle pole piece is fixed, but the upper one can be moved vertically by means of the brass control wheel (E), graduated in degrees, the pitch of which is 20 turns per in. The lower pole piece also has a vertical motion, controlled by a graduated brass rod (F) threaded into the soft iron cylinder, and held

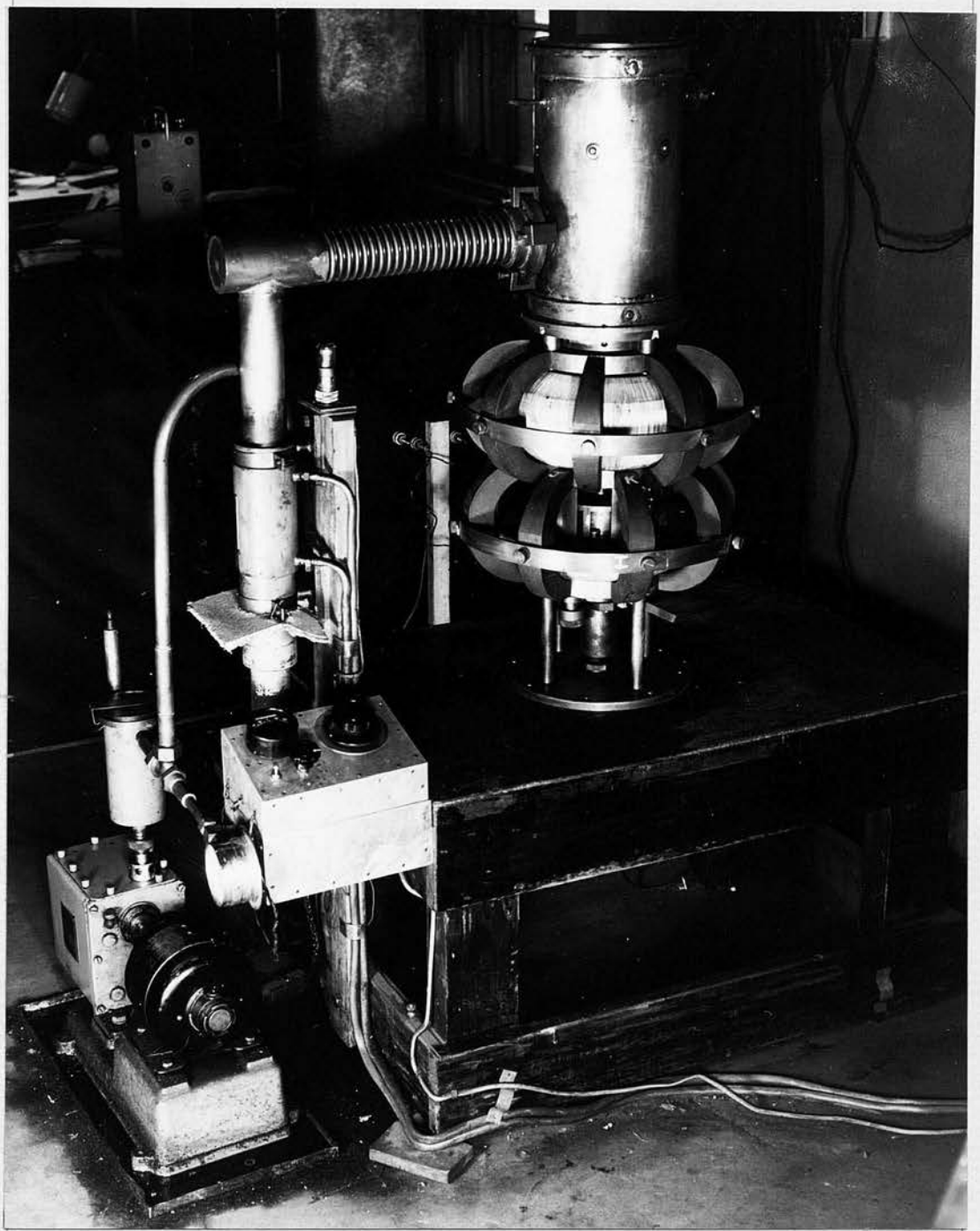

Plate I.

The Electron Emission Microscope and Auxiliary Equipment.

firmly by a brass bush in the base plate (G). The sleeve slides over the cylinder, and can be locked in any position. Reference to the scale on the brass rod gives the position of the lower pole piece and sleeve. Both gaps can thus be varied, the upper one having a maximum separation of 1¼ in.

(b) The Object Stage.

The specimen to be examined is placed in a holder which slides into the specimen chamber (H) through an opening which, when closed, makes a vacuum seal. The holder consists of ⅛ in. brass plate, shaped to fit the chamber, and has 3 projections on its underside, which fit into a groove on the floor of the chamber, to act as a guide. The specimen itself is held in a slide, the design of which depends on the type of specimen being examined. This slide fits into a groove on the holder which, together with a locking screw, governs the lateral motion of the specimen. Longitudinal adjustments are made by means of a screw projecting from the end of the holder, which can be locked in any position (see Plate II).

The specimen chamber is made of brass, and is cylindrical in shape. The top face, in its upper position, bears against the lower face of the middle

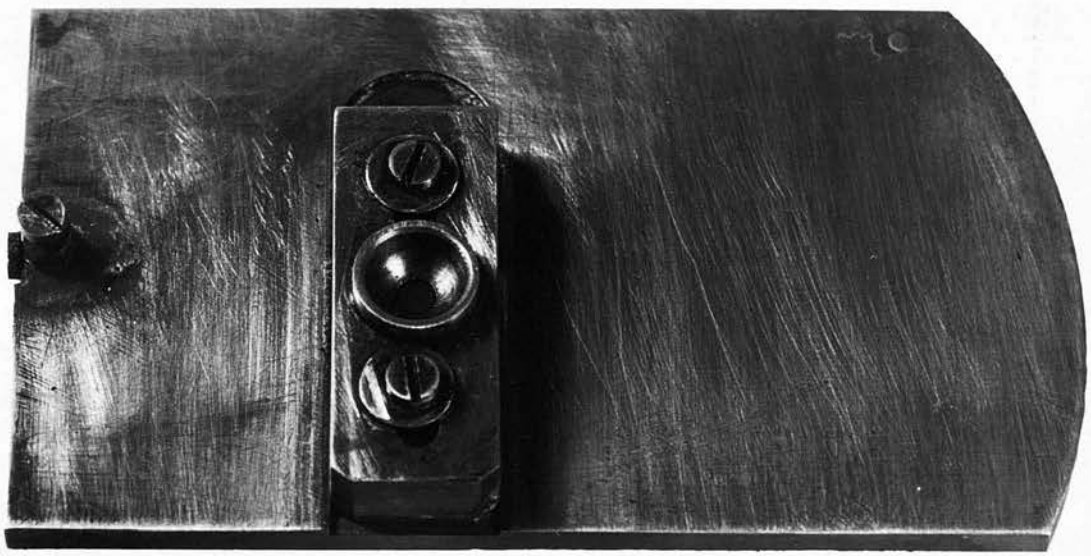

Plate II.

Specimen Holder (overall length $3^{3}/16"$).

pole piece. A 6½ in. long vertical hollow cylinder defines the boundary of the lens system, and allows the electron beam to pass up the axis of the lens. This axial tube leads into another hollow brass cylinder, of diameter $1\frac{3}{5}$ in., which projects down from the base of the camera mounting plate (K), the seal being made vacuum tight by means of a gasket and clamping ring. When the latter is loosened, the whole chamber can be moved vertically, by means of two threaded shafts (I), its position being read on a scale on the supporting brass frame work. The floor of the chamber can be moved, within the chamber itself, without destroying the vacuum, by means of a sylphon bellows (J). The screw operating the bellows moves over a scale, so that the position of the floor is known.

(c) The Image Stage.

The intensity of the image formed by the lens is such that photographic recording has to be used. The photographic plate is housed in a light- and vacuum-tight cylindrical brass chamber, which is screwed on to the camera mounting plate (K), while a gasket embedded in the latter ensures that the join is vacuum tight. Access to the plate is made through the top of the camera, which can be closed by means of a brass cover.

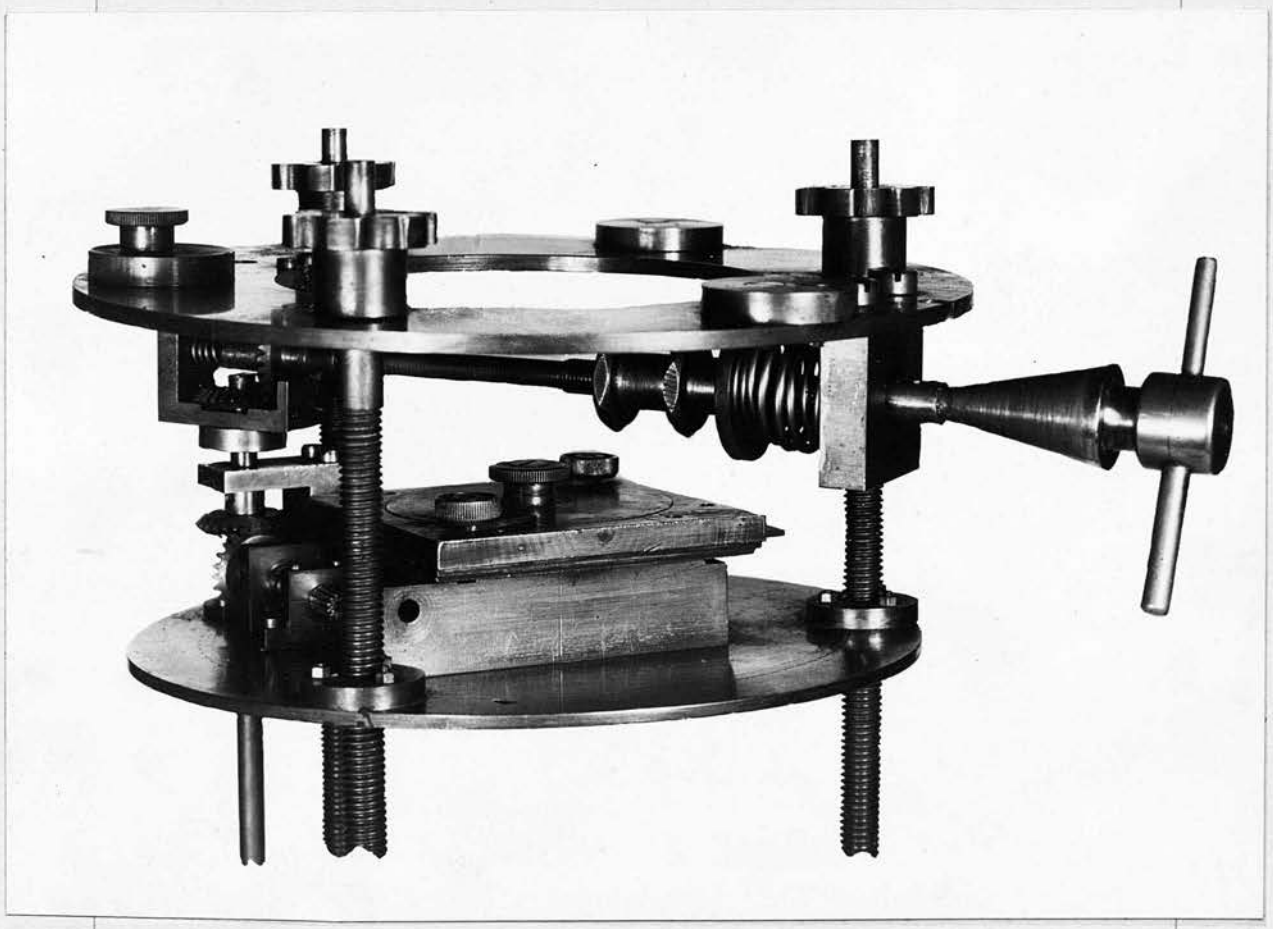

Plate III.

Plate Holder and Shutter Controls.

The plate, contained in a holder, is mounted on a stand, its height being varied by adjusting the length of the stand legs. When the chamber is closed, the control shutter on the plate holder can be operated from the outside, by a system of gears, moved by a shaft, which fits on a cone union mounted in the wall of the chamber. The arrangement is shown in Plate (III).

3. The Beam Limiting Aperture

The extremities of the lens system are defined by the hollow brass cylinder which leads vertically from the specimen chamber. The diameter of this tube is ¾in., so that the aperture has to be stopped down to decrease the spherical aberration of the system. This is done by a baffle system (see Fig. (3)), consisting of a thick brass ring supported on a fine centering spider. A centre stop of brass is also incorporated, in order to block out alpha-rays and low energy beta-rays which pass up the axis of the lens. The edges of the stop and ring, defining the aperture, are tapered away from the source, to prevent reflection and scattering of the electron beam. The resulting aperture is thus an annular hole, the size of which can be varied by changing the inner diameter

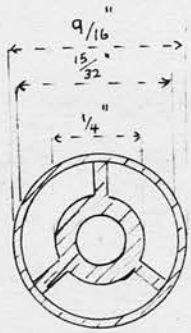

SPIDER

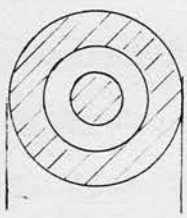

BAFFLE

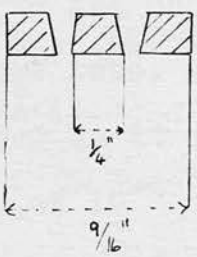

FIG. 3.

Baffle System.

of the outer ring. The arrangement is carried in a brass holder, which can be pushed down the axis to any desired position.

4. Auxiliary Equipment.

To increase the mean free path of the electrons, the specimen chamber, lens system, and camera have to be evacuated. This is done by means of a two stage oil diffusion pump backed by a two stage rotary vacuum pump fitted with a vapour trap. The vacuum line is taken from a 2 in. diameter hole in the side of the camera chamber.

Pressure measurements are made on a Pirani gauge and high voltage discharge tube. Precise measurements are not necessary, as long as it is known that the pressure is of the order of 10^{-4} mm. of mercury, but the gauges give an indication of when the camera shutter should be opened.

The magnets are held in position by their own magnetism, but are supported by brass clamping rings. The microscope is supported by four brass rods of length 6 in. and of diameter ¾ in., mounted on a brass base, fitted on a wooden table 22 in. in height. The top of the instrument is thus 5 ft. above floor level.

CHAPTER II.

A STUDY OF THE PROPERTIES OF THE MAGNETIC FIELD USED IN THE ELECTRON EMISSION MICROSCOPE.

A. Theoretical Investigations.

1. Spherical Aberration.

Magnetic electron lenses are subject to all the aberrations common to optical lenses, but by far the most important is the spherical error. In the electron emission microscope, the resolution is such that only spherical aberration need be considered.

The defect is due to the fact that a lens is more convergent for marginal rays than for paraxial rays, so that a point in the object becomes a disc of confusion in the image plane. There are two reasons for this effect. The marginal ray makes a larger angle (β in Fig. (4)) with the axis than the paraxial ray (α), so the former will recross the axis earlier than the latter, since its longitudinal component of velocity is smaller. This spherical aberration is positive, by definition, and it cannot be corrected.

A second factor, independent of the one above, is that the longitudinal component of the magnetic field usually gets stronger as the distance from the axis increases. With this positive gradient, the

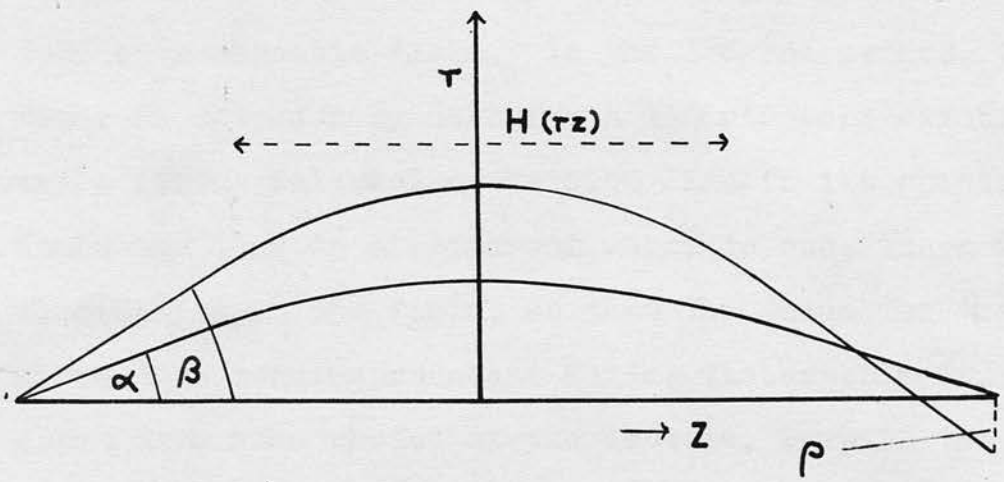

FIG. 4.

Diagram to show Spherical Aberration.

marginal electron is refracted more than one nearer the axis, resulting in a positive contribution to the error.

2. Chromatic Aberration.

This is due to the fact that electrons of different wavelength (i.e. energy) are brought to different foci by a magnetic field. In the present method, the error is cut down by choosing a radioisotope exhibiting a strong internal conversion line in its spectrum. Since the lens is a permanent magnetic one, there is no fluctuation in the field, so that the focus for the given line remains constant during the experiment. Apart from wise choice of the isotope, keeping the area of the object as small as possible, and precautions to prevent self absorption in the source, very little can be done to reduce the chromatic error due to the continuum.

3. General Discussion of Spherical Aberration in Magnetic Lenses.

The amount of spherical aberration present in a lens system depends on the aperture of the lens (α), and a constant (C_s). The dependency is best shown as follows:

$$\rho_s = C_s \alpha^3 M \qquad (1)$$

where M is the magnification of the system, and is the radius of the circle of least confusion due to the aberration. The spherical aberration constant (C_s) is given by the expression:

$$C_s = \frac{e}{96mV} \int_{z_o}^{z_i} \left(\frac{2e}{mV} H_z^4 + 5H_z'^2 - H_z H_z'' \right) r^4 \, dz \qquad (2)$$

where the integration is taken over the electron path, r(z), from object z_o to image z_i. V is the accelering potential applied to the electron beam, e and m are the charge and mass of the electron respectively, and H_z represents the value of the field strength at any point z on the axis; primes represent the derivatives of H_z with respect to z. Eqn. (2) applies only to a strong lens, and when the lens is weak (as in the electron emission microscope) the derivatives of H_z may be neglected ~~are small compared with H_z itself~~, so the value of C_s depends mainly on the first term in the brackets. It is, therefore, approximately proportional to the inverse square of the voltage, for a given field. However, an approximate value for the focal length (f) of a weak lens is given by the Busch formula:

$$f = \frac{8mV}{e \int_{-\infty}^{+\infty} H_z^2 \, dz} \qquad (3)$$

and since the focal length is usually fixed by the

geometry, the field being varied when the voltage is changed, Cosslett[13] has pointed out that the spherical aberration of a given lens would, to a first approximation, be independent of the voltage.

The factors affecting the spherical aberration in magnetic lens systems have been discussed by Glaser,[14] Dosse[15], Marton[16], Cosslett[17], and many others, but most of the work refers to strong lenses. Scherzer[18] has shown that there is no possibility of a complete correction for electron lenses, but there have been many attempts to reduce the error.

Glaser[19] has calculated a field form that should give zero spherical aberration. By equating to zero the integrand in eqn. (2) and solving the differential equation, the required field form is obtained. This is shown in Fig. (5), but cannot be realised in practice as the field strength increases to infinity at two points, but only a small error is introduced if the field is given finite values at these points. However, Rebsch[20] pointed out that the refractive power of such a field is very low.

The electron emission microscope lens was designed with this type of field in view, and the rest of this chapter deals with this lens in theory and practice.

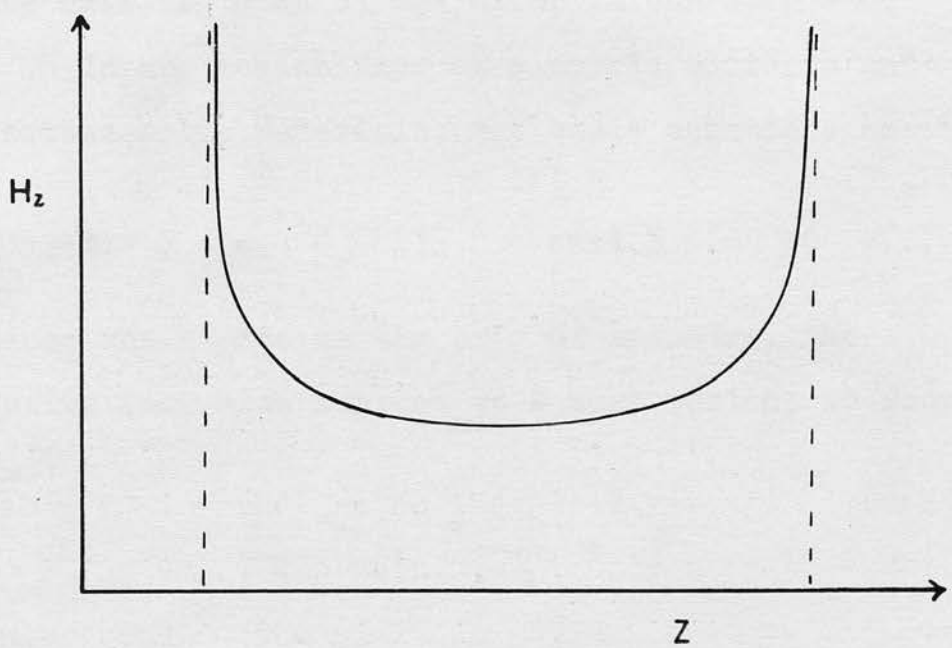

FIG. 5.

Zero Spherical Aberration Field (Glaser).

4. Theory of the Electron Emission Microscope Lens.

Consider a non homogeneous magnetic field, possessing axial symmetry, expressed in cylindrical coordinates (z, r, θ). Let the axial component of the field strength be H_z, and the radial component H_r. It is intended to derive an expression which gives the value of the axial field at any point off the axis in terms of the axial values at r = 0.

In any region free of electric currents and ferromagnetic materials, the basic equations are:

$$\text{div } \underline{H} = 0 \quad ; \qquad \text{curl } \underline{H} = 0 \quad \ldots\ldots (4)$$

Since the z-axis is the axis of symmetry, the derivatives with respect to θ must vanish, so from (4):

$$\frac{\partial (r H_r)}{\partial r} + r \frac{\partial H_z}{\partial z} = 0 \qquad (5)$$

and

$$\frac{\partial H_r}{\partial z} - \frac{\partial H_z}{\partial r} = 0 \qquad (6)$$

Combining (5) and (6):

$$r \frac{\partial^2 H_z}{\partial r^2} + r \frac{\partial^2 H_z}{\partial z^2} + \frac{\partial H_z}{\partial r} = 0 \qquad (7)$$

Expanding $H_z(r,z)$ by means of Taylor's Series, we can write

$$H_z(r,z) = \sum_{n=0}^{n=\infty} \frac{r^n}{n!} \left(\frac{\partial^n H_z}{\partial r^n} \right)_{r=0} \qquad (8)$$

Evaluating each term in eqn. (7), using the value of H_z from (8), we get

$$\left(\frac{\partial H_z}{\partial r} \right)_{r=0} + \sum_{n=2}^{n=\infty} \frac{r^{n-1}}{(n-2)!} \left[\left(\frac{\partial^n H_z}{\partial r^{n-2} \partial z^2} \right)_{r=0} + \frac{n}{(n-1)} \left(\frac{\partial^n H_z}{\partial r^n} \right)_{r=0} \right] = 0 \qquad (9)$$

Eqn. (9) holds for all values of r, so each coefficient of r vanishes separately. Hence:

$$\left(\frac{\partial H_z}{\partial r} \right)_{r=0} = 0 \quad ; \quad \left(\frac{\partial^n H_z}{\partial r^n} \right)_{r=0} = - \frac{n-1}{n} \left(\frac{\partial^n H_z}{\partial r^{n-2} \partial z^2} \right)_{r=0}$$

By a process of mathematical induction it can be shown that

$$\left(\frac{\partial^n H_z}{\partial r^n} \right)_{r=0} = 0$$

for odd values of n, and

$$\left(\frac{\partial^n H_z}{\partial r^n} \right)_{r=0} = (-1)^{\frac{n}{2}} \frac{(n-1)(n-3) \cdots \cdots 1}{n(n-2) \cdots \cdots 2} \left(\frac{\partial^n H_z}{\partial z^n} \right)_{r=0}$$

for even values of n.

Substituting these values into the Taylor expansion (8) we get

$$H_z(r,z) = \sum_{n=0}^{\infty} \frac{(-1)^n}{(n!)^2} \left(\frac{r}{2}\right)^{2n} \left(\frac{\partial^{2n} H_z}{\partial z^{2n}}\right)_{r=0} \tag{10}$$

If the field strength along the axis $(H_z)_{r=0} = H(o,z)$ is written H(z), and H'(z) represents its first derivative with respect to z, the first few terms of (10) are

$$H_z(r,z) = H(z) - \frac{r^2}{4} H''(z) + \frac{r^4}{64} H''''(z) + \cdots \tag{11}$$

Glaser and Lammel[21] have derived this relationship by a different method, finding an expression for the flux ψ (r, z) and relating this to H_r and H_z.

As previously stated, positive spherical aberration is mainly due to the positive gradient of H_z in the r-direction. This gradient from (11) is given by

$$\frac{\partial H_z(r,z)}{\partial r} = -\frac{r}{2} H''(z) \tag{12}$$

Now if a field had a negative H_z gradient it would at all points make a negative contribution to the spherical error. The condition for this is:

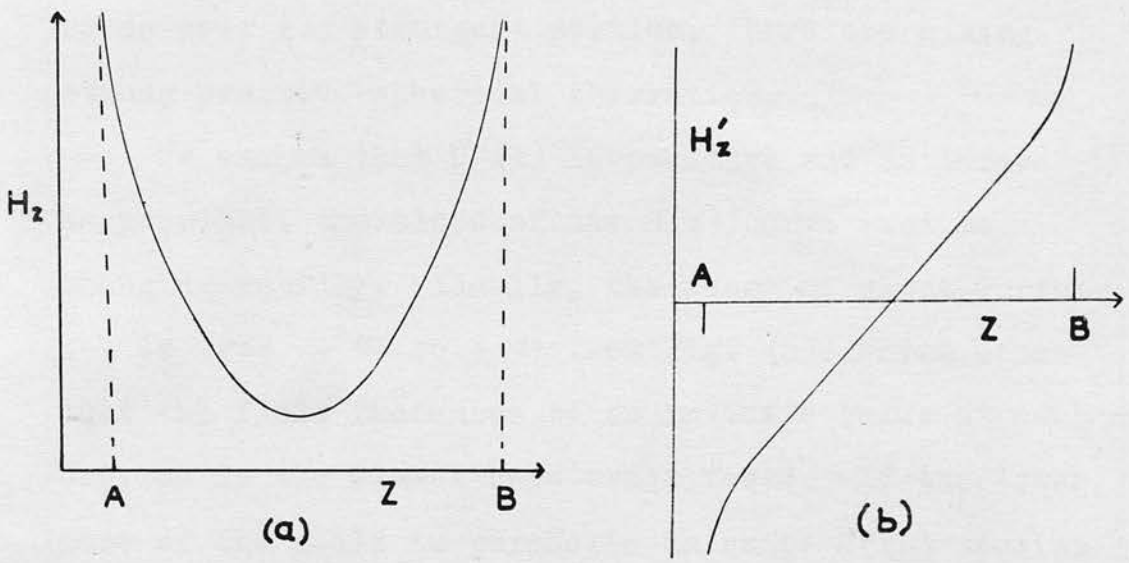

FIG. 6.

Parabolic Field Shape (H''_z constant).

$$\frac{\partial H_z(r,z)}{\partial r} < 0$$

We see from (12) that in order to fulfil this condition H"(z) must be positive, that is the field shape should be convex downwards. The usual bell shaped field used in magnetic lenses is convex upwards over its strongest portion, therefore giving strong positive spherical aberration.

To ensure that H"(z) is positive and as large as possible, the slope of the H(z) curve must be changing rapidly. Ideally, the range of slope variation is from $-\infty$ to $+\infty$ (see Fig. (6)) which means that the field increases to an infinite value at each end, as in the Glaser zero error field. If the lower part of the field is parabolic in shape H"(z) remains constant, the actual value depending on the slope of the tan θ curve, which for given boundary values is governed by the width of the field (AB). It is important that H"(z) is large over all parts of the field so that an electron passing through the lens field is under the influence of the negative value of $\partial H_z / \partial r$ all the time. Fig. (7) shows two extreme cases where all the change of slope takes place at one or two points. This is not desirable.

From these considerations it can be concluded that the best shape of field would be intermediate between (a) and (b) in Fig. (7), that is approximately

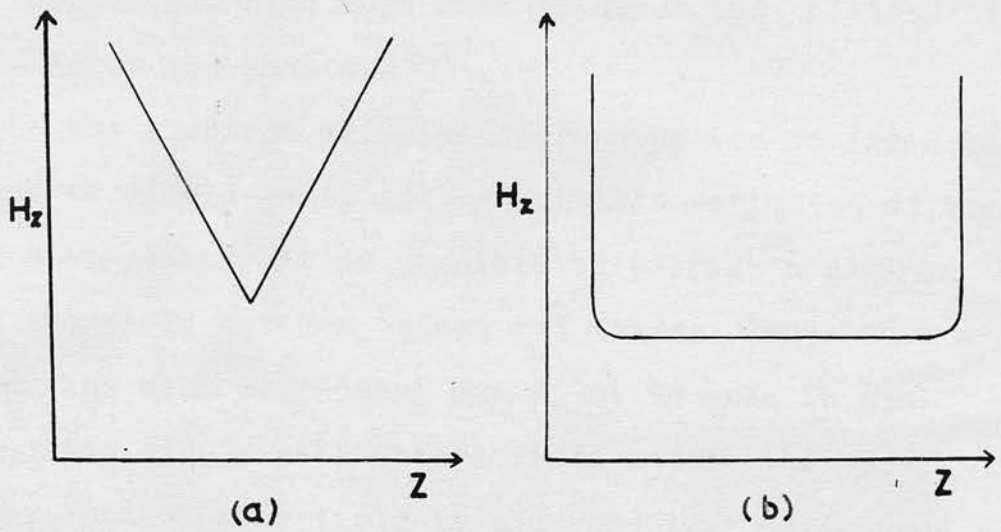

FIG. 7.

Extreme Cases of Change of Slope of H_z.

parabolic with H_z as large as can be tolerated by the operating conditions.

A magnetic field with a minimum between object and image was used by Slatis and Siegbahn[22] in a beta-ray spectrometer, giving reduced spherical aberration and improved transmission properties. The principle has also been used by Quade and Halliday[23], and Agnew and Anderson[24].

The electron emission microscope was designed to have two field gaps, and by suitable variation of the lens components it is possible to produce a minimum in the field between object and image. Since such a lens has weak refracting power, it is used in conjunction with a bell shaped field across the upper gap. This latter field is the same type as is used in transmission electron microscopy, and can be represented by the Glaser[14] expression

$$H(z) = \frac{H_o}{1 + \left(\frac{z}{a}\right)^2}$$

where H_o is the maximum field strength, and a is the coordinate where H(z) has the value $H_o/2$. Glaser has made a thorough investigation of this type of field, and has deduced expressions for the focal length and spherical aberration constant. The latter is given by

$$C_s = a\left[\frac{\pi k^2}{4(k^2+1)^{3/2}} - \frac{1}{8}\,\frac{4k^2-3}{4k^2+3}\,\sin\frac{2\pi}{\sqrt{k^2+1}}\right]\frac{1}{\sin^4\frac{\pi}{\sqrt{k^2+1}}}$$

where

$$k^2 = \frac{e H_o^2 a^2}{8 m V}$$

The lens strength also is characterised by the factor k^2 . For values of the various parameters used in the emission lens it is found that $k^2 \ll 1$, so that the lens is classified as weak, a condition which favours agreement between the Glaser and Busch expressions for the focal length.

The combination of the two field shapes results in the field form shown in Fig. (8). From the extremity (A) to the point of inflection (B) the gradient of H_z in the r-direction will be negative, from (B) to (C) will be strongly positive, and from (C) onwards it will be negative again. So it would be an advantage to keep the points of inflection as high up the bell curve as possible. Using this combined field an overall improvement in the spherical error might be expected over the bell shaped field when the latter is used alone. The whole field is asymmetric about the centre point, and conforms with Dosse's[15] conclusion that the aberration constant

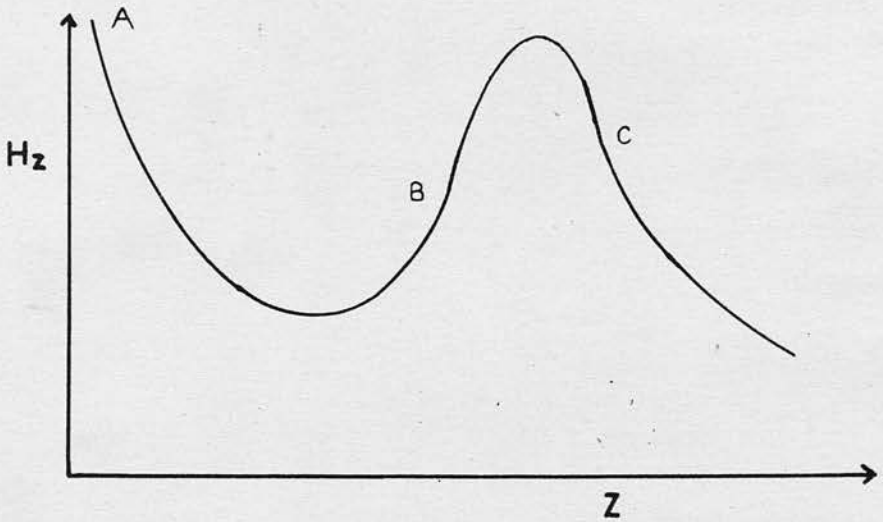

FIG. 8.

Combination of Bell and Dip Fields.

is smaller for less steep fields on the object side, particularly for low values of k.

Since the gap widths can be varied, it is an advantage to use the optimum separation of the pole pieces. The width of the lower gap is chosen to give the best field shape, and cannot be varied much without destroying that shape. Also, it depends on the position of the object, which is immersed in the field. In order to keep spherical aberration to a minimum, the upper gap should be fairly wide, and for a given electron energy the field strength can be adjusted to compensate for a larger gap width.

5. Realisation of the Field Shape.

The magnetic circuit of the lens system is shown in Fig. (1), the field being maintained across two gaps by the two banks of permanent magnets. The latter are initially energised by means of a D.C. current through two sets of coils ((L) Fig. (2)) wound around the axis of the instrument, between the horseshoe magnets and the pole pieces. The upper magnets are arranged symmetrically with their N-poles attached to the ring (A), and their S-poles to the ring (B). Hence, there is a strong field across the upper gap,

which is similar to the short magnetic lens, with a maximum field strength mid-way between the poles.

The lower magnets have their N-poles attached to the ring (B), and are arranged so that each one has a S-pole of the upper magnets equidistant on either side of it. The magnetic circuit is completed by joining the S-poles of the lower magnets on to the ring (C). To ensure good magnetic contact for the poles, small areas on the outside of the rings have been cut away to present a flat surface at the junction points.

Figs. (9) (a) and (b) are quadrants of a section through the rings (A) and (B), perpendicular to the lens axis, illustrating the magnetic lines of force in the soft iron. To ensure symmetry of the field it is important that the magnets in any particular bank are equally magnetised, but the upper and lower sets may have different strengths. If all magnets are equal the middle ring will have no magneto motive force, but free poles are bound to appear on the surface. The middle pole piece then approximates to a soft iron ring placed between two strong poles. Any irregularities in the field due to the free pole distribution will be well away from the central part of the field used for focusing.

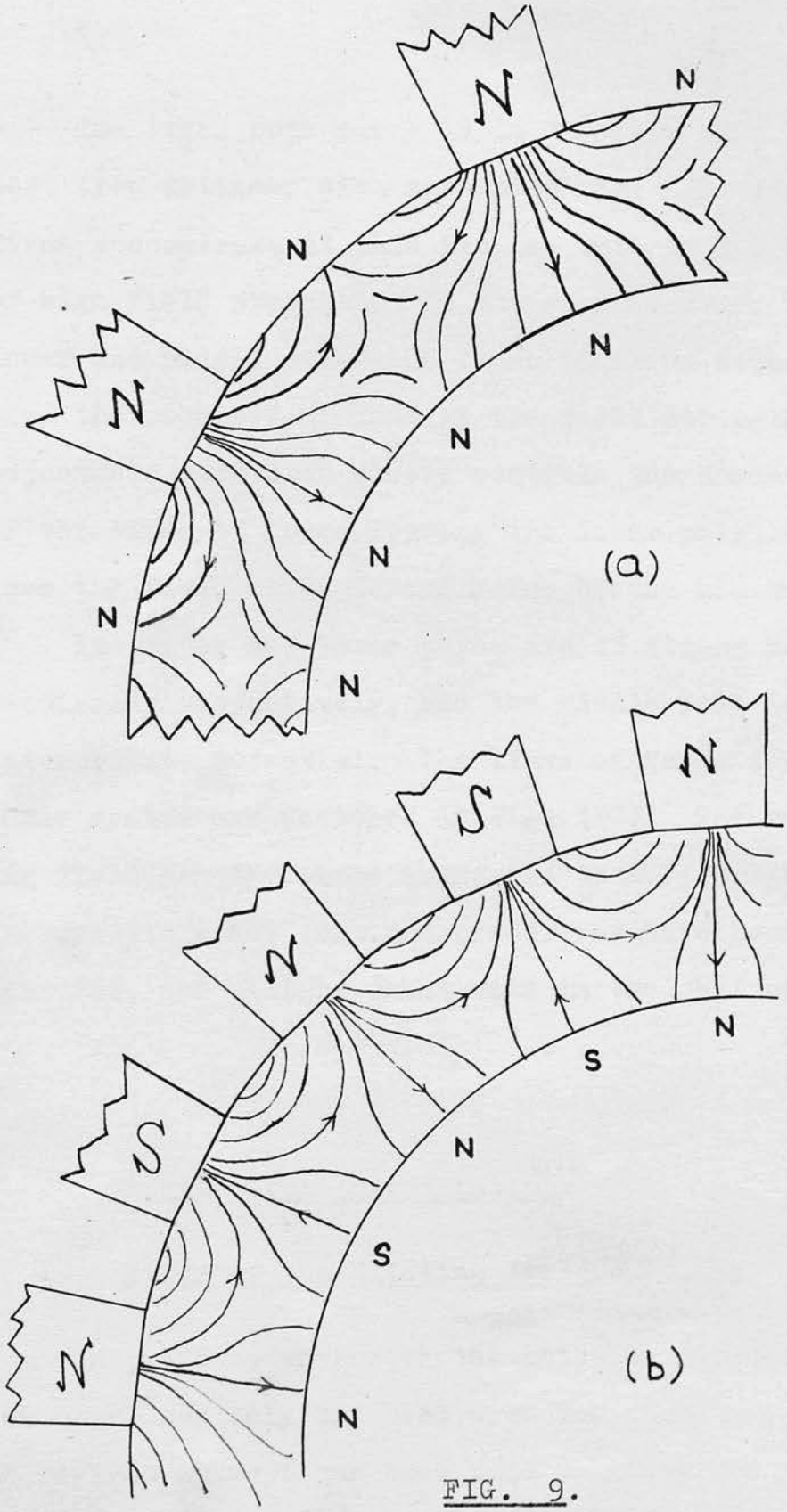

FIG. 9.

Sections through Soft Iron Rings.

The lower pole piece is in the form of a solid soft iron cylinder with a pointed tip. The lines of force concentrate at this tip, so this is a region of high field strength. In the space between the lower and middle poles the lines of force diverge and give the required minimum in the field strength. The adjustable soft iron sleeve controls the concentration of the lines of force leaving the lower pole, and thus the field strength and value of the minimum.

The upper and lower poles are of strong N- and S-polarity respectively, and the middle pole is of intermediate potential. The lines of force for the whole system are sketched in Fig. (10). The resulting field has the shape suggested by the foregoing theory; its exact form and properties have been measured, and will be dealt with in the next section.

B. Experimental Investigation.

1. Study of the Existing Field.

In previous work with the emission microscope the upper gap only had been used for focusing, and no serious attempt had been made to study the

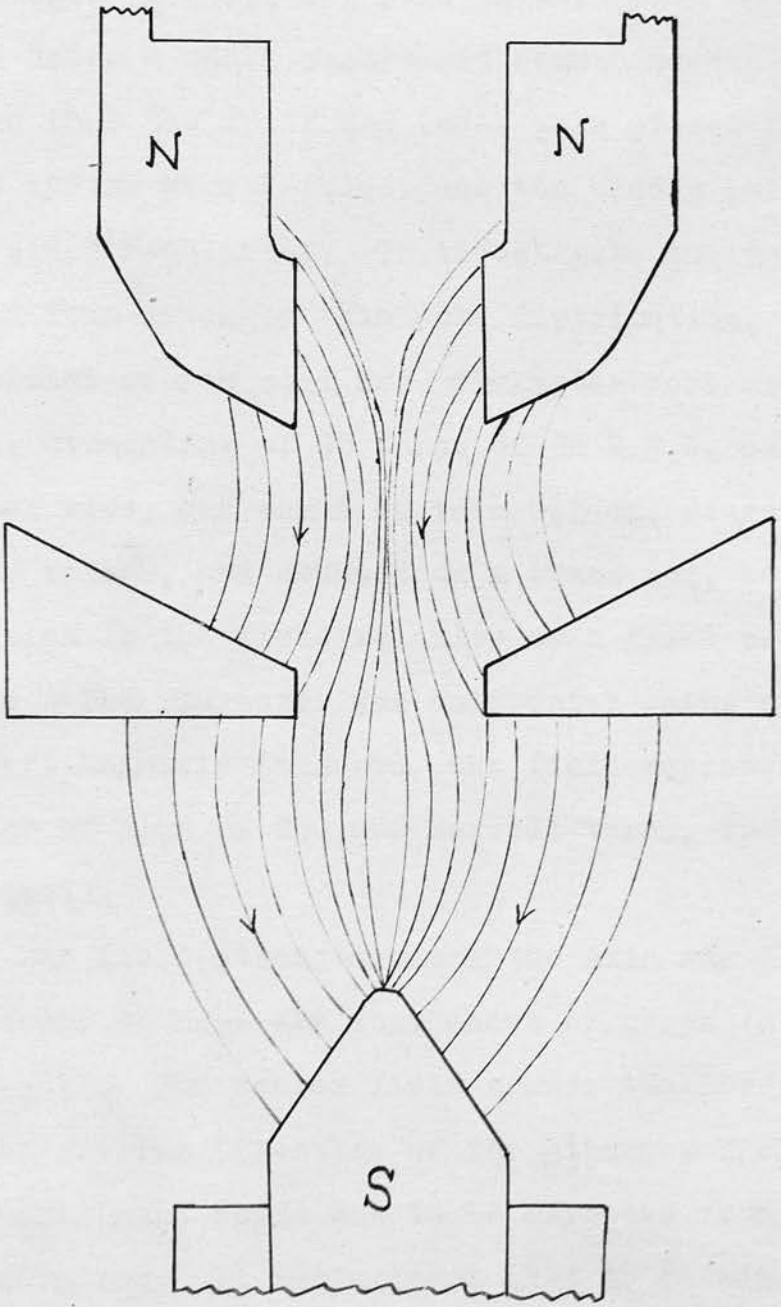

FIG. 10.

Lines of Force in Lens System.

influence of the lower pole piece.

Using a small magnetised search needle, it was found that the upper and lower pole pieces in the lens system were S-poles, and the middle pole piece exhibited N-polarity. To investigate the actual field form given by this pole distribution, a conventional search coil and fluxmeter were used. The coil, consisting of 90 turns of 38 S.W.G. enamelled copper wire, was wound on to a 0.5 cm. diameter brass former, and mounted on a brass rod, so that its position in the field relative to a fixed point was known. The fluxmeter was calibrated using a Hibbert Magnetic Standard, the field representing a change of flux of 230,000 Maxwell turns, for a 10 turn coil.

The field strength along the axis was plotted, and found to have the form shown by graph (a) in Fig. (11). The weaker field across the lower gap was in the reverse direction of the stronger field across the upper gap, which was to be expected from the pole distribution. It was evident that to obtain the desired field shape, complete remagnetisation of the Alnico magnets was necessary.

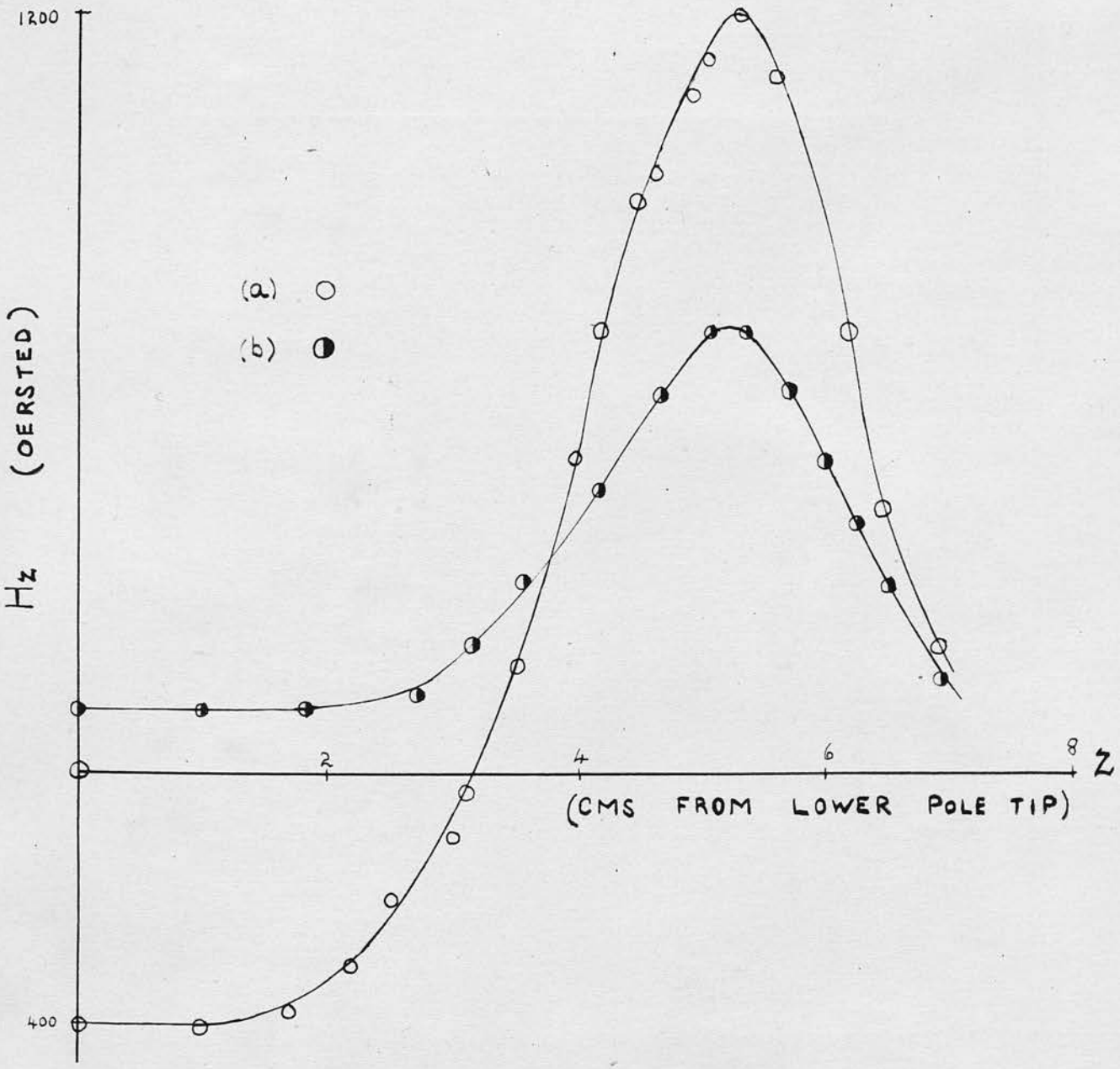

FIG. 11.

Study of Existing Field.

2. Model of the Required Field.

Before attempting to change the field form in the microscope lens, a model of the proposed arrangement was made, in order to confirm the previous conclusions.

Ordinary bar magnets were arranged on the bench so that they represented a section through the lens system similar to Fig. (1); the pole pieces were made of ¼ in. flat strips of mild steel, cut to the shape that the pole pieces of the lens present in section. By suitable adjustment of the components it was possible to get two strong poles of opposite polarity with a central pole of intermediate strength. The field lines were then observed by sprinkling iron filings on to a cardboard sheet placed over the magnets. The pattern was photographed and is shown in Plate IV. The pole pieces can be identified as the areas free from filings. Although the model was a rough one, the main characteristics could be observed, and agreed with previous deductions (compare Fig. (10)).

Much valuable data, such as the influence of the position of the lower pole piece and sleeve on the field shape, and the effect of varying the strength of the magnets joining the middle pole piece, were

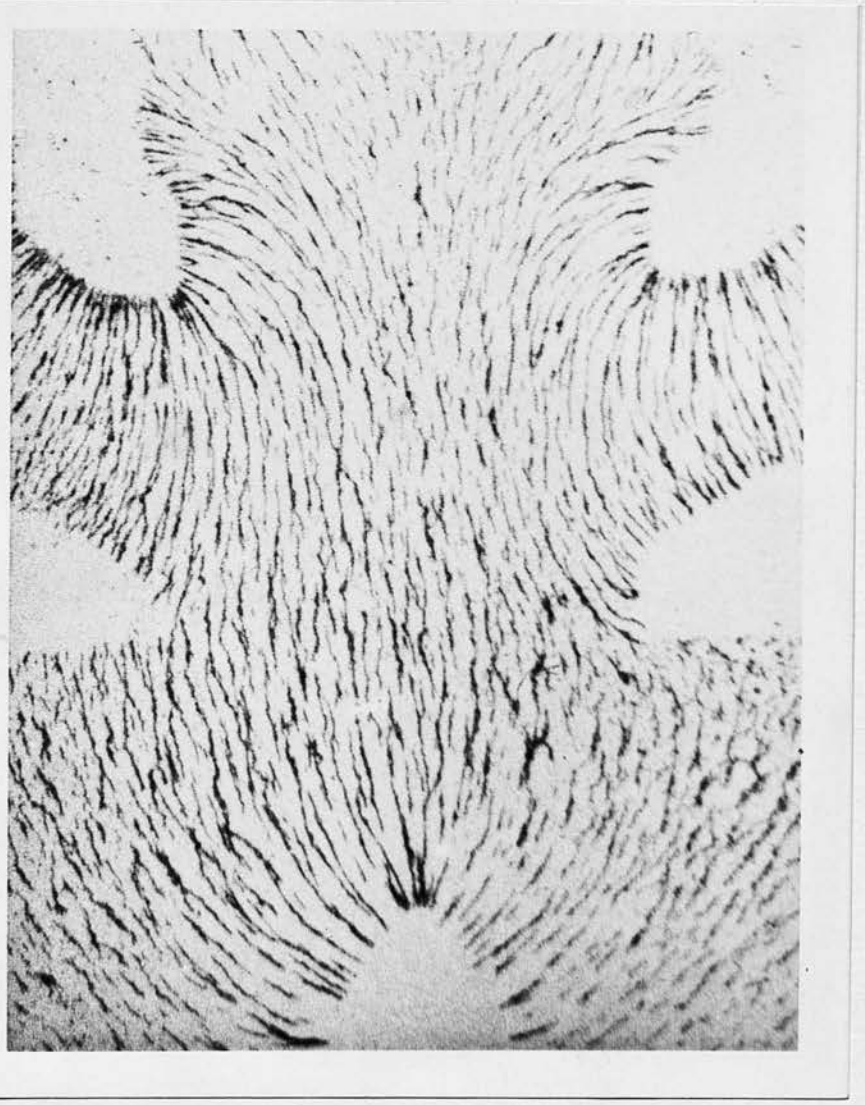

Plate IV.

Model of Lens Field.

obtained from this model.

3. Remagnetisation and Study of the New Field.

It was intended to make the lens field strong enough to focus the F line of thorium B which has an energy of 147.8 keV, and as the refractive power of the proposed dip field across the lower gap was not known, only a rough estimate of the value of the required field could be made. From consideration of the existing field it was concluded that the new field should have a maximum value of approximately 900 oersted across each gap, which entailed remagnetising the lower magnets only.

The instrument is supplied with two sets of copper coils to supply the necessary magnetising field. The lower coil was joined in series with an external circuit of variable, high wattage resistances to the D.C. mains. Due to the position of the specimen chamber, it was impossible to get a complete path in iron for the flux through the lower coil, but the reluctance of the circuit could be reduced to a minimum. The chamber was raised to its uppermost position, and a piece of mild steel placed between the floor and roof of the chamber. A mild steel pole

tip was made for use with the lower pole piece during magnetisation only; this had a flat top to ensure a larger area of contact with the underside of the chamber floor. The lower pole piece and sleeve were raised to their highest position, and the upper gap opened as wide as possible.

Small currents were first passed so that the correct direction of the current could be decided, using the fluxmeter and search coil. This was to ensure that the direction of the field across each gap was the same. A current of 70 amp. was then passed for 5 sec., and the field replotted under standard conditions. Very little change in the field form was found, and the reversal of field direction in the lower gap still existed.

It is recommended by the National Bureau of Standards [25] that the magneto motive force in magnetisation should exceed $5\ H_c \times l$, where H_c is the coercive force of the magnetic material, and l the length of the magnet in cm. For Alnico H_c is approximately 500 oersteds, and in this case $l = 25$ cm. so the M.M.F. should be at least 62,500 gilberts, that is about 50,000 amp.-turns. The number of turns in the lower coil was not known but by measuring the dimensions and resistance of the coil, and the gauge

of the copper wire, it was possible to arrive at an approximate value viz. 350 turns. Thus the M.M.F. previously used was equivalent to 24,500 amp.-turns, which is less than the recommended value. The number of turns is limited by the dimensions of the apparatus, and the fuse rating of the wire in the coil is 102 amp., so it was concluded that some exterior circuit, producing a high value of current of very short duration was necessary. The following impulse methods of magnetisation were considered.

(a) Discharging a high capacitance condenser through the coil windings.

(b) Using a transformer with a secondary winding of large cross section; the primary is supplied with rapidly interrupted D.C.

(c) Blowing a fuse in the external circuit.

(d) Employing a high speed circuit breaker set to open at a current corresponding to $5H_c$.

Methods (a), (b) and (d) involve technical difficulties and expense, whereas (c) is comparatively simple.

The principle involved is to connect the magnetising coils through a fuse to a D.C. voltage supply. When the switch is closed we have:

$$L\frac{di}{dt} + iR = E$$

where i is the current, L and R values of the inductance and resistance, and E the D.C. voltage. Solving we have

$$i = \frac{E}{R}\left(1 - e^{-\frac{R}{L}t}\right) \qquad (13)$$

which represents the current at any time t. Thus when the switch is closed, if E is high and R low, the current in the circuit rapidly rises to a large value according to eqn. (13). The time to reach a maximum depends on the time constant of the circuit but it may approach the value E/R before the fuse blows. If the fuse rating is suitably chosen, the circuit is ruptured long before the magnetising coil acquires any appreciable rise in temperature.

A circuit (Fig. (12)) was designed to supply the high impulse current to the coils, and then to reduce the current in steps for safety. The resistance R_1, consisting of a series of carbon discs, had a very high current carrying capacity. With all switches closed and $R_3 = 0$ the circuit was connected to the D.C. mains. On throwing the main switch the current rose to a high value, then the fuse blew, bringing in R_1 which immediately reduced the current to a safe value. Breaking switch 2 brought in R_2;

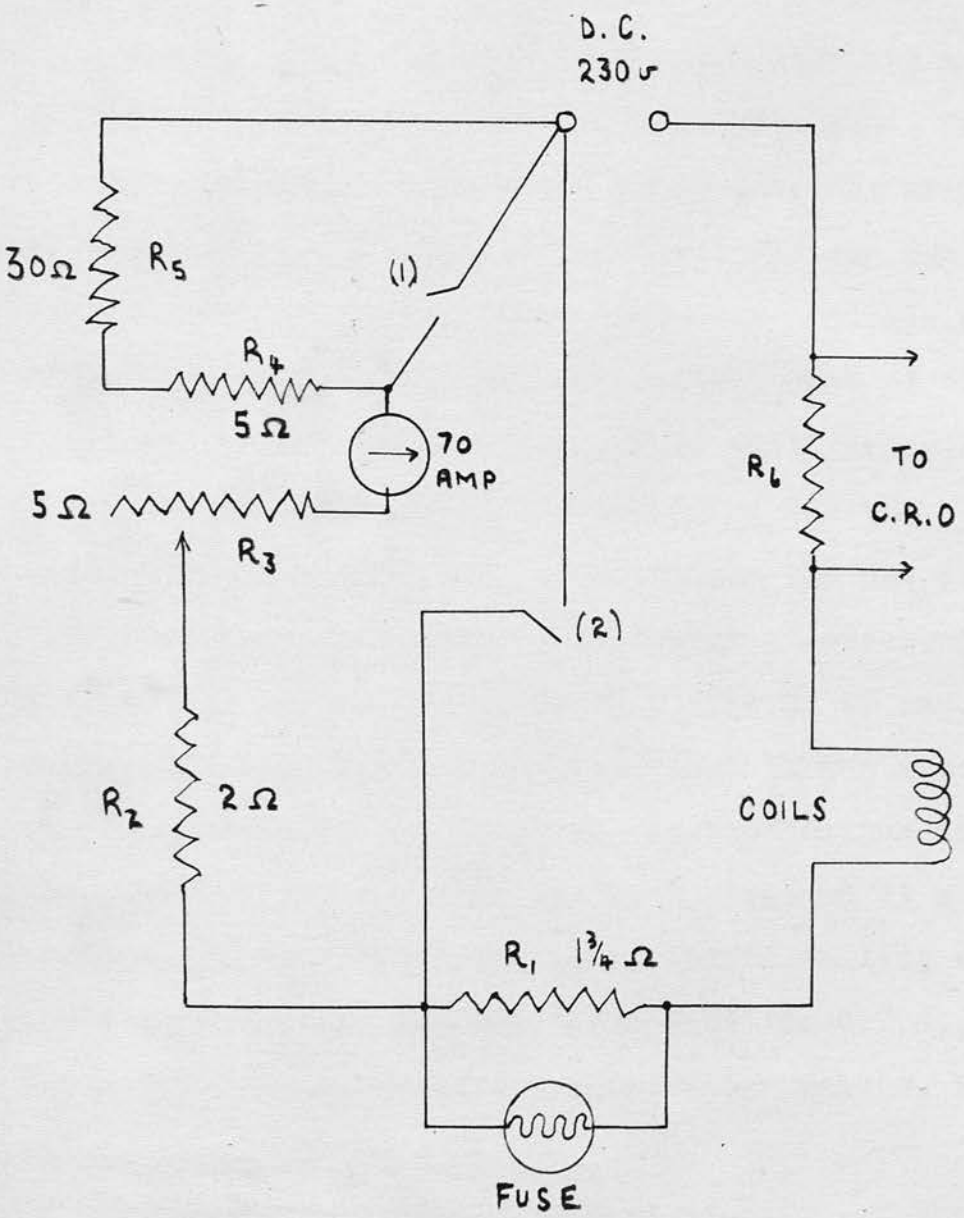

FIG. 12.

Circuit Used in Remagnetisation of Magnets.

R_3 was then increased, and switch 1 broken. This reduced the current to 5 amp., when the mains could be switched off with safety.

A very low resistance R_6 was put into the main circuit to enable the current to be measured. The voltage difference across the resistance was examined by means of a D.C. amplifier and cathode ray oscilloscope. The C.R.O. was first used with a single sweep time base which showed the exponential rise of current, but even on the slowest range of 50 milli seconds the rise time of the current was too great for the maximum to be reproduced. Accordingly the use of the time base was discontinued, in favour of observations of deflections of the spot. Using a fuse of 15 amp. rating the time lag was so small that it was impossible to deduce whether the spot had reached maximum deflection. With a 30 amp. fuse the spot remained at a maximum for an appreciable time, before falling when the fuse blew. At maximum deflection the C.R.O., which had been calibrated against known values, indicated a current of 126 amp.

After ensuring that the magnetisation of the magnets was a maximum, the field was replotted under the standard conditions. The distribution along the lens axis (Fig. (11b)) indicated that although the

neutral point had been eliminated, there was no minimum in the field, and the shape did not approach that required.

At this point it was decided to examine the magnetic hysteresis cycle of the Alnico, and this was done on one of the spare magnets. Some difficulty was experienced in finding suitable coils to give the necessary high flux, but eventually three coils were obtained which gave a total of 8,080 turns. These were not of ideal shape, and only one could be fitted over the magnet; the other two were slipped over the yoke, which consisted of 2 x 2 in. mild steel. The coils, each of resistance 40 ohms, were joined in parallel to allow a high current to be passed. The magnetic induction (B) of the magnet was measured by means of a 5 turn search coil wound around the axis of the magnet and connected to a fluxmeter. The magnetising field (H) was found in terms of the energising current (I). We have

$$\text{M.M.F.} = \int H \, d\ell = \frac{4\pi n I}{10} = H\ell$$

where n is the total number of turns used, and ℓ is the length of the magnet. The potential drop in the yoke may be neglected since its area and

permeability are large. Hence $H = \frac{4\pi n I}{10\ell}$.
The maximum number of amp.-turns that could be used was 43,000 and the hysteresis curve (Fig. (13)) showed that the Alnico was almost saturated. The values obtained for the more important properties of Alnico are listed below. These are in agreement with those values given by Hoselitz[26].

Remanence	(B_r)	8,550 gauss
Coercive Force	(H_c)	460 oersted
$(B\,H)_{max}$		1.8×10^6 gauss-oersted.

The number of amp.-turns used in the impulse method of magnetisation was 44,000, and the results of the hysteresis experiment show that this should be adequate to magnetise fully the magnets. Also it approaches the recommended value of $5H_c \times \ell$ which is equivalent to 50,000 amp.-turns. The poor result obtained with the lens system may have been due to a high reluctance in the magnetic path, caused by the brass roof of the chamber. To investigate this the hysteresis cycle was repeated with a piece of brass, of the same thickness as the chamber roof, included in the yoke. No significant change in the cycle was observed.

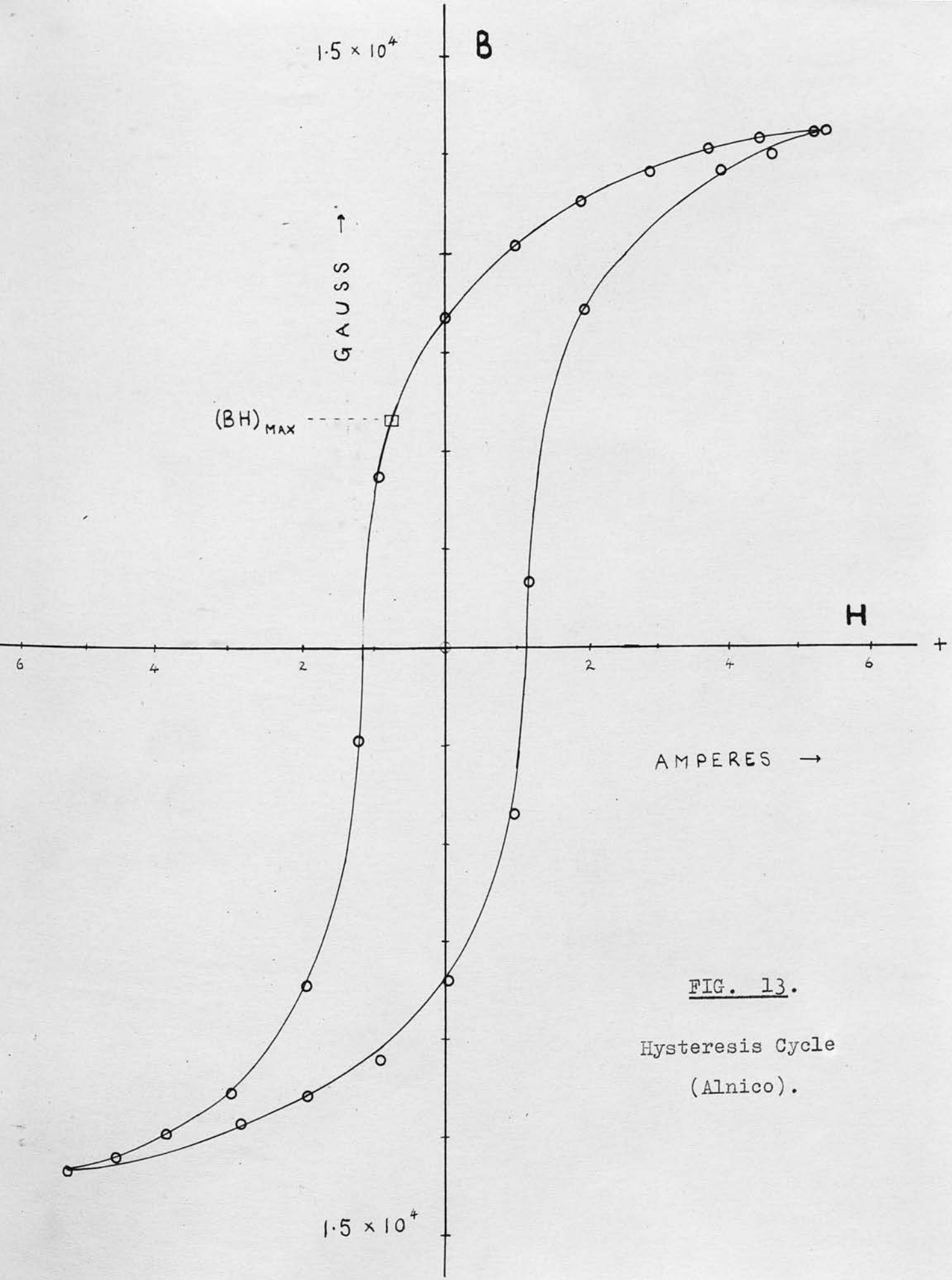

FIG. 13.

Hysteresis Cycle

(Alnico).

One of the lower magnets was removed from the bank to measure its remanence, and it was found that it possessed a N-pole at each end and a S-pole in the middle. A simple experiment showed that this was due to uneven demagnetisation. Using the hysteresis apparatus with the coil around the axis of the magnet removed, the magnetising field was supplied at the yoke only (as in the lens system) and the brass introduced as before. In this way it was possible to reproduce the result obtained with the microscope magnets.

The effect is due to the combination of two factors, viz. the gap in the magnetic circuit and the fact that the magnetising coils are not symmetrically distributed around the circuit. Since there is not a complete path in iron the lines of force tend to bend back close to the coil, so that more go through one end of the magnet than the other, as shown in Fig. (14), producing a greater magnetic influence at the corresponding pole. In the microscope the conditions are probably accentuated by placing the steel strip between the floor and roof of the chamber. In addition there was some demagnetisation of the upper magnets.

From these experiments it can be seen that the

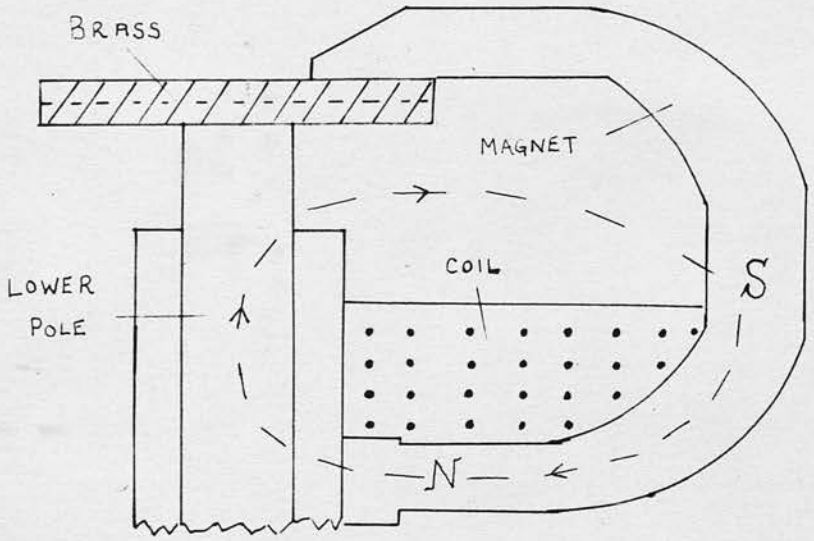

FIG. 14.

Diagram to Illustrate Demagnetisation Effect with Lower Coil.

lower coil has no useful function and any other means of magnetisation is prevented by the geometry of the magnet arrangement. However, tests showed that the magnets could be disconnected without any appreciable demagnetisation effect, so that it should be possible to energise each magnet separately. All the lower magnets were removed and the upper set remagnetised using the impulse method (since there were no gaps in the circuit the upper coil could still be used). The lower magnets were energised on the bench and replaced in their correct position.

The field was then plotted and it was found to possess the desired minimum in its distribution. The positions of the lower pole piece and sleeve were then varied and the field checked for each position. The higher the position of the lower pole piece the greater is the value of H_z at the limit of the field. Hence the pole piece should be kept in contact with the floor of the chamber for all positions of the specimen chamber. The position of the soft iron sleeve was found to govern the shape and value of the minimum. The sleeve was clamped in that position which resulted in a rapidly changing slope of the H_z curve. Two types of pole tips were tried with the

lower pole piece, one hemispherical and the other conical. The latter gave a greater concentration of the field lines at the tip, thus improving the shape of the field, and it has been used throughout the experiments. Variation of the separation of the pole pieces of the upper gap did not alter the maximum value of the bell field, and had very little influence on the shape of the minimum. This meant that the wheel controlling the upper gap width could be used as a fine focusing control, while the object position remained fixed. In choosing the position of the specimen chamber a compromise had to be made between a narrow gap which would give a more rapidly changing field, and a wider gap which would mean that the transit time of the electrons in the negative gradient field would be longer. A plot of the field distribution used in focusing the F line of ThB is shown in Fig. (15).

It was decided to examine the field at points off the axis to find if the axial component of the dip field did in fact have a negative gradient in the radial direction. The diameter of the space to be explored was ¾in., so a new search coil was made. It consisted of 600 turns of 40 S.W.G. enamelled copper wire wound on a brass former of internal diameter

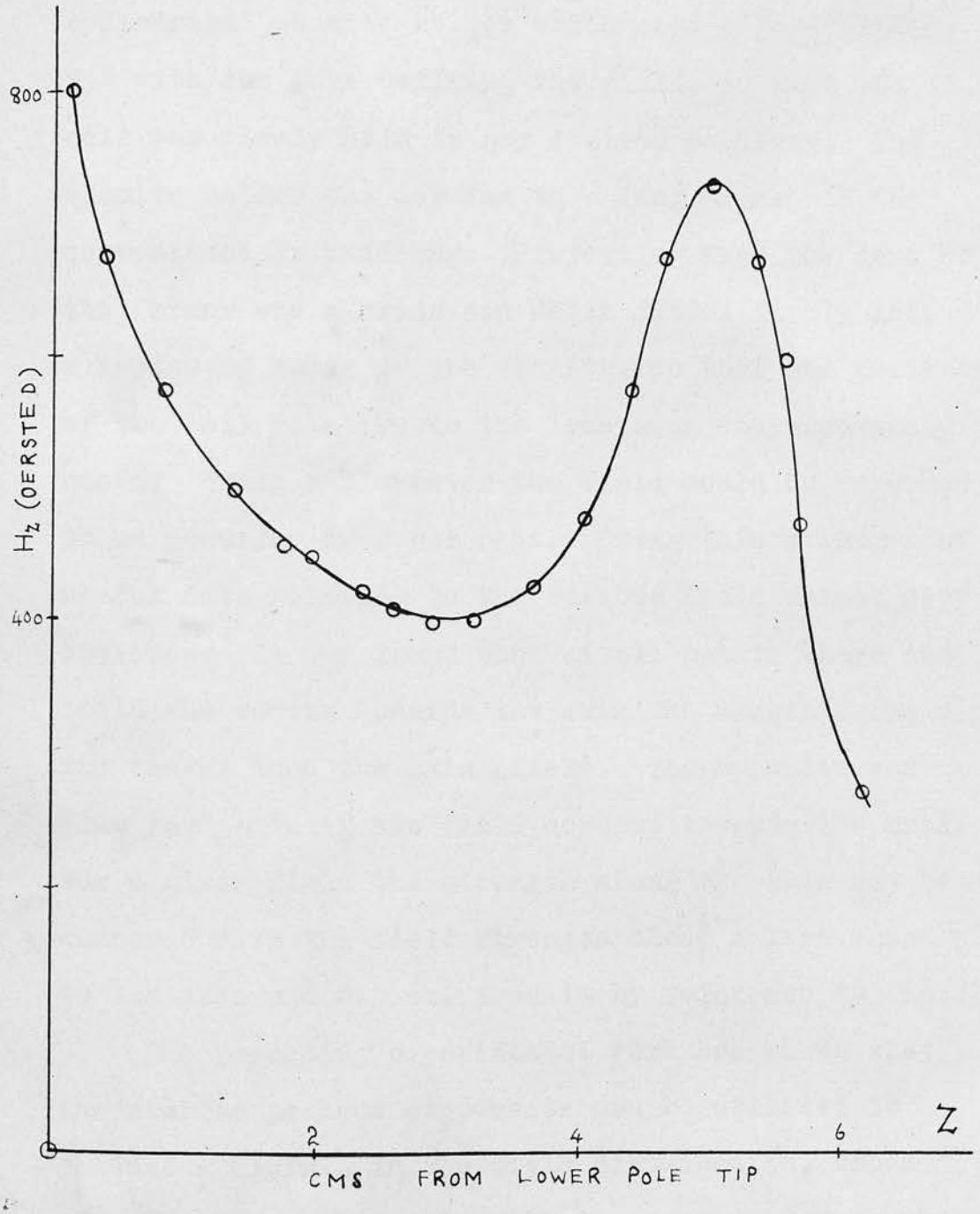

FIG. 15.

Field Form Used to Focus 148 keV Electrons.

0.17 cm. and length 1 cm. The outside diameter of the coil was 0.51 cm. The former was attached to a cylindrical ebonite holder which made a good sliding fit with the tube defining the field, so that the coil was firmly held in any desired position. The ebonite holder was screwed to a long brass rod for convenience in handling. Projecting from the core of the former was a brass pin which fitted firmly into a series of holes in the ebonite, so that the position of the coil relative to the lens axis was accurately known. Using a fluxmeter the field could be measured to an accuracy of 2 per cent. Using this arrangement useful data relating to the various field shapes were obtained. It was found that at all points where the field was convex towards the axis the marginal field was weaker than the axial field. The opposite was true for parts of the field concave towards the axis. For a given field the strength along the axis can be compared with the field strength along a line parallel to the axis and 0.5 cm. from it by reference to Fig.(16).

The preceding experimental work has shown that the microscope lens components can be utilised to produce a minimum in the field distribution, whose properties agree closely with those predicted by the

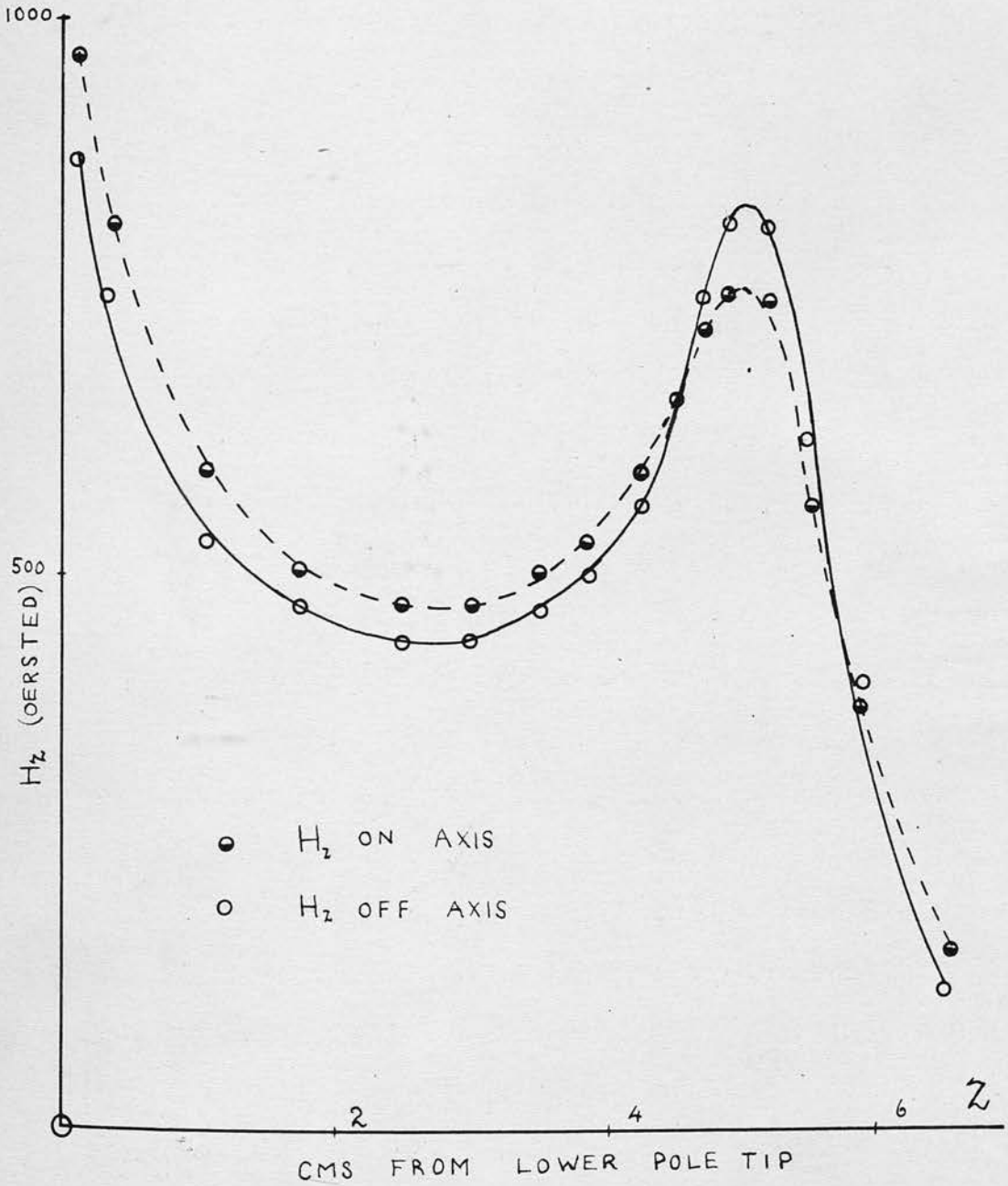

FIG. 16.

Comparison of Field Strength along Axis with Extra-axial Field Strength.

theory. The general form of the field has remained unaltered throughout the experimental procedure with the lens system, but the value of the field strength used has depended on the energy of the electron line emitted from the source.

CHAPTER III.

GENERAL PERFORMANCES OF THE INSTRUMENT.

A. Operational Procedure.

1. Preparation of Sources.

Thorium B ($_{82}Pb^{212}$) was chosen as the most suitable isotope for tests with the instrument since it emits a number of strong lines of internal conversion electrons, in particular the A line (energy 24.5 keV) and the F line (energy 148.1 keV). Also it has a convenient half value period of 10.6 hr., and is easily prepared from a stock of radiothorium. The F line was used in most of the work. This has an absolute intensity of 0.288. However, the ThB products are also present, so the number of F electrons emitted is approximately 10 per 100 disintegrations.

In the preparation of a test object, the ThB had to be deposited on a surface so that the deposit formed a regular pattern of activity. A 5 B.A. screw was turned down at one end to a diameter of 1 mm., and the face polished. A series of lines was then engraved on the face, using a special steel tool which had a very fine point. Many techniques were tried in order to improve the quality of the scratches; the best

method was to place the screw in a holder and draw the tool, which was held in the stationary head of a small milling machine, slowly across the surface. This operation was repeated a number of times in order to clean out the grooves. The depth and separation of the scratches could be varied and it was found that the separation could be made as small as 10 microns. The screw length was 5 mm. which meant that when in the microscope, the object did not project too far into the field and also ensured convenient handling.

The object was screwed into a brass holder which was supported by a cylindrical ebonite plug. The latter was pushed into a stainless steel pot containing an emanating source of radiothorium. This consisted of a precipitate of ferric hydroxide containing the radiothorium which gave rise to thoron gas. A high potential was applied to the object through the brass holder so that the charged ThA atoms were attracted to it. Most of the activity formed on the face of the screw and very little in the grooves, so that the object constituted a known pattern of activity. A rubber disc was slipped over the stem of the screw to prevent accumulation of activity on other parts of the screw, which would fog the final image.

It was very important that the activity on the

face should be uniformly distributed and in this respect the method of collection gave considerable trouble. When a new plug was employed the activity tended to collect on the rim, but after some use the active deposit formed on a small area in the centre of the object. Examples of this effect, are shown in Plates V(a) and V(b). Many attempts were made to standardise collection. These included the use of an earthed plate on the face of the ebonite, but this merely impeded collection. Plugs made of polystyrene, polythene, tufnol, perspex and micalex were tried with poor results. During exposure a conducting layer was formed on the face of the plug and this may have disturbed the collecting field. Evidence of an electric wind effect was observed in some of the distributions. The best results were obtained when the ebonite face was some distance (about ½ in.) from the screw head. A positive or negative potential could be applied to the object. Sometimes the former gave more efficient collection, sometimes the latter. It was found that the efficiency of collection was independent of the magnitude of the applied voltage. Despite the improvement mentioned above, good distribution on the object has always been largely a matter of chance. The radiothorium was dried out

periodically in order to maintain its emanating power.

2. Focusing.

The field strength necessary for focusing a particular electron energy could not be calculated exactly. Approximate values of the field were estimated and using the method described previously, the strength of the magnets was adjusted accordingly and a suitable baffle was set in position. A small sheet of aluminium was placed between the object and the photographic film, and in contact with the film. The thickness of the aluminium (in mgm. per $cm.^2$), chosen from the range-energy curves of Katz and Penfold[27], was just sufficient to absorb completely the electrons of the line to be focused. Two exposures were then taken, at minimum and maximum separation of the upper field gap. If after development there was no image on the film, the field was too weak, but the presence of an image indicated that the energy of the focused electrons was greater than that of the line and the field was too strong. Adjusting the field strength and repeating the exposures eventually gave an image with the largest gap, but no image at the minimum setting.

Fine focusing could then be achieved by removing the aluminium foil and studying the clarity of the pattern in the image at different settings. Since the action of the microscope is similar to a β -ray spectrometer, when the line is just out of focus, a ring appears around the image formed by electrons selected from the continuum. The change in diameter of this ring with change in gap width is another aid in fine focusing. The sensitivity of the focusing control was such that a change in the gap of 0.03 cm. from the true forms gave a slight blurring of the image.

3. Baffle Adjustments.

Before remagnetisation, experiments were carried out to find the largest aperture that could be used without affecting the resolution of the lens. Using the annular hole baffle system the maximum solid angle of collection was 0.01% of 4π . The variation of the quality of the image was also studied for different settings of the baffle along the lens axis. It was found that the best position was at the edge of the field nearer the image. The setting was not critical, however, and the baffle could be moved over a range of 1 cm. without deterioration of the image.

The effect of moving the centre stop was also examined. When the stop had been removed, the pattern of the image was still visible, but a dark spot showing no structure and having about the same size as the object, was superimposed on the image. It had previously been thought that this was due to alpha-rays, but simple tests showed that the spot was due to low energy electrons. A 200 micron thick nuclear emulsion was used for recording, and the image was studied under a microscope, using high power, when the spot was observed to be composed mainly of short electron tracks. Also it was possible to deflect the spot by the field of a small magnet placed inside the camera and near the axis. Absorption experiments showed that the energy of the electrons was less than 25 keV.

This central spot was used in aligning the source along the lens axis. The object was considered to be in the correct position when the spot was in the centre of the image.

4. Recording the Image.

To obtain a satisfactory record of the image, the photographic material used must satisfy the following requirements: low background fog, high contrast, fine grain, and high sensitivity. The last is extremely important because the electron beam falling on the plate is of low intensity. For test purposes it was convenient to use X-ray film, since the development time was short. The three types used were Kodirex, Ilfex, and Ilford Industrial G. These are high contrast films and are relatively fast, but they are not entirely suitable for permanent records as some fading of the image over a long time has been observed. Electron sensitive nuclear emulsions do not suffer from this disadvantage and exhibit high sensitivity and fine grain. Ilford G5 plates with emulsion thickness of 50 microns have been used extensively. Although there is some scattering in the emulsion, the resolution is better than with the coarse grained X-ray films. The G5 emulsion quickly gathers cosmic ray and other background, so fresh plates were always used.

Using the F line of ThB, for a given source strength the exposure times necessary to produce satisfactory blackening of G5 emulsion, Industrial G,

Ilfex, and Kodirex were 4 : 6 : 9 : 12. The sensitivity of the G5 emulsion varied with electron energy and there was less blackening for low energy electrons.

5. Magnification.

The magnification of the lens system was deduced directly from the diameter of image and object. Since the object was usually in a fixed position the magnification of the image depended on the position of the plate and the width of the lens field. The principal planes of the lens system were crossed so the magnification was larger for small gap widths. The greatest magnification that could be obtained with the new lens field was 7.5x.

B. Resolution Tests.

1. Introduction.

The resolving power of the lens system is determined by the values of the chromatic and spherical errors. Any improvement in the resolution of the image, produced by changing the magnetic field shape, will be due to a reduction in the spherical error. To check the performance of the instrument either a method of measuring the spherical aberration, or a means of estimating the resolution, had to be devised. The former proved impracticable but a method of comparing the resolution of different micrographs has been developed.

2. Investigation of Spherical Aberration.

The measurement of spherical aberration in electron optics usually involves some variation of the "pepperpot" method, in which the separation of the marginal and paraxial focal points of an originally parallel beam is measured. The success of such a method depends on the value of the separation to be measured. Since the microscope lens system had a small aperture and low magnification it was thought that the method could not be applied. To

check this a pepperpot disc was made. This was of thin brass and in the form of a cylinder open at one end so that it could be pushed down into the lens. The cylinder served to stop the disc from slipping and to keep it perpendicular to the lens axis. Holes $^{8}/_{1000}$ in. in diameter were drilled in the disc at distances 0.35 cm. and 0.85 cm. from the centre. The source of electrons was the end of a fine brass wire activated with ThB. A long exposure was taken on a G 5 emulsion but no separation of the images was observed and no displacement could be detected by microphotometer tracing.

3. Discussion of Possible Methods.

One method for checking resolution is to use a test object possessing fine structure with a separation ranging from 1 to 10 microns, and determining how much of the structure can be resolved in the image. Satisfactory objects with lines separated by less than 10 microns could not be made in the workshop. Also in activating these objects some activity was deposited on the sides of the grooves so that there was no sharp cut off of activity. Hence the lines in the image would merge before minimum resolution (measured in terms of the separation of the lines

in the object) had been reached. A grid with a suitably fine mesh would be an ideal test object. However, grids with such a fine pattern could not be obtained. Those used as specimen supports in transmission electron microscopes were the best available but these were made of copper strips, of width 40 microns, with a separation of 50 microns.

The possibility of using naturally occurring specimens was considered but no suitable objects could be found. In particular, the use of diatom skeletons as test objects was investigated without success. This will be described in more detail in the next chapter. Attempts to activate small fragments of brass and lead filings deposited on the face of a screw also failed.

A resolution test due to Stevens[28] is often used in contact autoradiography. A test chart is reduced photographically on to a Maximum Resolution plate and the silver image reconverted into silver halide, which is then converted to radioactive iodide using I^{131}. This attractive method can not be employed in checking the resolution of the emission microscope, because the amount of I^{131} taken up by the chart image is not great enough to give blackening of the recording plate.

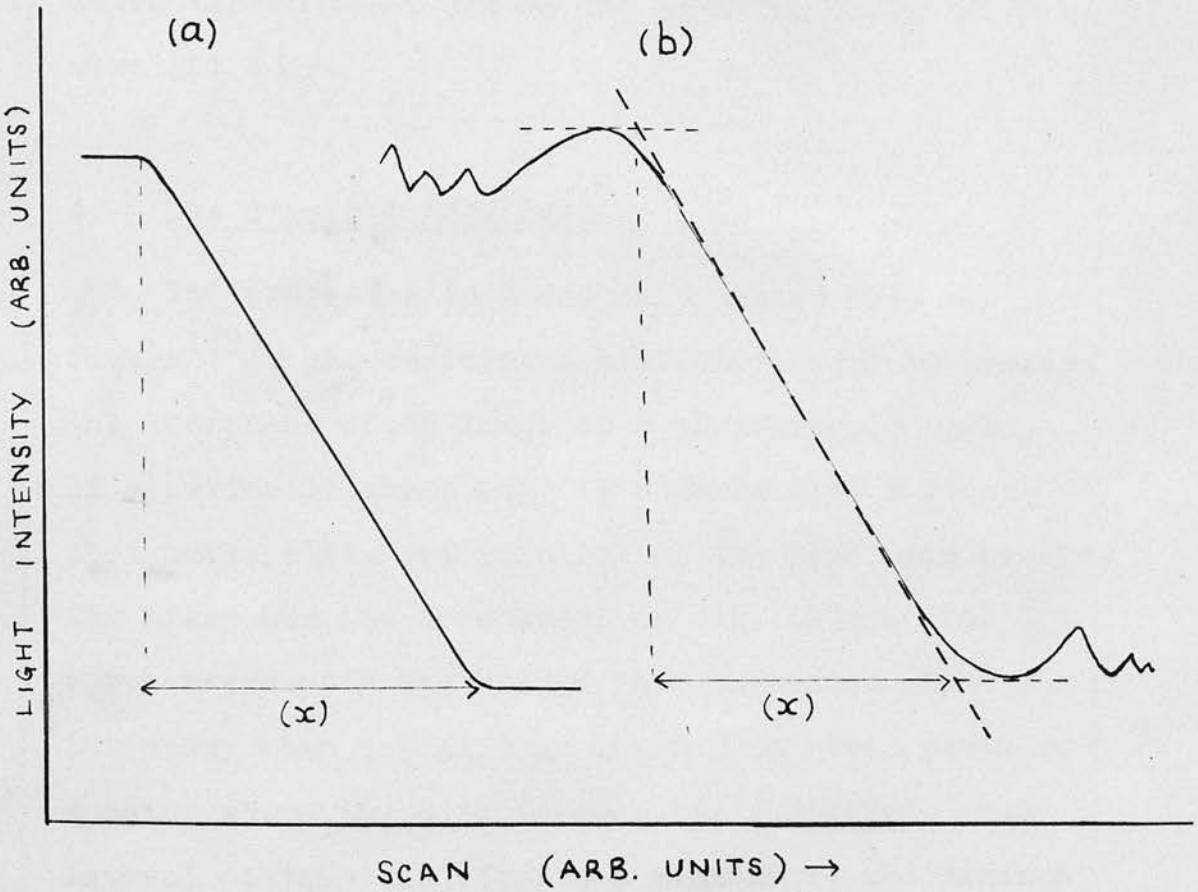

FIG. 17.

Microphotometer Traces Across Image of Sharp Edge (theoretical).

In view of the difficulties mentioned above, a method called "the straight edge test" was developed. In this test the resolution of different images was compared from information obtained from microphotometer traces taken across the electron image of a straight edge.

4. The Straight Edge Test.

The procedure is based on a method used by Tugman[29], who employed a microphotometer to measure the sharpness of an image on a photographic plate. If a perfectly sharp edge is scanned with a microphotometer slit, set parallel to the edge, the resulting trace has the form shown in Fig. 17(a). The curve represents the change in transmitted light intensity when the slit is moved from clear plate to a point where the slit is completely covered. The lateral distance (x) from the maximum to the minimum depends on the width of the slit (d) and the ratio of the speed of the recording film (v_F) to the speed of the scanning slit (v_S). The exact relationship is:

$$x = d \times \frac{v_F}{v_S}$$

The value of the vertical displacement depends only on

the density of blackening and is independent of the sharpness of the image.

If an object possessing a sharp edge is activated and the electron optical image scanned, the value of (x) obtained depends on three factors viz. the sharpness of the edge in the object, the broadening of the edge in the image due to aberrations of the lens system, and the transmission characteristics of the slit. If the object is perfectly sharp and the slit width kept constant, the value of (x) can be used to compare the resolution of the lens system under different operating conditions. If the slit behaves as a true rectangle, the increase (δx) in (x) can also be used for different slit widths. Both quantities can be translated to a size in the object by dividing by the magnification (M). It should be emphasised that the values obtained are only functions of the resolution, and can be used as a measure, but not as an absolute determination of the resolution in an image. The quantity $\delta x/M$ has very little physical significance; in the present work it is denoted by (q).

The trace obtained in practice resembles Fig. 17(b). The graininess of the plate affects the smoothness of the curve, and there may be some doubt in selecting

the correct distance (x). To overcome this uncertainty the following criterion was adopted. The straight line portion of the curve was extended to cut the ordinates of the maximum and minimum. The interval between these two points, in the x-direction, was the required distance.

5. Preparation of Test Objects.

To ensure the presence of a sharp edge in the image there must be a sharp cut off in the activity on the object. It was decided that the best way to achieve this was to activate an object that possessed such an edge, so that there would be no activity on one side and maximum activity on the other. It was important that the edge used in the object should be sharp, since any irregularities would appear in the image and produce errors in the microphotometer trace. Most objects that possess sharp edges are made of steel or some other magnetic material which would disturb the microscope field. So the usual brass test object was modified as follows.

After polishing, the screw was clamped firmly in a holder (see Fig. 18). A steel tool was made with its cutting edge shaped as shown in the fig., and sloped away towards the rear to prevent irregular

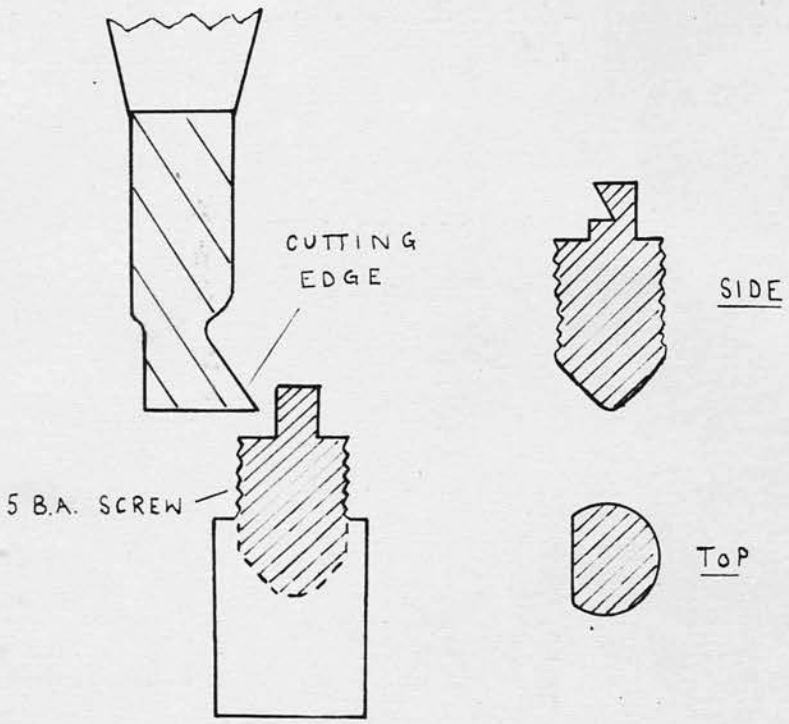

FIG. 18.

Preparation of Straight Edge.

cutting. The tool was lowered until it was 2 mm. below the face of the screw and in contact with the stem. It was drawn slowly forward, then moved laterally $\frac{1}{1000}$ in., and the operation repeated. This was continued until enough brass had been cut away to form an edge about 0.7 mm. in length. A small lip was left on the edge, but this was removed by polishing without destroying the sharpness of the edge. Objects prepared in this way were studied under a microscope and it was found that parts of the edge were so sharp that no irregularities could be detected. The selected test object was activated in the radio-thorium pot.

6. Experimental Procedure.

With the source in position and the field set to focus the F line, a set of exposures was taken with 50 microns thick G 5 emulsions. The exposure times were varied from 10 to 60 min. so that images of different densities of blackening could be examined. During processing of the plates a certain amount of surface stain appeared on the emulsion. This was removed either by rubbing the surface gently with the finger after development, or using a lens tissue soaked in methyl alcohol after the plates had dried.

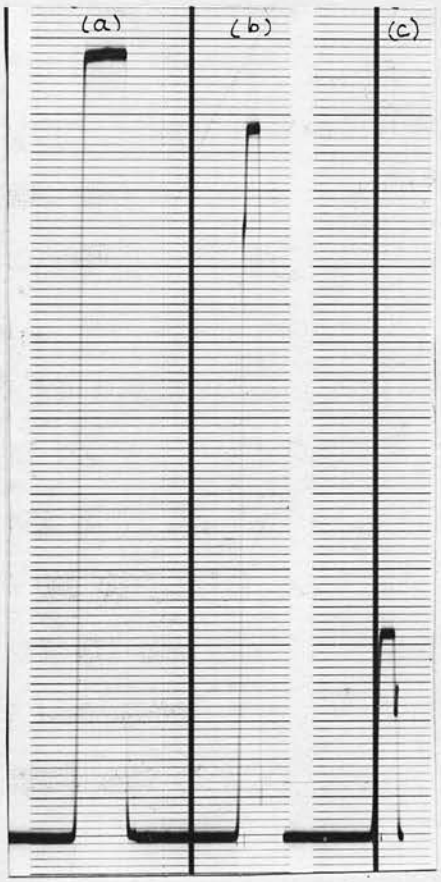

Fig. 19.

Microphotometer Traces of Razor Edge.

(Self Recording Instrument)

Slit Widths:

(a) 15 microns

(b) 10 microns

(c) 5 microns

Great care was taken to ensure that the top surface of the image was not damaged.

Two microphotometers were used in the analysis of the plates. The first was a Kipp microphotometer* with automatic recording. In this instrument the plate moved continuously across the slit and the motor controlling the motion of the plate was locked to that driving the recording drum, so that the speed ratio remained constant. Fig. (19) is a photograph of the trace obtained when a slit of width 5, 10, and 15 microns was moved across the edge of a new razor blade. A serious disadvantage of the instrument was that the maximum speed ratio that could be used was 50 : 1. This gave rise to large errors in the measurement of $(x\acute{})$. For this reason, use of the Kipp instrument was discontinued in favour of a Hilger and Watts non recording microphotometer which was subsequently available at the Department of Natural Philosophy.

Greater accuracy was possible with the Hilger and Watts instrument since the fine control, governing the motion of the plate, could be read to 1 micron. Fig. 20(a) shows a trace across a razor edge. The value of (x) agreed with the value for the

* The writer wishes to thank Professor Greaves and members of the staff of the Royal Observatory, Edinburgh, for the use of this instrument.

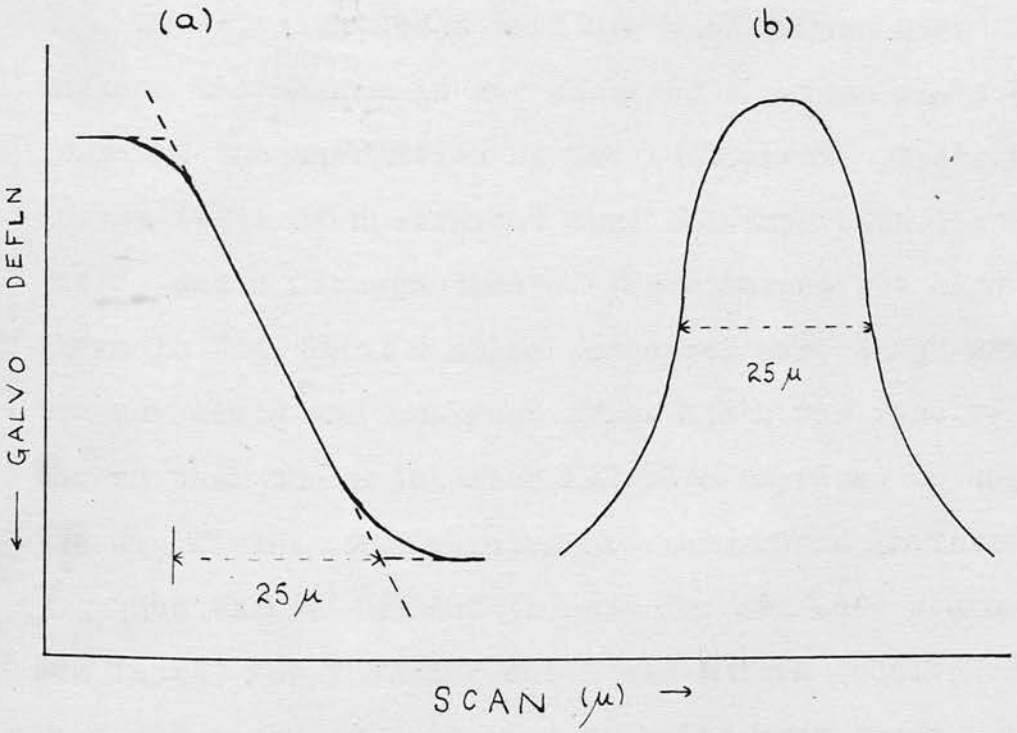

FIG. 20.

Microphotometer Slit Width Measurements.

slit width, measured by the width at half height of the trace in Fig. 20(b). The latter was obtained when the slit was moved across a fine line in a microscope test graticule. This result, and the shape of Fig. 20(a), supported the assumption that the slit could be regarded as rectangular. In addition it was found that, for a given plate, the value of (δx) was unchanged for different values of the slit width.

The straight edge test was used to discover whether the change in the shape of the lens field had improved the resolution of the instrument. Plate VI is the image of a straight edge obtained with the old field, and a microphotometer trace across the edge is shown in Fig. 21(a). Similar exposures were taken with the new field and analysed (Fig. 21(b)). The results showed that the resolution had been improved by using the dip field. The results are summarised in Table 1.

The values (a) and (b) are for the same source but in (b) the focusing wheel was ¼ turn (equivalent to a gap width of 0.03 cm.) from the true focus position. The distance (x) could be measured to ± 1 micron. The smallest value of (δx) obtained throughout the experiments is given in (c).

Fig. 22 is a Kipp microphotometer trace equivalent to (c). The value of x is approximately

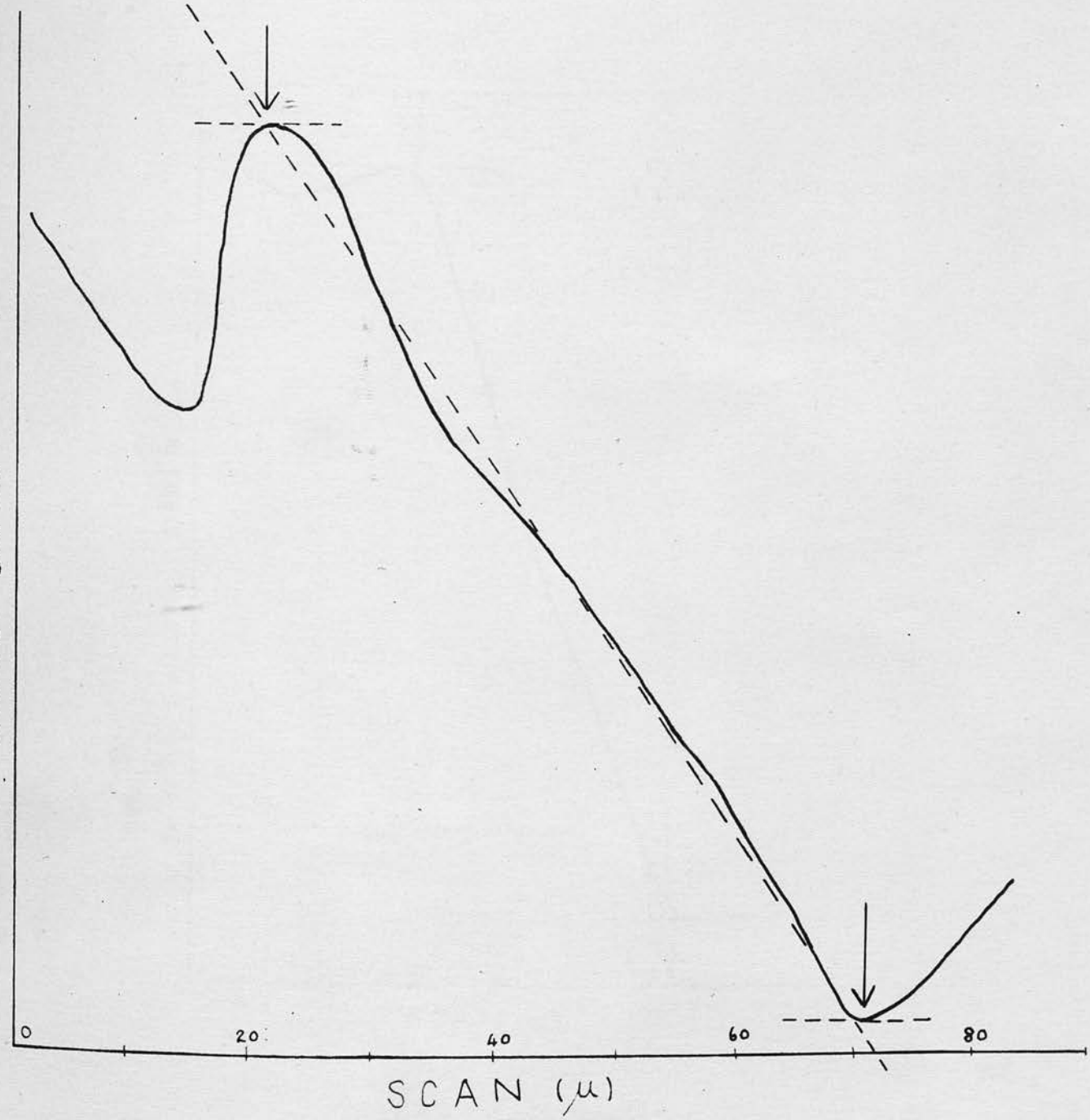

FIG. 21(a).

Microphotometer Trace across Image of Sharp Edge (Old Field).

x = 50 microns.

TABLE (1).

	Slit Width (μ)	x (μ)	δx (μ)	M	q (μ)
Old field	12	50	38	7	5.5
New field (a)	12	22	10	6	1.7
(b)	12	26	14	6	2.7
(c)	20	28	8	6	1.3

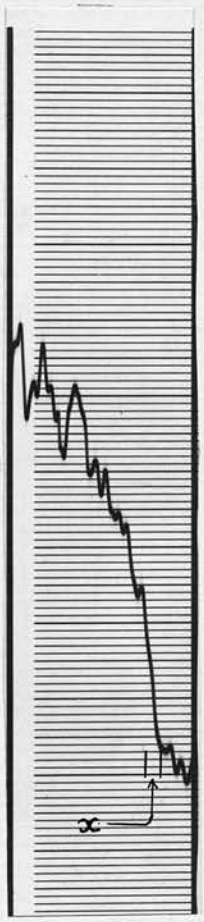

Fig. 22.

Microphotometer Trace across Image of Sharp Edge.
(Self Recording Instrument).

2 mm. which corresponds to q = 3.3 microns.

After this test had been developed, it was found that a similar resolution check had been recommended by Kinsinger et al.[30] in the Report of the Electron Microscope Society of America's Committee on Resolution.

7. Variation of the Size of the Aperture.

The tests had shown that the new lens field had improved the resolution obtained with the lens system so experiments were performed to determine the effect on the image of opening up the aperture. A set of baffles was made, with diameters ranging from the original value of 7.32 mm. to 11 mm., and each baffle was tested in the lens. It was found that good resolution was preserved until the collecting power was 0.02% of 4π (i.e. twice the original collecting power), which corresponded to a baffle diameter of 8.3 mm. Plates VII are a set of exposures taken with baffles of different diameter. The lines in the object had a separation of 15 microns and it was seen that, for detail of this size, the pattern was preserved even when the diameter of the aperture was 8.76 mm. (2.5 x original collecting power). The plates were slightly over exposed and have not made good prints.

8. Transmission Resolution.

A further check on the resolution of the instrument was made by studying the image of fine particles formed when a specimen was placed in the path of monokinetic electrons. Th. B was deposited on the flat face of a screw which then acted as a source of F line electrons. The specimen to be examined was suspended on collodion film and placed almost in contact with the activated face of the screw. The film was very thin and did not affect the transmitted electrons in any way. This was verified by the fact that the image of a fine pattern showed no deterioration when the film alone was interposed between object and image. The film was prepared by placing a drop of a 2% solution of collodion in amyl acetate on water. After a short time the film which floated on the water surface was picked up on a wire frame and transferred to the specimen support. The support consisted of a brass cylinder 0.3 cm. in length. The top of the cylinder had a small lip, to which fine copper wires were soldered to give added support to the specimen.

Various fine powders, such as bismuth oxide, were tried as specimens but these were not dense enough to absorb the F line electrons and give sufficient

contrast in the image. (Since the magnification is small, differential scattering of the electrons is less important than in normal transmission electron microscopes). Eventually fine lead filings were sprinkled on the collodion film and these produced good "shadow" images. (see Plates VIII and IX). The specimen was then studied under a light microscope and the separation of the lead chips measured. It was found that particles separated by 2¼ microns had been resolved in Plate VIII. (see Fig. (23)). This gave an upper value for the resolution of the lens system. When the microscope is used in this manner, there is some scattering and absorption of the electrons at the particle edges, so it is probable that the resolution obtained by emission methods is better than the above value.

9. An Estimate of the Resolution.

The evidence from the transmission test indicates that a resolution better than 2¼ microns is attainable with the emission microscope. The straight edge test does not give an absolute measure of the resolution but, making certain assumptions, it is possible to arrive at an approximate value. Hillier[31] has used the half width of the contour in the image of a sharp

edge, taken from external maximum to internal minimum, to obtain a value for the resolution of an image of polystyrene latex particles. No account is given of a correction made for the microphotometer slit width although the width of the contour (approximately 22 microns) is of the same order of magnitude as the slit width.

The previous experiments have shown that the value (δx), for the same place in a given image, is the same for different slit widths and that the slit may be regarded as truly rectangular. Thus the value (δx) may be regarded as a measure of the sharpness of the image and the quantity (q) corresponds to the contour width used by Hillier. If irregularities in the edge in the object can be neglected the value $q/2$ can be used as a quantity indicating the resolution possible with the instrument. This gives a value of 0.9 microns for the resolution corresponding to Table 1(a) and 0.7 microns for the best resolution attained in the course of the experiments.

It should be pointed out that the measurement of the resolution obtained with any electron microscope cannot be made with any degree of certainty. When measured in terms of the sharpness of the image, it may vary over different parts of the image depending

on the type of detail and to some extent on the contrast conditions. Under normal working conditions it is probable that the resolution limit of the emission microscope is about one micron.

10. Examples of Electron-Micrographs.

The plates described below are examples of the type of micrograph obtained with the emission microscope, using various kinds of objects and recording film.

Plates X, XI, XV, XVI, XVII and XVIII were obtained using objects prepared by the engraving technique described on page 39. Plates X and XI exhibit patterns of parallel lines; the separation in the former is large but in the latter it varies from 12 to 60 microns. Plates XV and XVI have coarse and fine patterns of crossed lines respectively. The inclination of the lines is 45°. Plates XVII and XVIII show lines inclined at 90°. The same object was used in this case but the image was recorded on G 5 emulsion (XVIII) and X-ray film for comparison. For the same exposure the G 5 emulsion gave more blackening and a sharper image. Plate V(c) has some lines separated by 10 microns and is a further example of the poor distribution of activity obtained with the radiothorium pot.

Plate XII is a micrograph of an electron microscope grid. The grid which was 3 mm. in diameter was kept in close contact with the face of a brass pin by means of an ebonite cap, and exposed to the radiothorium. In this way it was possible to deposit Th B on only one side of the grid. The activated grid was placed in a special holder (to be described in the next chapter), in the microscope and a small circular mask, with a one mm. hole in the centre, was used to limit the size of the object and thus cut down the general background. An image of the same grid was obtained by transmission (Plate XIII). It can be seen that this image is not as sharp as the one obtained by self emission and the background is more intense. This is due to increased chromatic aberration caused by the electrons which pass through the grid itself.

An attempt was made to produce a sharp cut off in activity on a brass screw head by covering part of the face with fine wires. The wires were removed after activation and a micrograph of the face taken. The result (Plate XIV) was poor as the line of no activity was too broad and the edge was not sharp.

CHAPTER IV.

APPLICATIONS OF THE INSTRUMENT.

A. EXPERIMENTS WITH DIATOMS.

1. Introduction.

The silica skeletons of diatoms exhibit a highly regular fine structure and are often used as test objects in light microscopes. There are many varieties of these algae and their varied configurations cover a large range of distances. In particular the diatom Pleurosigma angulatum has a fine structure with distances of separation varying from 0.1 to 5 microns. Since this range of separations represented the limit of resolution of the emission microscope, an attempt was made to impregnate these diatoms with radioactivity and study them in the microscope.

The siliceous shells of diatoms normally consist of two layers with a series of chambers between them which open both inwards and outwards. The holes are very small and often have complicated shapes. There is considerable controversy about the composition of the diatom frustule, particularly that of Pleurosigma angulatum (e.g. Hamly and Watson[32]). It has been suggested that the observed pattern of the

~~of the~~ valve could be due to a number of causes viz. projecting points, small cavities, large holes, depressions of the surface, or thickenings in the silica.

It was hoped that the activity would be taken up in such a way that the regular pattern would be visible in the image. In addition to the usefulness of the diatoms as resolution test objects the results of the experiments would give valuable information regarding the uptake of radioactivity in a specimen by chemical action.

2. Experimental Technique.

A stock of diatoms was obtained and studied under a light microscope when the Pleurosigma angulatum variety was easily identified. Each specimen was about 200 microns in length, with a fine structure separation of 0.7 to 1.2 microns. It was found that the diatoms did not take up enough activity when exposed to the radiothorium directly; also it was impossible to obtain an image by transmission methods.

ThB was collected on a clean platinum foil and the activity dissolved off with concentrated hydrochloric acid in a crucible. The latter was a hemispherical cavity scooped out of a block of polystyrene.

This was used to prevent activity sticking to the walls of the container. The diatoms, contained in distilled water, were added and the liquid evaporated off. The diatoms were collected in a small volume of distilled water and placed on a flat screw head. The water was evaporated under an infra-red lamp and the activated diatoms remained on the screw face. The image obtained from this source showed that the activity had spread over the face of the screw and had not been confined to the diatoms.

To overcome this difficulty the following micro-technique was developed. The activated diatoms were deposited on a glass slide and observed under a low power microscope. Single diatoms were then picked up on the end of a sharp needle and deposited on the face of the holder, the whole operation being carried out under a microscope. The activity of the diatoms was very low and no image was obtained. The uptake of activity was improved when the solution containing the diatoms was saturated with hydrogen sulphide before adding to the active solution. It is probable that the di-sulphide decomposed to form gelatinous silica which increased the adsorption of ThB. The evaporation was carried out in a small flat bottomed container, made by shaping out a cavity in heated glass with a

steel wire. This confined the activity to a small area and facilitated manipulation under the microscope. Diatoms selected after this procedure exhibited much greater activity and produced some blackening of the plate. Many attempts were made to increase the activity, but the results were poor and the experiments abandoned as impracticable.

The best image obtained (after a 40 hour exposure) is shown in plate XIX. Two diatoms are visible; the oval shaped one is Surirella gemma and the other Pleurosigma angulatum. The former variety had a line separation of 2 to 5 microns and was very suitable for the tests due to the robust nature of the specimen. No structure is visible in the image. This is probably due to the fact that the adsorption of activity was not uniform, or it might indicate the presence of a continuous unperforated shell.

B. Experiments with Radioiodine.

1. Introduction.

Autoradiography has often been employed in the study of metal surfaces. A particular example is the investigation of friction and lubrication in which the autoradiographic technique is used to detect

fragments of metal transferred when one metal slides over another. The method used is to impregnate either the slide or the surface with a radioactive tracer, the autoradiograph being taken after the sliding experiment (e.g. Gregory[33]). This could be done with ThB but it was decided to use some other isotope with the microscope and other methods of source preparation.

Rabinowicz[34] has described a method which uses the different chemical reactivities of various metals towards a radioactive substance, which in his case was radioiodine. The published autoradiograph showed poor resolution and it was thought that better results could be obtained with the emission microscope.

Radioactive iodine has been used extensively in biological investigations and medical tracer experiments. The isotope $_{53}I^{131}$ has a convenient half value period of 8.1 days and its 80 keV γ-ray is internally converted in the K-shell, giving rise to an electron line of energy 45.42 keV. From data given by Kern, Mitchell and Zaffrano[35] the number of K-electrons per 100 disintegrations can be found. The value is 2.7 per 100 disintegrations but there is considerable disagreement about the magnitude of the conversion coefficients and γ-ray intensities. The above

properties indicate that I^{131} is suitable for use in the emission microscope.

The experiments described below did not give a positive result but the procedure has been described in some detail since the experiment illustrates some of the difficulties encountered in the operation of the instrument.

2. Design of Source Holder.

The magnetic field strength was altered to give an approximate focus for the 45 keV electrons. This was done in the usual way. A source for fine focusing was then prepared. Rabinowicz reported that copper reacted strongly with iodine so it was decided to use an electron microscope grid as a test object. A new source holder was designed to accommodate the grid. The holder itself was similar to that described on page 8 and the slide was made to fit into a $\frac{1}{32}$ in. deep groove in the holder. The slide dimensions were: thickness ¼ in., length 1¼ in., breadth ½ in. A brass cup shaped as shown in Fig. (24) was made to fit into a hole in the slide. The slide could be locked in any position by means of two screws on either side of the cup. The grid rested on a $\frac{1}{16}$ in. recess at the bottom of the cup.

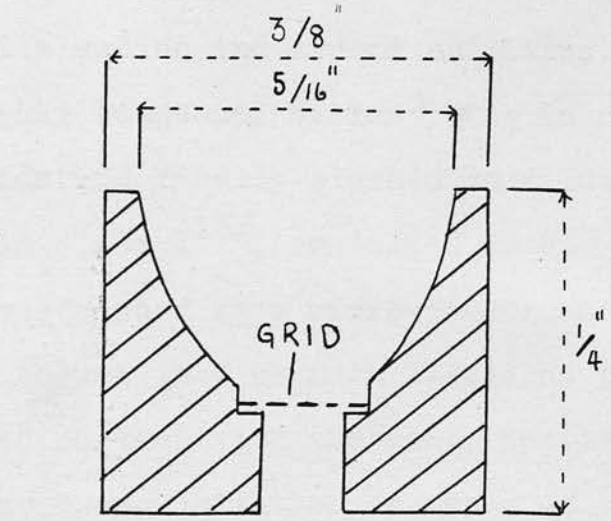

CUP

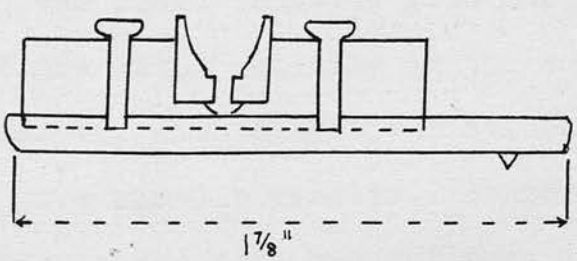

HOLDER & SLIDE

FIG. 24.

Source Holder, Slide and Cup.

3. Activation of Copper Grids.

A 2 mc. source of carrier free I^{131} was obtained from Harwell in the chemical form of iodide together with a little sodium and sodium sulphate. The grid was thoroughly degreased by immersing in carbon tetrachloride and finally cleaned in dilute hydrochloric acid. The I^{131}, contained in 0.2 ml. of solution, was placed in a micro-beaker and the grid added. To ensure that as much liquid as possible was brought into contact with the grid, the liquid was kept in continuous agitation by means of a mechanical shaker.

After 10 hours' exposure to the radioactive solution it was found that the grid had taken up about 5% of the total activity in the solution. Further attempts, with slight variations in the chemistry, gave similar results. Evaporation of the I^{131} solution on the grid brought down a thick layer of impurities. Blackening of a plate was obtained from these sources but the exposure time was too long to enable adjustments of the field to be made.

4. Activation of Silver Grids.

The Radiochemical Centre, Amersham, recommended that a greater uptake of activity might be obtained if silver or silver plated grids were used. Some electron microscope grids were silver plated and immersed in 0.3 ml. (5 mc.) of iodine solution which had been acidified to 1N with hydrochloric acid. After two hours it was found that nearly half the activity of the solution had been taken up by the grid.

Focusing experiments were carried out with this source but it was impossible to obtain a clear image of the grid although absorption tests showed that the in-focus position had been reached. The quality of the image showed little change when the field strength was varied. It was thought that this effect might be due to self absorption in the silver coating so new grids were plated with a very thin layer of silver. This gave no improvement in the image. The grids were examined in the spectrometer used by Kyles et al.[36] and the β-spectrum plotted. It was found that the 45.42 keV line was quite broad and the peak to continuum ratio was much smaller than the expected value.

It was concluded that the poor image produced was

due to the fact that activity on the back of the grid gave rise to electrons which passed through the grid and produced a high background fog. Examination of the β-spectrum of I^{131} (see ref. 35) confirms this. The I^{131} spectrum has an end point of approximately 600 keV and a large percentage of the electrons emitted have energies in the range 100-400 keV. The grid (approximately 0.01 mm. thick) absorbs electrons up to 70 keV only, so that the transmitted electrons increase the intensity of the continuum considerably and reduce the value of the ratio of the peak to the surrounding continuum. The F and A lines of ThB (Flammersfeld[37]) have a much greater intensity and, under similar conditions, ThB sources would not suffer as much from this disadvantage.

Attempts were made to remove the activity from one side of the source by floating the grid on nitric acid. 5N acid was required to remove any activity and this damaged the grid. Since the uptake of activity was much greater for silver than for copper, only one side of the grid was plated. The other side was covered with a film of polystyrene. This was done by floating the grid on the surface of a solution of polystyrene in benzene. Surface tension prevented the upper side from coming into contact with the liquid.

The grid was removed by means of a small wire scoop and left for the benzene to evaporate off. The grid was then put in the plating bath for ½ min.; on removal it was found that only one side had been plated.

A grid prepared in this way was impregnated with I^{131} by floating it, silver side down, on the surface of a solution containing 5 mc. of the isotope. After 3 hours the grid was taken out of the solution and the film removed with benzene solvent. Much better results were obtained with this source. Rearrangement of the field and focusing was continued. After some time had elapsed it was decided to make another source since the exposure time in the focusing tests was quite long. At this stage the best image of the grid obtained showed that the grid was almost in focus. This image can be seen in plate XX. The patches of no activity correspond to unsilvered parts of the grid.

A fresh source of I^{131} solution was obtained from Amersham but only minute quantities of activity could be deposited on a grid under exactly the same conditions as before. Other sources gave the same, poor result. Silvered grids were sent to Amersham for activation. No improvement in the uptake of

activity was achieved, and no explanation could be offered for the sudden change in reactivity of the iodine. Thus it was impossible to continue with the focusing experiments.

5. Sliding Experiment.

It had been found that aluminium reacted less strongly with the iodine than copper and silver, and it was decided to use this as the sliding surface. The slide consisted of a hemispherically ended rod. In principle, if the iodine was applied to the friction track, the silver wear fragments would take up much more activity than the aluminium and would show up in the electron-micrograph. Sliding experiments were performed with slides made of copper, lead and silver on aluminium discs. The latter were then placed in the I^{131} solution and after removal placed in the microscope. Exposures of 5 days gave no trace of blackening on the recording plate although contact autoradiographs showed the activity distribution (plate XXI).

It is believed that the experiments would have been successful if the later supplies of I^{131} had possessed the same properties as those with which the

earlier tests had been performed. Although considerable time was spent on these experiments no conclusive results were obtained.

C. INVESTIGATION OF A DEFORMED STATE BY RADIOACTIVE ISOTOPES : A PRELIMINARY STUDY.

1. General.

In the experimental investigation of a specimen under plastic deformation, one method used is to study the change in shape of a network of mutually perpendicular lines, or circles, marked on the surface of a body; e.g. in the process of deformation the circles become ellipses. A disadvantage of this method is that the network can be drawn only on the surface of the specimen (or plane of symmetry when cut along that plane), so that it is impossible to study the deformation at a given place inside the body. Also the pattern may be erased during the experiment.

Gubkin and Dovnar[38] have described a method which employs a radioactive network within the metal. Wires of the metal are coated with a thin layer of radioisotope and inserted in holes drilled in the specimen. The wires weld into the specimen on heating

and macroscopic deformation can be observed by auto-radiography of sections. Dr. A.F. Brown, of this Department, has considered the possibility of using this method for the detection of coarse slip. Preliminary experiments were carried out by the writer to determine if the emission microscope could be used in the project.

2. Experiments with Aluminium Wire.

Thick aluminium wire was drawn out to a diameter of approximately 1 mm. A small aluminium holder (see Fig. (25)) was made which fitted into the brass cup (Fig. (24)) of the source holder. A hole was made through the centre of the aluminium holder so that the wire could be drawn through it. The correct diameter of wire was chosen to give a tight fit in the hole.

The wire was exposed to radiothorium emanation. A small rubber washer was slipped over the wire to confine the activity to the end of the wire (exposed length about 2 mm.). After removal from the radio-thorium pot the end of the wire was cut off (at a point 1 mm. from the end) with a sharp razor blade. If the ThB had deposited uniformly over the wire an end view of the wire should show a ring of activity

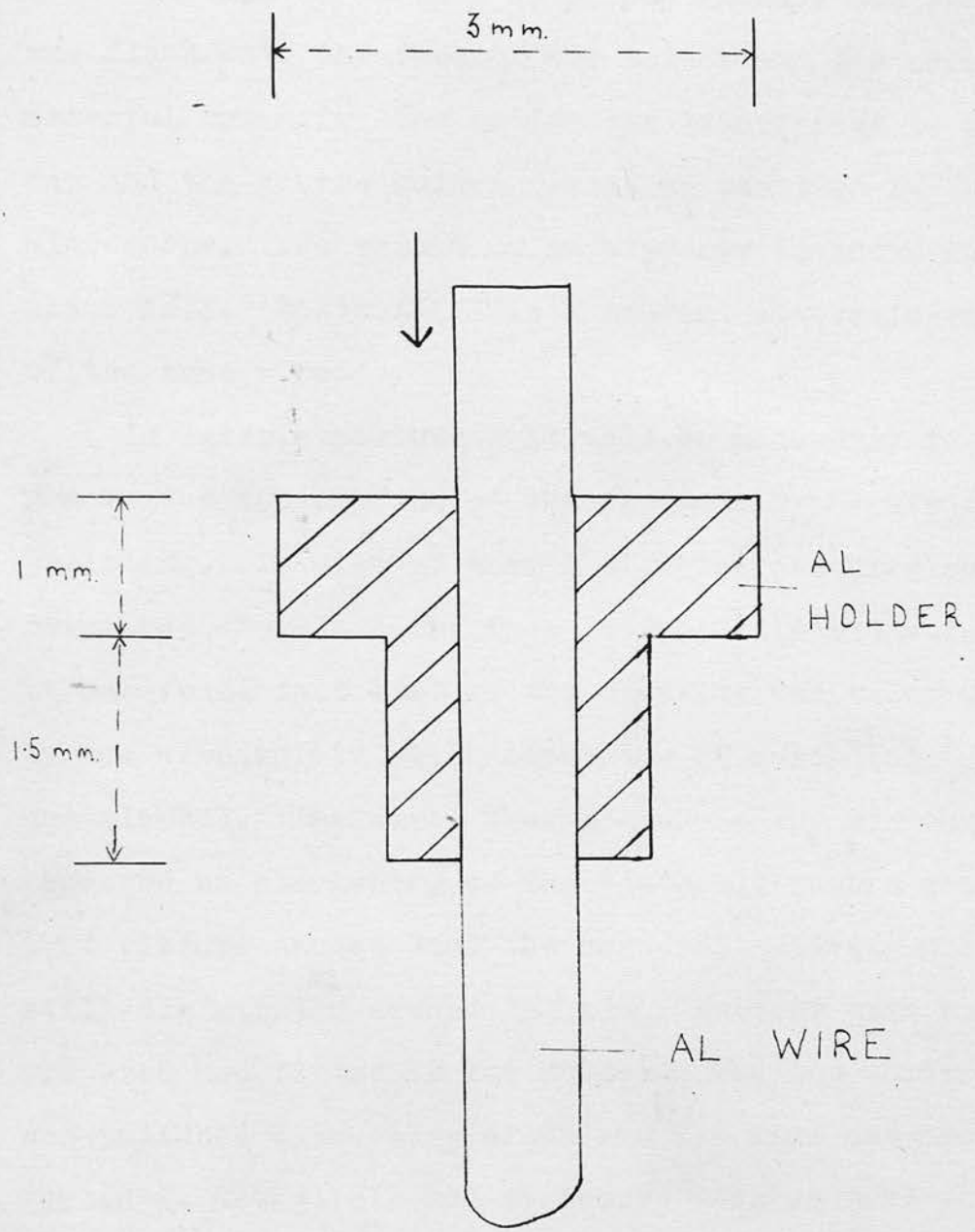

FIG. 25.

Holder for Aluminium Wire Experiments.

around the perimeter of the face. The wire was drawn through the holder until the freshly cut end was flush with the face of the holder and the surplus material cut off. The holder was transferred to the cup and the source holder placed in position in the microscope. The result of an exposure is shown in plate XXII. Plate XXIII is a contact autoradiograph of the same wire.

In later experiments it will be necessary to remove the top surface of the specimen by electrolytic polishing. In view of this a wire was prepared as described above and the face polished electrolytically. It was found that most of the activity was taken up by the electrolyte which consisted of perchloric acid and alcohol. The wire, when placed in the microscope, produced no blackening of the plate although a contact picture showed that the residual activity was still distributed around the rim. Another wire was prepared and fitted in the holder. The top surface was polished with emery cloth and the wire and holder rinsed in methyl alcohol to remove surplus activity. This time most of the activity remained on the wire and a ten hour exposure in the microscope gave the picture shown by plate XXIV. This can be compared with the contact autoradiograph of the same wire after polishing, illustrated by plate XXV.

3. Conclusions.

Although refined methods were not used in the contact autoradiography, comparison of the contact and electron optical photographs indicates that the latter gives a better quality image with less fogging, due to the selection of one electron energy by the lens system. This, together with the initial electron optical magnification obtained, would facilitate any measurements that would have to be made on the circles or ellipses. The size of the specimen used would be limited to about 4 mm. diameter by the field of view of the microscope but, using fine wires, useful information could be obtained. The good resolution of the microscope would enable deformation effects over a small area to be observed.

No welding or deformation experiments were carried out and certain problems have still to be solved but these do not appear to be unsurmountable. The results of these initial experiments were encouraging and it is probable that the instrument will be useful in the programme under consideration.

CHAPTER V.

INVESTIGATION OF NON-VISUAL METHODS OF STUDYING IMAGES OF LOW DENSITY.

1. Introduction.

Since the emission microscope has poor transmission properties the source strengths used must be large. This disadvantage is critical since it limits the application of the method as can be seen from the results of experiments described in Chapter IV. The direct interpretation of the image depends on the intensity of blackening of the photographic plate. The possibility of identifying weak images by indirect methods (thus enabling weaker sources to be used) will be considered in this chapter. The work described gives useful information on a method for recording the exact distribution of radioactivity in a specimen.

2. Sensitivity of the Photographic Emulsion.

The amount of radiation required to produce blackening of a photographic plate varies considerably with the type of emulsion used. Axelrod and Hamilton (see ref. (2)) stated that for Agfa X-ray film, 5×10^6 β-particles must strike each square

cm. of film to produce blackening. The sensitivity of an emulsion is usually defined as the intensity of radiation required to produce a density of 0.5 above background fog. Berriman, Herz and Stevens (see ref. (6)), using this criterion, found that autoradiographic stripping emulsions (Kodak N.T. 2A, 4 microns thick) had a sensitivity of 5×10^8 electrons per unit area when exposed to I^{131} radiation; they found that X-ray film was 100 times faster than the stripping emulsion.

No information on the Ilford G5 (electron sensitive) emulsion has been published but Digby, Firth and Hercock[39] found that at 66 keV a density of 0.5 was produced in Type B2 emulsion (25 microns thick) by 10^{-11} coulombs/cm.^{2}, i.e. 6×10^7 electrons/cm.^{2} Ilford state that the G5 emulsion is 50% faster than the B2. Allowing for the greater number of grains produced per electron track* by the 148 keV F line of ThB, it can be deduced that for the F line 8.8×10^6 electrons/cm.^{2} are required to give blackening. This argument assumes that all the ionisation effects are confined to the emulsion. This assumption was supported by observation of tracks in the emulsion.

* The correction factor was obtained from grain count/energy curves compiled in this Department.

Experiments were performed to check this value. The strength of a ThB source was measured using the apparatus to be described in section (3), and the number of F electrons falling on the emulsion to form an image of known area was calculated. Different exposure times were used until a density of blackening of 0.5 was obtained. The latter was deduced from microphotometer observations when the density was taken as $\log_{10} I_o/I_T$ where I_o is the intensity of the incident light and I_T that of the transmitted light at a point in the image. It was found that 3.0×10^6 electrons/cm.^{2} gave a density of blackening of 0.5 above the surrounding background. This result showed that the sensitivity of the G5 emulsion was greater than the value deduced from the results of Digby et al. The discrepancy is probably due to the different experimental conditions and the improvement in sensitivity of the grains of more recent emulsions. The sensitivity compares favourably with that obtained by Berriman et al. when a correction for the emulsion thickness is applied.

A similar experiment showed that the number of F electrons required to give the same density of blackening on Ilford Industrial G film was 4.5×10^6 per cm.^{2}

The sensitivity of the G5 emulsion varies with

the energy of the electrons. Hence for the 25 keV line of ThB and the 45 keV line of I^{131} the estimated values of the sensitivity of 50 micron thick emulsion are 4.0×10^7 and 1.8×10^7 electrons/cm.^{2} respectively. The reduced sensitivity had been noticed when focusing the A line of ThB although no quantitative observations were made.

Assuming that the sensitivity of Industrial G film remains constant with electron energy, calculations show that the film and G5 emulsion are equally sensitive at approximately 115 keV. Hence if exposure time is the limiting factor, Industrial G film should be used for recording electrons with energies below 115 keV.

3. Measurement of Source Strengths.

An object consisting of a screw turned down to 0.1 cm. at one end was exposed to radiothorium until the active deposit had reached equilibrium. The screw was removed from the pot and its source strength measured using the apparatus shown in Fig. (26). The Geiger-Muller counter had a thin mica window (1.9 mgm./cm.^{2}) and its distance from the source was adjusted so that the ~~long range~~ α-particles from ThC' could be counted. The solid angle of collection

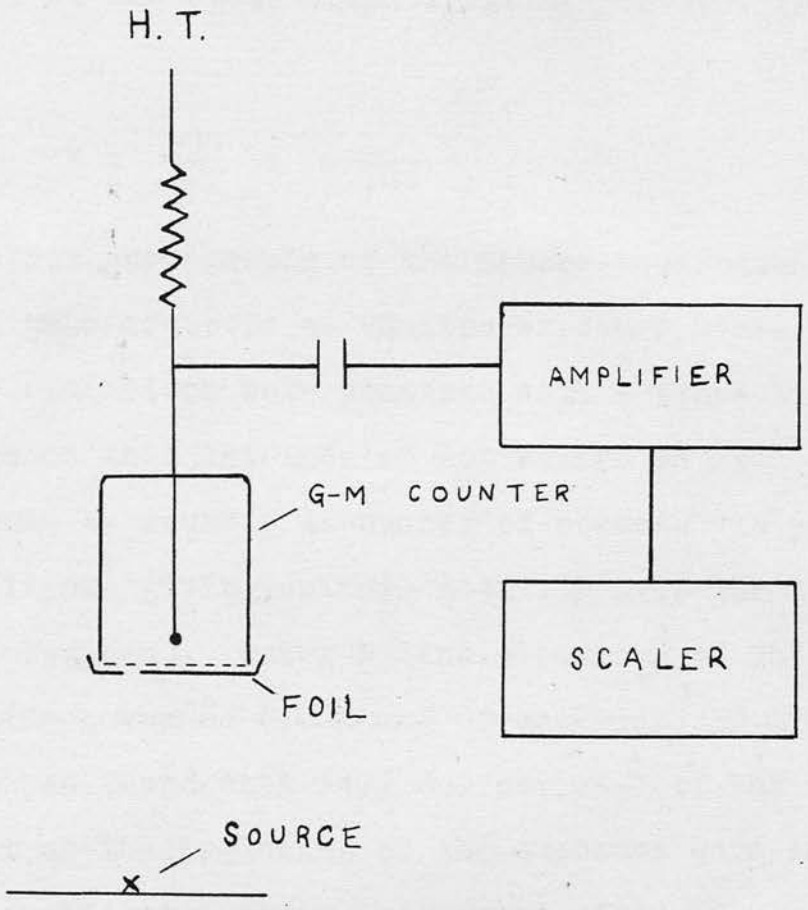

FIG. 26.

Apparatus used in Measurement of Source Strengths.

was defined by a ⅛in. hole drilled in a thin copper foil. The ThB activity could then be calculated. If the α-activity (N per sec.) is measured at a minimum of 4 hours after removal from the radiothorium pot the number of ThB atoms disintegrating per sec. is given by

$$N \times \frac{100}{65} \times \frac{1}{1.106} \quad .$$

Electron photographs of the source were taken in the emission microscope at various exposure times. The image dimensions were measured with a travelling microscope so that the area of activation in the source could be found. (A number of sources was prepared until one giving uniform activity over the active area was obtained). Using F line electrons of ThB at a collecting power of 0.02% and G5 emulsion (50 microns thick) it was found that 14.2 mc. per cm.^{2} of ThB on the object at the beginning of the exposure gave an image of density 0.5 above background after 60 min. The magnification was 6X. This represented approximately 4.1 mc. per cm.^{2} of F line electrons.

It was considered that the optimum density of blackening for viewing the image was 1.0 but much less intense blackening could be detected with the eye. Plates XXVI (a), (b) and (c) illustrate images

with densities of blackening of 1.0, 0.5 and 0.14 respectively. The latter corresponded to an exposure time of 10 mins. with the standard source strength of 14.2 mc. per cm.^{2} of ThB. In fact exposures as low as 4 min. gave an image that could be detected by careful visual inspection of the negative. The latter represents an exposure of 0.28 mc.-hrs. (F electrons of ThB).

4. Track Counting.

The method of track counting to interpret low intensity images was investigated. It was hoped to scan the image, counting the number of electron tracks in a given area, and deducing the form of the image from the observed track densities. Preliminary tests to determine the optimum development conditions were carried out and the tracks were observed at a magnification of 970X using oil immersion. A 30 micron square aperture was used in scanning. Ilford G5 (50 micron thick) plates were used but the tracks were confused and it was impossible to follow single tracks through the emulsion so that the 148 keV tracks could not be identified. To overcome this difficulty an attempt was made to count the ends of all tracks at the emulsion surface. This method proved unsatisfactory due to back scattering of

electrons at the surface of the emulsion and the fact that some grains were only slightly developed. Observations were also made with Industrial G film but the grains were very irregular and it was difficult to determine whether a developed grain represented one or more events. Also large clusters of grains were observed so that a number of grains may have represented only one event.

In order to obtain good resolution it would have been necessary to make a large number of counts so that the method would have been very tedious. Preliminary scans showed little correlation with the known distribution in the image. In view of these difficulties the method was considered to be impracticable.

5. The Microphotometer Method.

The possibility of scanning the image by a microphotometer technique was considered. This method also provided a means of recording the intensity distribution throughout the image i.e. a detailed picture of the distribution of activity in the source. Since very little work has been done on this subject a detailed investigation was carried out.

(a) Processing of Plates to be Studied.

Ilford G5 electron sensitive plates were used throughout the experiments. The emulsion thickness was 50 microns. Some plates were exposed to electrons of various energies and for different exposure times. Tests using a number of developers and different development times were then carried out to determine the best development conditions. Elon developer gave the best results.

The plates were immersed in the developer for 30 min. at 21°C. No stop bath was necessary and the plates were kept in the fixing bath for 2 hrs. They were then washed and dried in a dust free atmosphere. The solutions used in the processing are specified in Table II.

(b) Preliminary Investigation and Method of Analysis of Microphotometer Readings.

The source strengths obtained with the radio-thorium pot varied considerably so that the exposure times necessary to give a certain density of blackening on a plate were different for each source. All exposure times quoted in the remainder of this chapter refer to the standard source used in section (3) e.g. an exposure of 10 min. for any source

TABLE II.

PROCESSING SOLUTIONS.

Developer:

Solution A. (Prepared immediately before use)

Crystalline Sodium Sulphite ($Na_2SO_3.7H_2O$)	25 gm.
p-Methylamino-Sulphate (Elon) $\{(CH_3NHC_6H_4OH)_2H_2SO_4\}$	3 gm.
Distilled Water to	1,000 ml.

Solution B. (Prepared fortnightly)

Anhydrous Sodium Carbonate (Na_2CO_3)	50 gm.
Anhydrous Sodium Bicarbonate ($NaHCO_3$)	50 gm.
Distilled Water to	1,000 ml.

Fixing Bath:

Crystalline Sodium Thiosulphate ($Na_2S_2O_3.5H_2O$)	300 gm.
Distilled Water to	1,000 ml.

indicates the blackening that would be produced if the plate had been exposed to the standard source for 10 min. In arriving at this value corrections were applied to allow for the distribution of activity in the object, different initial strengths, decay of the source at the time of exposure and decay during exposure.

An object consisting of a screw face engraved with parallel lines was activated and plates exposed for exposure times equivalent to 1, 5, 60 and 90 min. With the microphotometer slit set parallel to the lines in the image, a trace across the 90 min. plate was taken. It was thought that this plate would give the more accurate picture of the blackening. The result is shown in Fig. (27). To abstract any useful information from the readings some kind of smoothing had to be applied to the curves. The shape of Fig. (27) indicated that the distribution of activity about a ridge in the object was sinusoidal. Therefore it was assumed that the true distribution (i.e. galvanometer deflections) could be represented by the first harmonic of a sine-cosine series:

$$y = F(x) = A_0 + A_1 \cos x + B_1 \sin x$$

where x takes the values 0, $\frac{2\pi}{m}$ .... $\frac{2(m-1)\pi}{m}$ and m

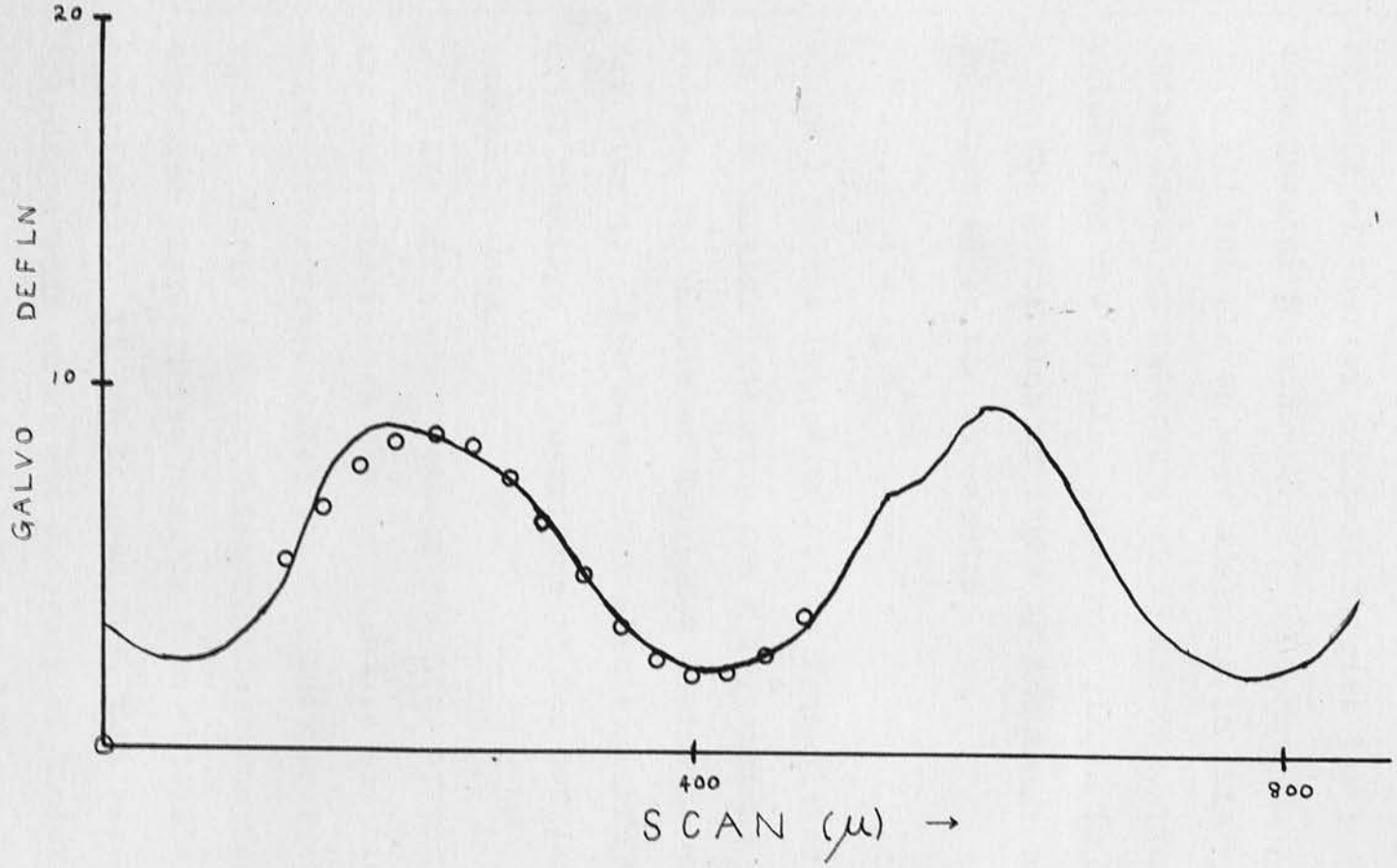

FIG. 27.

Microphotometer Trace showing Sinusoidal Distribution of Activity.

is the total number of observations (taken at equal intervals) per wavelength. The values of the coefficients A_0, A_1 and B can be deduced by the methods of Fourier analysis to give the best fit with experimental points.

All the plates were analysed in this way, readings being taken at intervals of 25 microns. The smoothed values for the 90 min. plate are ringed in Fig. (27).

The absorption of light by the image can be represented by the expression

$$I = I_0 \, e^{-kt}$$

where I is the intensity of the transmitted light, I_0 is the initial intensity and k is a constant which relates the number of developed grains to the exposure time t. This means that when comparing galvanometer readings the logarithms of the deflections should be used.

The difference between the log. of the smoothed and observed values for any point on the microphotometer trace represented the fluctuation from the true value. Table V shows these fluctuations for a 10 min. exposure plate (these results were obtained in a later experiment). It can be seen that they are random and therefore come under the category of "noise", the concept of which can be extended from the original

electrical meaning to the readings under discussion. Two methods of defining noise were used. In the first case the noise was taken as the R.M.S. value of deviations taken over one wavelength. Hence

$$\text{Noise (1)} = \sqrt{\frac{\sum (F(x)_c - F(x)_o)^2}{m}}$$

where $F(x)_c$ and $F(x)_o$ are the calculated and observed values of the galvanometer deflections respectively. The second definition, referred to as noise (2), was similar but the R.M.S. value was taken over the signal portion of the curve only (i.e. the denser part of the image). This involved 8 or 9 readings depending on the shape of the curve.

The detection of an image would depend on the differential between readings taken in a region of minimum blackening and readings taken in an area of relatively dense blackening. Hence the strength of the signal was taken as the difference between the logarithms of the maximum and minimum values of the smoothed sine curve:

$$\text{Signal} = \log_{10} F(x)_{max} - \log_{10} F(x)_{min}$$

Each wave form was characterised by a signal-to-noise ratio. The value of this ratio would limit the

usefulness of the method and establish the conditions under which the method could be used.

The preliminary experiments indicated that this method of analysis could be used but further information was required over a range of exposure times and new plates were ordered to ensure that the cosmic ray background would be at a minimum.

The analysis was applied to equal density images recorded on G5 emulsion and Industrial G film. The results showed that, for this work, the G5 emulsion was superior to the coarse-grained Industrial G film.

(c) Tests with Different Sizes of Aperture.

The 5 min. exposure plate was used in this test. Scans were taken across the same portion of the plate with apertures of different areas , and the resulting curves were analysed. The size of slit that could be used was limited since at widths greater than 40 microns the slit width was greater than the width of the illuminating light beam. Also the pattern in the image restricted the height of the slit that could be employed and in any case a long, relatively narrow slit was not to be desired.

The results are given in Table III and illustrated graphically in Fig. (28). The graph has been drawn

TABLE III.

Exposure Time : 5 min.

Slit Area ($cm^2 \times 10^3$)	Signal	Noise $\times 10^3$	Signal/Noise
0.048	0.038	(1) 12.4 (2) 15.8	3.1 2.4
0.072	0.049	(1) 11.8 (2) 13.9	4.2 3.5
0.096	0.051	(1) 11.3 (2) 13.4	4.5 3.8
0.120	0.053	(1) 10.5 (2) 11.6	5.0 4.6
0.144	0.044	(1) 7.3 (2) 6.9	6.0 6.4

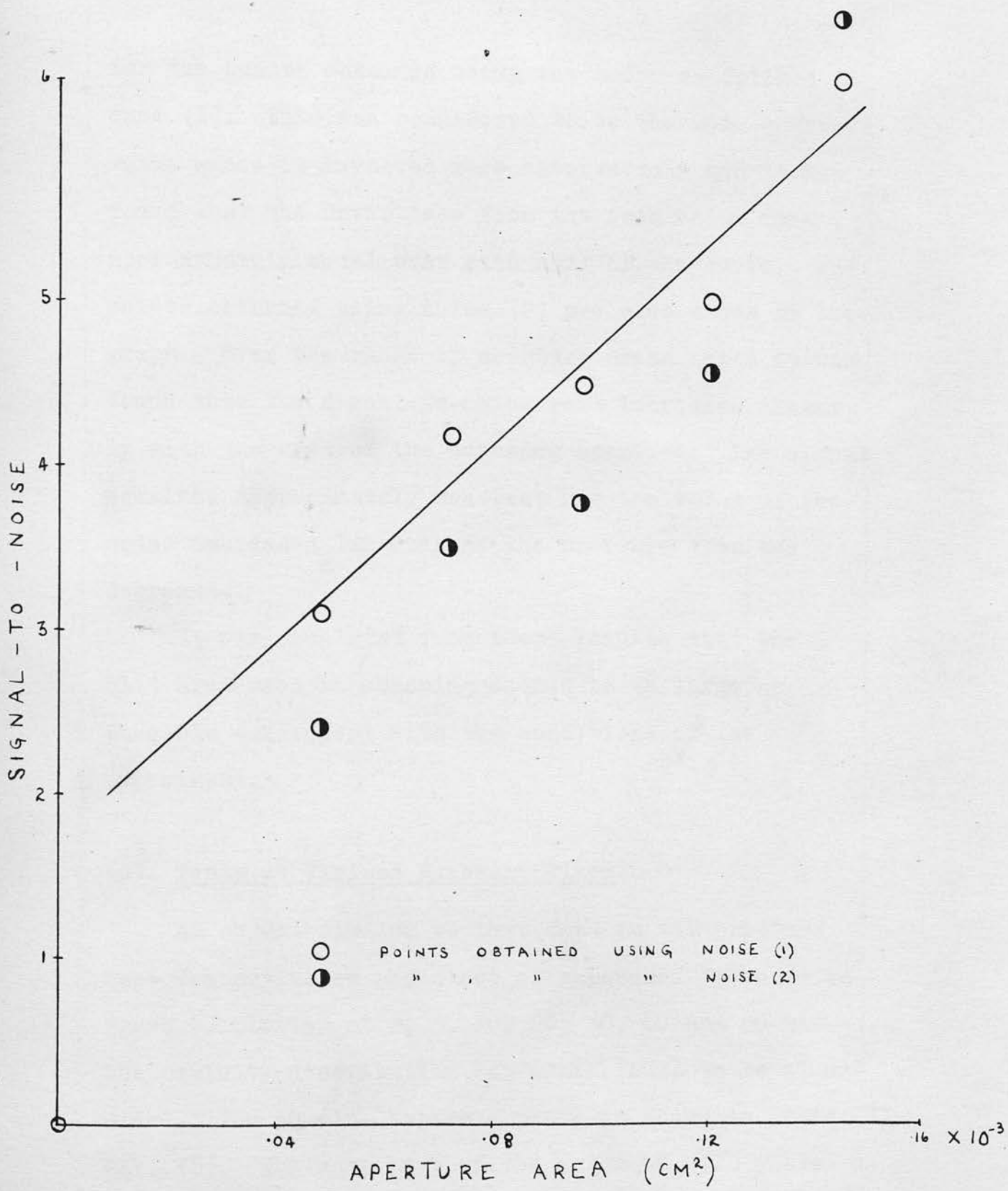

FIG. 28.

Signal-to-Noise Ratio against Aperture Area.

for the points obtained using the noise as defined in case (1). This was considered to be the more accurate value since it involved more observations and it was found that the deviations from the true value were approximately equal over each half of the curve. The points obtained using noise (2) are also shown on the graph. Over the range of aperture areas taken it was found that the signal-to-noise ratio increased linearly with the area of the scanning aperture. The signal remained approximately constant and the value of the noise increased linearly as the aperture area was decreased.

It was concluded from these results that the slit area used in scanning should be as large as possible consistent with the conditions of the experiment.

(d) Tests at Various Exposure Times.

An object similar to that used in the previous test was activated and a set of exposures taken (with fresh G5 plates) at 2, 5, 10, 20, 40, 60 and 90 min. The activity distribution was again found to be sinusoidal. The 60 min. exposure plate is shown in plate XXVI (b). The same part of the image on each plate was scanned using a slit of area 0.128×10^{-3} cm.^{2}

TABLE IV.

Area of Aperture : 0.128×10^{-3} cm^2.

Exposure Time (mins.)	Signal	Noise x 10^3	Signal/Noise
90	0.630	(1) 29.0 (2) 30.0	21.7 21.0
60	0.455	(1) 25.7 (2) 32.1	17.7 14.2
40	0.367	(1) 20.3 (2) 23.0	18.1 16.0
20	0.197	(1) 14.2 (2) 15.0	13.9 13.1
10	0.104	(1) 13.4 (2) 10.6	7.8 9.8
5	0.056	(1) 14.6 (2) 12.3	3.8 4.6
2	0.013	(1) 12.3 (2) 14.1	1.1 0.9

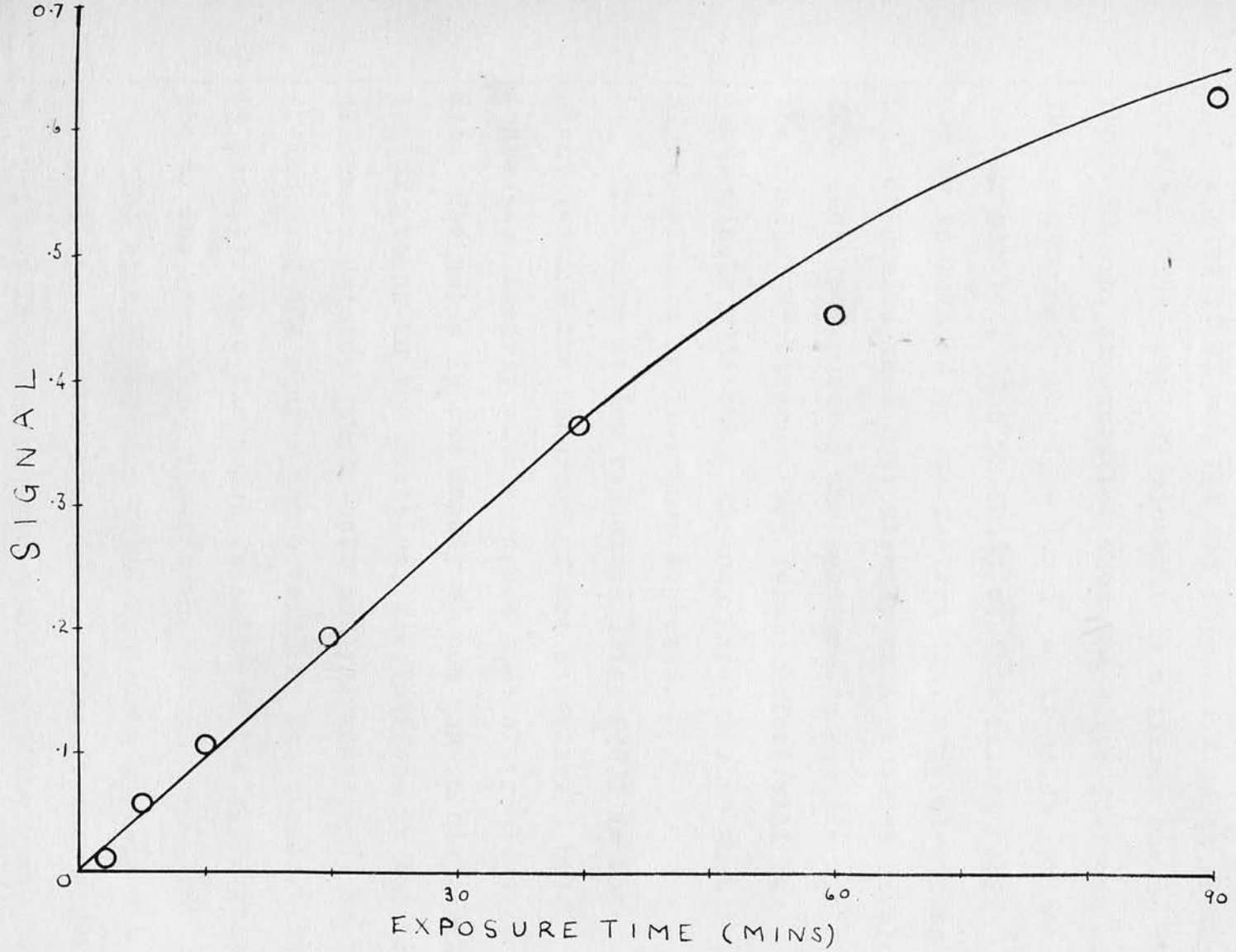

FIG. 29.

Signal against Exposure Time.

The curves were analysed and the values of signal, noise and signal-to-noise calculated (see Table IV).

A plot of signal against exposure time is shown in Fig. (29). The relationship is a linear one up to about 50 min. exposure and then the curve flattens out. The relationship $\log I_o - \log I = kt$ holds for the linear portion. The validity of this relationship may be influenced by two factors viz. some electrons fall on grains that have already been rendered developable (double exposure) and some grains may lie "in the shadow" of others. The former effect will be particularly noticeable at long exposures so that the signal will be smaller than expected.

The noise at low exposures (Fig. (30)) is constant (within the accuracy of the experiment) but increases linearly with exposure time after about 20 min. The noise is due mainly to non random distribution of grains in the emulsion, fluctuations in the recording apparatus (photo-cell and galvanometer), background from the source and cosmic ray background. It is probable that the constant noise at low exposure is due to the cosmic ray background.

The signal-to-noise value increases rapidly with exposure time for low exposures. After 20 min. exposure the rate of increase becomes smaller and the curve tends to a maximum value (see Fig. (31)).

Exposure time 10 min.

TABLE V.

log (observed reading)	log (smoothed reading)	Deviation $\times 10^2$	(Deviation)^2 $\times 10^6$
1.509	1.496	+13	169
1.490	1.519	-29	841
1.553	1.538	+15	225
1.568	1.550	+18	324
1.554	1.556	-2	4
1.548	1.554	-6	36
1.538	1.543	-5	25
1.507	1.526	-19	361
1.520	1.505	+15	225
1.491	1.484	+7	49
1.467	1.465	+2	4
1.459	1.453	+6	36
1.455	1.452	+3	9
1.439	1.459	-20	400
1.477	1.476	+1	1
	Totals	-1	2709

Noise (1) = 0.0134

Signal = 1.556 - 1.452 = 0.104.

Signal/Noise = 7.8.

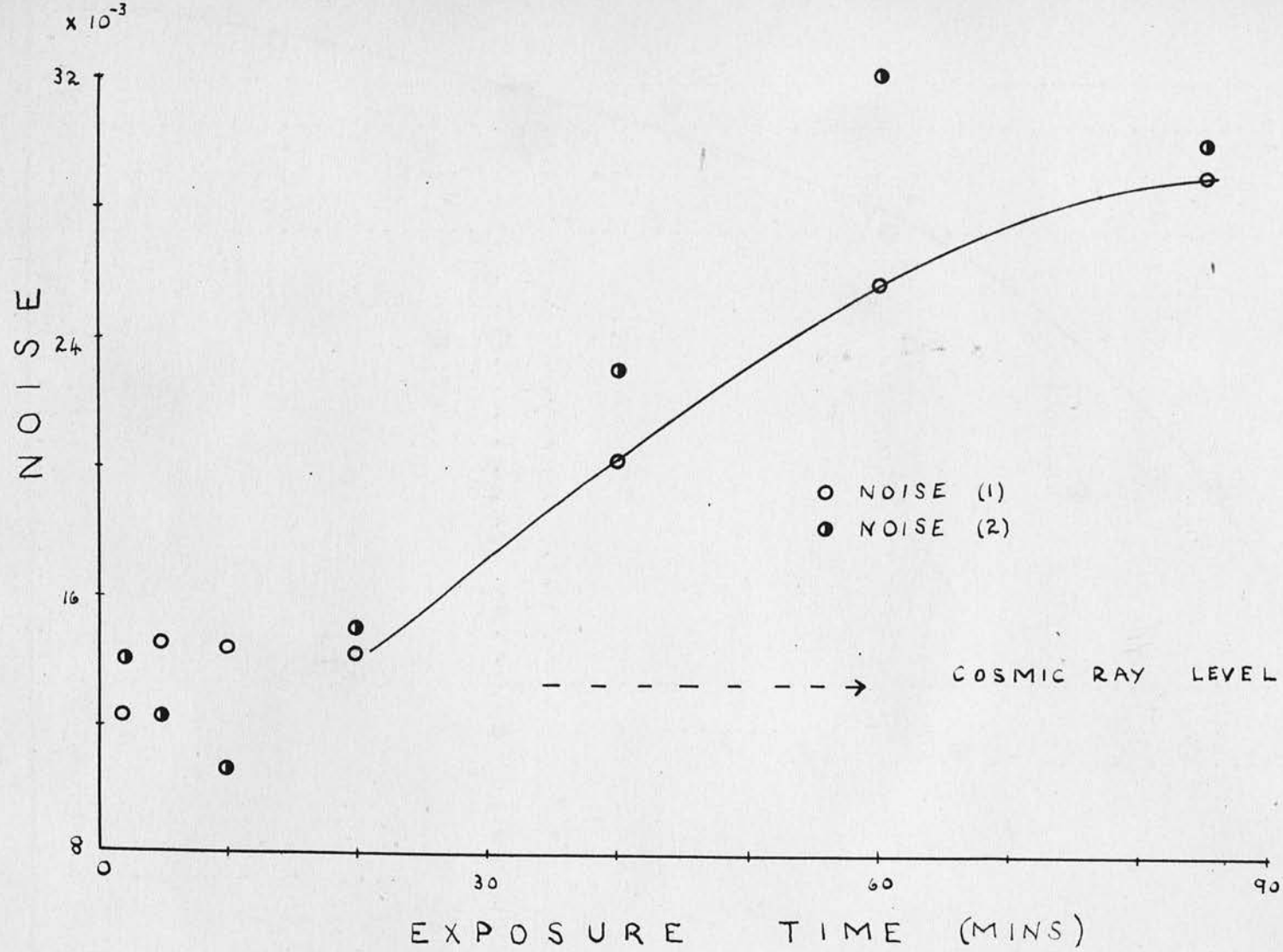

FIG. 30.

Noise against Exposure Time.

(e) Application of the Method.

In order to check the validity of the results obtained in sections (c) and (d) and to find out if the method gave useful information about the image, the following procedure was carried out.

An electron microscope grid was activated with ThB in the usual way. It was found that the activity of this type of specimen could not be measured accurately by counting ThC' α-particles. The amount of ThB actually present was greater than that calculated from the α-count due to the fact that activity gathered on the back of the grid and on the sides of the holes. Plates were exposed to the grid for different times and the equivalent exposure time calculated by comparing the densities of the images obtained with the densities of images of the standard source. The 10 min. exposure plate was selected and examined by the method of "block scanning".

A square aperture should be employed in the scan but it was not possible to do this. The smallest aperture that could be measured accurately was selected. The use of a narrow rectangular slit was excluded since this would give poor definition in the results. The size of the aperture used was 80 microns x 40 microns. The aperture was moved across the plate

in the x-direction and galvanometer readings taken at 50 micron intervals. The aperture was displaced by 50 microns in the y-direction and another scan carried out. In this way a set of readings was obtained which represented the density of the image at points separated by 50 microns (which corresponded to a distance of 9 microns in the object) in the x- and y-directions (see Table VI).

The readings were inspected and contours drawn to separate the regions of greater image density (small deflections) from those of lower density. The blocks of numbers of high values represented the holes in the grid and the dimensions of these blocks were found to correspond to the true dimensions of the holes in the grid. Differences in the density of distribution of activity in the object could be detected from the readings. A micrograph of the grid taken at optimum exposure is shown in plate XXVI(a). The block scan represents a section of this grid.

The signal-to-noise ratio for this set of readings was calculated. Two adjacent regions of high and low density were selected and the mean of the logarithms of the deflections over 45 readings was calculated for each region. The difference of these two values was taken as the signal and the R.M.S.

TABLE VI

(Block Scan)

208	196	180	161	148	154	140	148	154	152	171	161	182	192	210	191	206	198	148	122	155	143	154	154	168	182	184
205	210	175	176	155	162	132	143	155	142	163	165	190	192	208	198	204	186	152	122	140	154	148	160	163	175	186
205	224	181	175	172	148	125	124	140	135	176	169	200	194	204	184	206	191	151	118	165	144	137	144	160	181	184
187	206	184	168	176	147	129	120	130	130	176	168	187	191	191	190	189	181	146	128	156	136	142	141	160	180	168
162	168	176	143	133	142	117	140	136	134	142	149	145	148	145	160	134	146	147	120	126	140	156	140	136	150	143
132	146	150	142	129	143	141	165	135	136	129	140	143	150	134	126	136	141	150	124	122	130	138	116	132	152	145
142	138	135	150	133	132	148	160	120	128	125	139	148	160	145	139	134	125	142	122	131	115	131	121	122	135	140
135	158	155	154	144	131	146	157	121	107	142	145	137	138	142	140	134	115	138	132	138	115	162	129	134	128	148
152	158	172	151	151	145	153	160	129	114	153	156	139	156	146	139	155	150	155	146	144	126	161	125	130	138	144
148	144	186	156	126	121	135	117	134	148	174	186	165	178	189	174	183	182	175	156	148	166	138	160	161	175	171
188	186	198	160	129	124	137	139	137	130	175	181	157	185	212	188	195	176	186	146	118	144	126	143	180	179	177
197	175	196	172	135	146	134	122	142	151	176	170	184	220	201	188	212	184	184	145	121	141	122	142	170	173	160
196	179	198	165	152	139	145	119	146	158	164	166	178	217	198	184	210	195	168	122	115	160	125	135	164	181	160
195	201	187	152	156	146	150	135	148	162	158	165	170	208	182	195	210	184	167	120	119	124	136	132	155	200	158
179	190	182	145	140	160	145	148	146	149	168	164	176	198	180	205	190	185	181	140	118	103	138	114	137	180	165
180	181	186	150	144	160	134	150	137	150	154	158	184	191	191	204	185	182	182	148	114	114	136	117	152	170	176
195	176	178	149	156	136	140	146	114	144	139	161	188	180	182	189	181	185	165	130	130	116	142	136	180	160	202
184	183	157	149	150	130	144	130	134	147	168	169	160	187	176	166	164	172	160	126	148	140	142	141	171	158	176
164	172	166	146	144	128	136	140	132	142	154	156	148	178	184	170	156	164	154	126	141	152	144	155	155	156	165
138	154	154	150	125	120	137	148	146	152	124	134	160	164	156	152	135	156	152	131	120	144	125	160	135	141	141
140	144	142	150	122	145	152	142	148	152	125	116	158	146	142	115	122	147	140	137	130	126	100	148	112	140	138
146	148	154	155	130	152	154	128	140	141	127	114	147	122	130	118	147	144	137	138	150	106	117	137	111	131	142
146	155	150	152	134	134	142	132	134	136	150	138	154	132	126	140	160	130	145	134	132	132	144	142	136	144	136
160	**145**	146	137	145	128	138	136	136	138	154	172	152	147	166	172	156	178	160	150	122	120	146	148	140	152	150
189	191	172	165	156	145	146	142	128	145	150	174	195	187	202	202	171	163	167	161	138	100	128	149	160	180	192

↑

50 μ (Movement) ⟶

Electron Optical Magnification 5.7 x

Aperture Area: 0.032 x 10^{-3} $cm.^2$

Signal : 0.112
Noise (1) : 0.33
Signal/Noise : 3.4

value of the deviations from the corresponding means (which represented the smoothed readings) gave a value for the noise. The signal-to-noise ratio was 3.4 whereas the value calculated from the graphs in Figs. (28) and (31) was 4. The fact that these values were approximately equal indicated the method of analysis was valid and the results reproducible.

(f) Signal-to-Noise Permissible.

In order to examine the possibility of using the microphotometer method for interpreting low density images the smallest value of the signal-to-noise ratio that could be used had to be decided. The problem of how far noise limits the detection of the signal is a complex one and depends on the conditions for any particular experiment. Signal-to-noise values of 2 are accepted in some detecting instruments but the definitions are not consistent. In the method under discussion it was decided that signal-to-noise ratios below 3 could not be tolerated if the resolution in the plate was to be preserved and if the method was to give reliable information.

(g) Summary and Conclusions.

The 148 keV electron line of ThB has been used in the tests, and the images recorded on Ilford G5 (50 micron thick) electron sensitive emulsions.

The method of analysis was exploratory but consistent results have been obtained. Two definitions of noise were taken but the consequent results showed the definition (1) to be the more satisfactory one. All graphs have been drawn for points obtained using this definition.

Using a standard source of 14.2 mc./cm.^{2} of ThB the optimum exposure time for visual observation was 90 min. Images could be detected at exposures down to 10 min. (Under certain conditions images could be detected at exposure times as low as 4 min. but small details could not then be distinguished clearly).

Employing an aperture of 0.128×10^{-3} cm.^{2} in the microphotometer technique, the image can be detected on plates of equivalent exposure time 4 min. (signal-to-noise ratio 3). Thus only a factor of 2.5 is saved in the exposure time. This area represents a square of side 19 microns in the object. Even smaller scanning apertures are desirable but the exposure time would need to be greater to keep the

signal-to-noise ratio at a high enough value. A block scan was carried out using an aperture area of 0.032×10^{-3} cm.^{2} and the results agreed with the true distribution in the plate.

The method is very useful for obtaining a permanent record of the distribution of activity in the specimen. When minute scrutiny is required the aperture should be small and the movement of the aperture should be in small intervals (this can be as little as 1 micron). In this way the resolution is preserved and no information is lost.

CHAPTER VI.

1. Comparison with other Focusing Systems.

The focusing action of the emission microscope is similar to that of a magnetic lens β-ray spectrometer. It is interesting to compare the resolving power of some well known spectrometers with the resolution obtained with the microscope. The following treatment is very approximate but only orders of magnitude are required.

The relative line width (R) is an inverse measure of the resolving power of a spectrometer:

$$R = \frac{\Delta(H\rho)}{H\rho}$$

where ρ is the radius of curvature of the electron path in a uniform magnetic field of strength H. $\Delta(H\rho)$ represents the "half width" and two peaks are resolved when separated by this distance. $\Delta(H\rho)$ can be related to Δx the distance apart of two points in the object (or source) which are just resolved in the image.

The permanent magnetic double β-ray spectrometer used in this department (see ref. (36)) has a resolving power of 1% and in this case $x = 2\rho$, where x is the distance from source to recording device, so that $\Delta x = 2\Delta\rho = 2R\rho$. The value of Δx obtained is

0.06 cm. at a transmission of 10^{-1}%. In the case of the spheriodal field spectrometer [40] the field is not uniform so that the treatment is even more approximate. However, assuming $x \sim \rho$ a value of 0.2 cm. is obtained for Δx at a transmission of 4%.

Better resolution has ~~lower resolving powers have~~ been obtained, e.g. Quade and Halliday [23] (transmission 0.12%, relative line width 0.78%) and Schmidt [41] (transmission 2%, relative line width 0.4%), but the values of Δx are much larger than the resolution obtained in the emission microscope.

It can be seen that most of these instruments have much better transmission properties than the emission microscope but the improvement is achieved at the expense of resolution. On the other hand, the microscope has relatively good resolving power but poor collecting power. In this type of lens system it does not appear to be possible to combine high resolving power with useful transmission properties.

2. Conclusion.

Although the transmission of the lens system (at high resolution) has been doubled by employing a new field shape, the solid angle of collection is

still very small (0.02% of 4π). In addition, internal conversion electrons are selected from the continuum and these usually comprise about 5% or less of the total activity. This means that the amount of activity in a specimen must be large (and the half value period long) which appears to preclude the use of the instrument in biological tracer experiments. There is no point in improving the transmission of the instrument at the expense of resolution as the main advantage of the focusing method over contact autoradiography would then be lost.

The choice of isotope is limited to those emitting strong lines, which means that many of the isotopes (such as C^{14}, P^{32} and S^{35}) usually employed in tracer experiments cannot be used. When a suitable isotope has been found it must be deposited on the surface of the specimen (or very thin sections must be used) to prevent self absorption in the specimen. The difficulties of source preparation were illustrated in Chapter IV and little success was achieved in the applications attempted.

Attempts to reduce the source strengths necessary with the microscope by use of a microphotometer technique to detect low density images were not very

successful. The resulting improvement does not justify a large scale application of the instrument.

In view of the serious limitations of the instrument in its present form, it appears that any applications will be in specific problems encountered in metal physics. In this field strong sources can be permitted and the study of surface phenomena is important.

It is considered that the principles of the method are sound but that the applications are limited. Advances in electron optics may produce a more suitable lens system that will facilitate a wider application of the focusing method in autoradiography.

ACKNOWLEDGMENTS.

I am indebted to Professor N. Feather, F.R.S. for providing the opportunity for this research and for extending to me the facilities of his laboratory, also for his supervision and guidance throughout the work.

I wish to thank Professor H.O.W. Richardson (now Professor of Physics, University College, Exeter), who designed the magnetic lens system, for valuable advice in the early stages of this research.

Thanks are due to all members of staff for helpful discussions and advice. In particular, it is a great pleasure to record my thanks to Dr. M.A.S. Ross for help and supervision of the work contained in Chapter V, and to Dr. A.F. Brown for helpful suggestions concerning the work in Chapter IV (B) and (C).

In addition thanks are due to Mr. A. Headridge and the technical staff of the Natural Philosophy Department, whose help and cooperation at all times have been greatly appreciated.

BIBLIOGRAPHY.

1. Lacassagne, A. & Lattes, C., J. Radiol. et Elect. 9, 1, 1925.
2. Axelrod, D.J. & Hamilton, J.G., Amer. J. Path. 23, 389, 1947.
3. Evans, T.C., Proc. Soc. Exp. Biol. Med. 64, 313, 1947.
4. Belanger, L.F. & Leblond, C.P. ,Endocrinology 39, 8, 1947.
5. Pelc, S.R., Nature, 160, 749, 1947.
6. Berriman, R.W., Herz, R.H. & Stevens, G.W.W., Brit. J. Radiol. 23, 472, 1950.
7. Gomberg, H.J., Nucleonics 9, 28, Oct., 1951.
8. Fink, R.M., Science 114, 143, 1951.
9. Lawrence, J.H., Am. J. Roentgenol. 58, 31, 1947.
10. Marton, L. & Abelson, P.H. Science, 106, 69, 1947.
11. Barker, A.N., Thesis, Edinburgh, 1950.
12. Barker, A.N., Richardson, H.O.W. & Feather, N., Research 3, 431, 1950.
13. Cosslett, V.E., J. Sci. Instr. 22, 170, 1945.
14. Glaser, W., Z. Phys. 117, 285, 1941.
15. Dosse, J., Z. Phys. 117, 316, 1941.
16. Marton, L., Rep. Progr. Phys. 10, 204, 1946.
17. Cosslett, V.E., Proc. Phys. Soc. 58, 443, 1946.
18. Scherzer, O., Z. Phys. 101, 593, 1936.
19. Glaser, W., Z. Phys. 116, 19, 1940.
20. Rebsch, R., Z. Phys. 116, 729, 1940.

BIBLIOGRAPHY (Contd).

21. Glaser, W. & Lammel, E., Ann. Phys. 40, 367, 1941.

22. Slatis, H. & Siegbahn, K., Ark. Fys. 17, 339, 1949.

23. Quade, E.A. & Halliday, D., Rev. Sci. Instr. 19, 234, 1948.

24. Agnew, H.M. & Anderson, Rev. Sci. Instr. 20, 869, 1949.

25. Sanford, R.L., Circ. Nat. Bur. Stan., C448, Washington, 1944.

26. Hoselitz, K., J. Sci. Instr., 23, 65, 1946.

27. Katz, L. & Penfold, A.S., Rev. Mod. Phys. 24, 28, 1952.

28. Stevens, G.W.W., Brit. J. Radiol., 23, 723, 1950.

29. Tugman, O., Astrophys. J. 42, 321, 1915.

30. Kinsinger, W.G., Hillier, J., Picard, R.G., Zieler, H.W., J. Appl. Phys. 17, 989, 1946.

31. Hillier, J., J. Appl. Phys. 17, 307, 1946.

32. Hamly, D.H. & Watson, J.H.L., J. Opt. Soc. Amer., 32, 433, 1942.

33. Gregory, J.N., Nature 157, 443, 1946.

34. Rabinowicz, E., Nature 170, 1029, 1952.

35. Kern, D., Mitchell, A. & Saffrano, D., Phys. Rev. 76, 94, 1949.

36. Kyles, J., Campbell, C.G. & Henderson, W.J., Proc. Phys. Soc. 66A, 519, 1953.

37. Flammersfeld, A., Z. Phys. 114, 227, 1939.

BIBLIOGRAPHY (Contd).

38. Gubkin, S.I. & Dovnar, S.A., Dokl. Ak. Nauk, S.S.S.R. 91, 1089, 1953.

39. Digby, N., Firth, K. & Hercock, R.J., J. Photogr. Sci. 1, 194, 1953.

40. Braid, T.H. & Richardson, H.O.W., Proc. Phys. Soc. 64A, 163, 1951.

41. Schmidt, F.H., Rev. Sci. Instr. 23, 361, 1952.

ELECTRON-MICROGRAPHS.

Note:

Electron-Optical Magnification denoted by E.O.M.

Optical Magnification denoted by O.M.

All Ilford G5 plates had emulsion thickness of 50 microns.

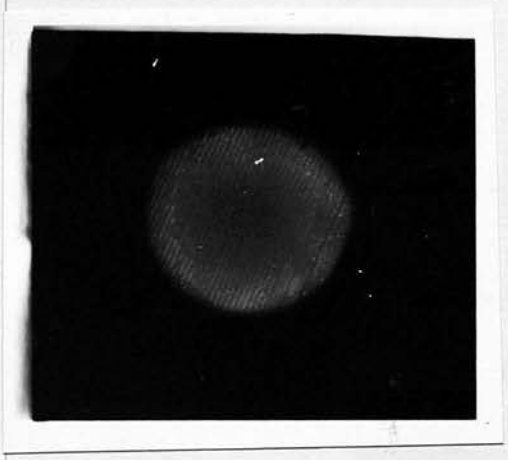

(a)

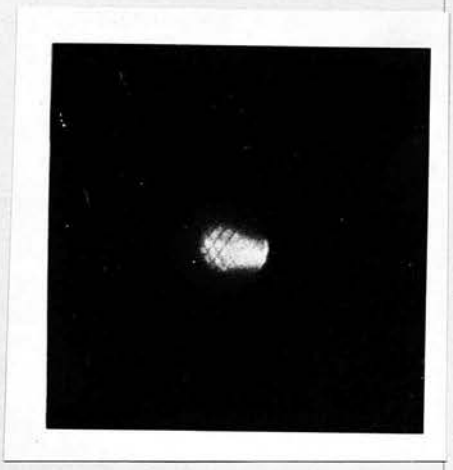

(b)

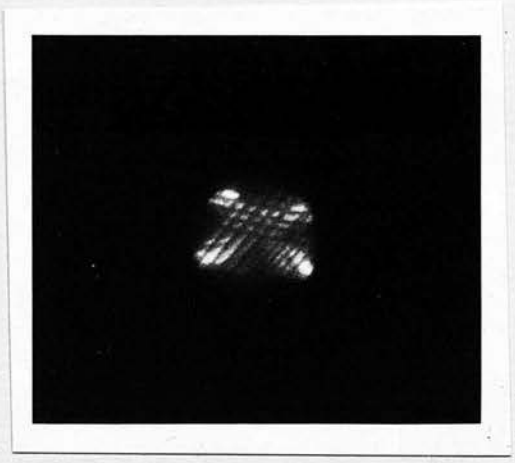

(c)

Plate V(a), V(b), and V(c)

Examples of Poor Distribution of ThB.

Ilfex film

E.O.M. : 7.5X

O.M. : 2X

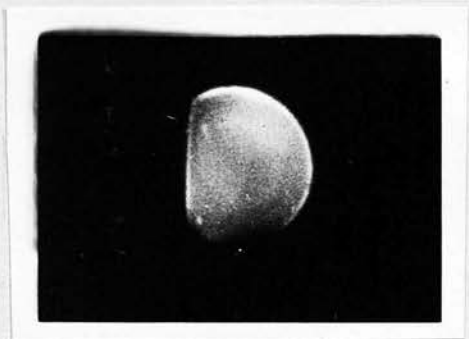

Plate VI.

Straight Edge (Obtained with Old Field).

Ilford G5

E.O.M. : 7X

O.M. : 2X

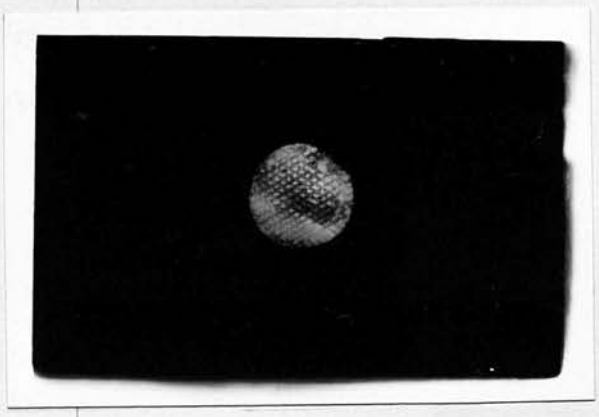

(a)

(b)

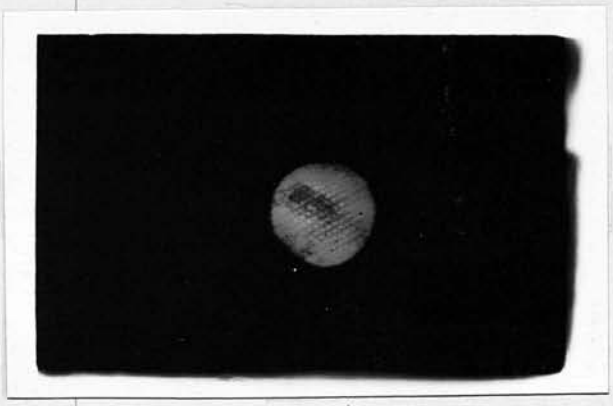

(c)

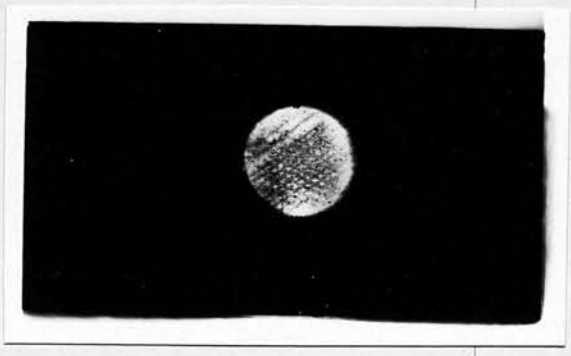

(d)

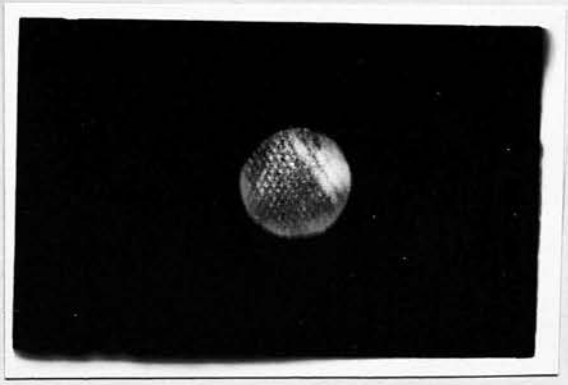

(e)

Plate VII.

(a)	Baffle diameter	:	7.32 mm.
(b)	" "	:	7.75 mm.
(c)	" "	:	8.30 mm.
(d)	" "	:	8.57 mm.
(e)	" "	:	8.76 mm.

Ilford G5

E.O.M.	:	6X
O.M.	:	2X

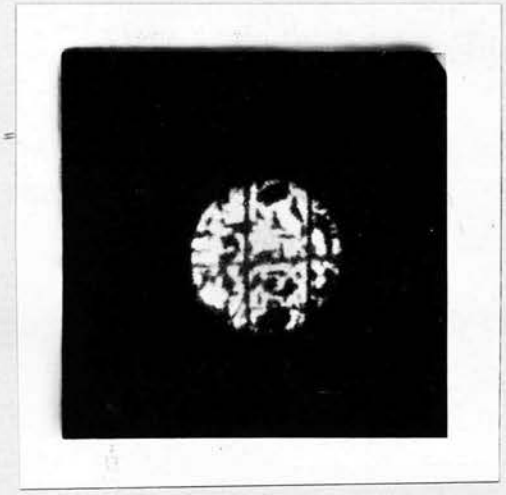

Plate VIII

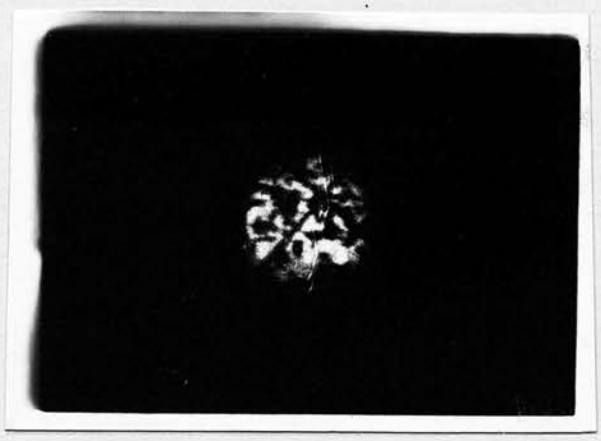

Plate IX

Plates VIII and IX.

Lead Filings on Collodion (Transmission).

Ilford G5.

E.O.M. : 7.5X

O.M. : 4 X

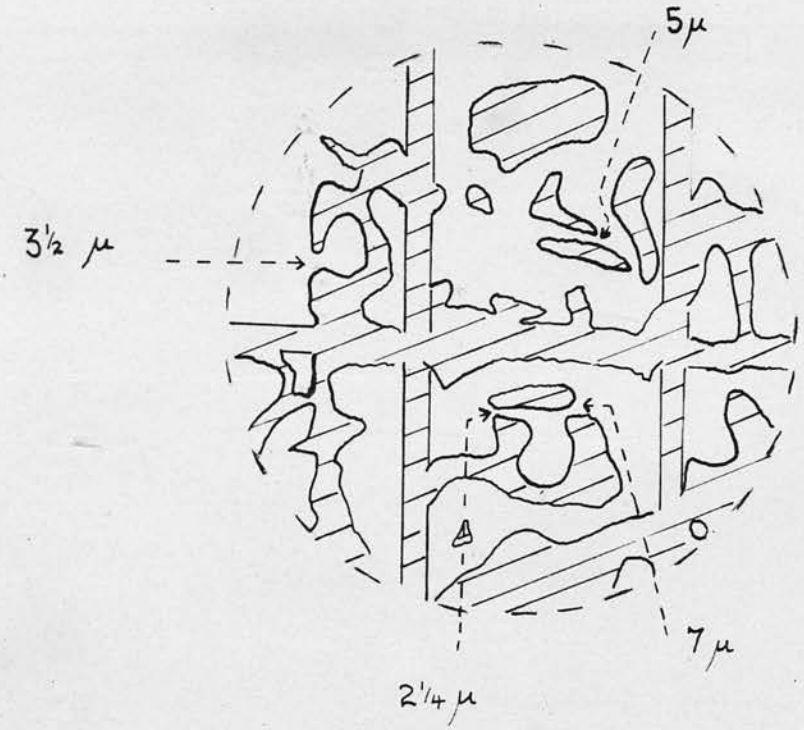

Fig. 23.

Key to Plate VIII.

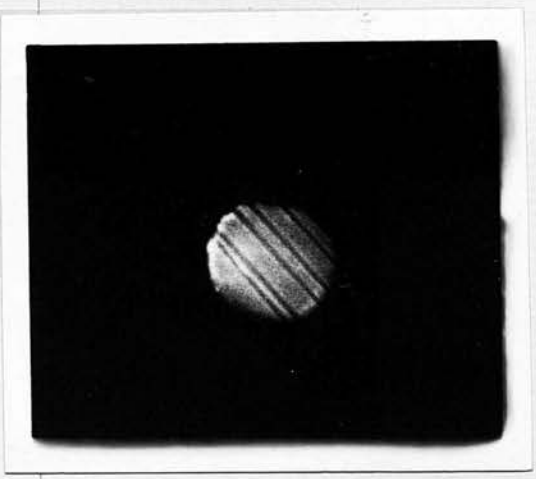

Plate X

Ilford G5
E.O.M. : 6X
O.M. : 3X

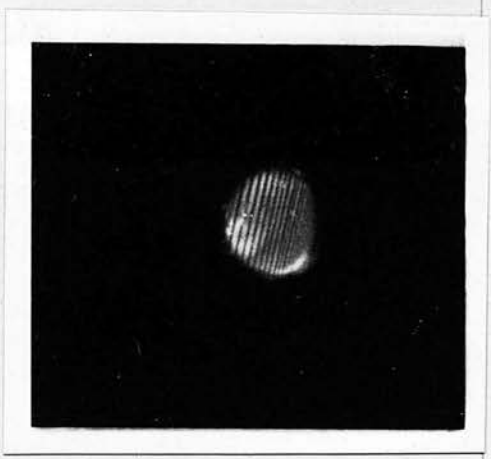

Plate XI

Ilfex
E.O.M. : 7X
O.M. : 3X

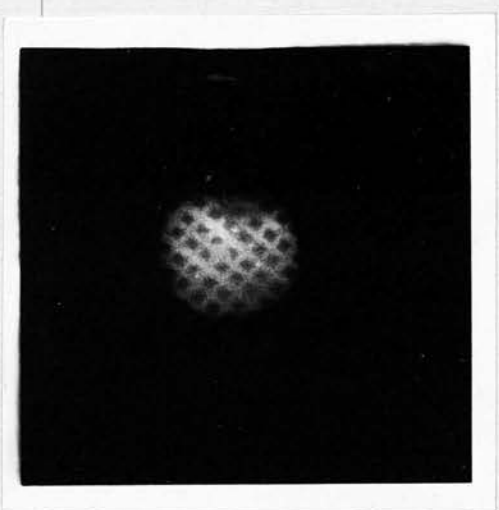

Plate XII

Ilfex
E.O.M. : 6X
O.M. : 3X

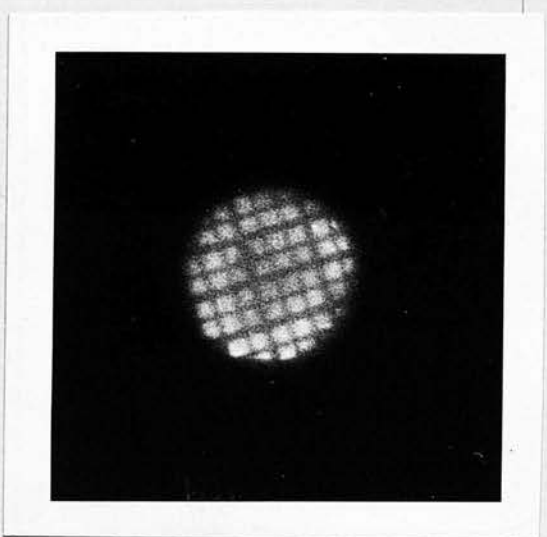

Plate XIII

Ilfex
E.O.M. : 6X
O.M. : 4.5X

Electron Micrographs of Various Objects

(see page 60 for details).

Plate XIV.

Ilford G5
E.O.M. : 6X
O.M. : 3X

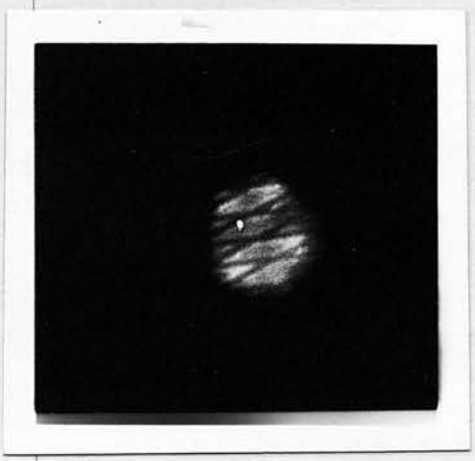

Plate XV

Ilford G5
E.O.M. : 6X
O.M. : 3X

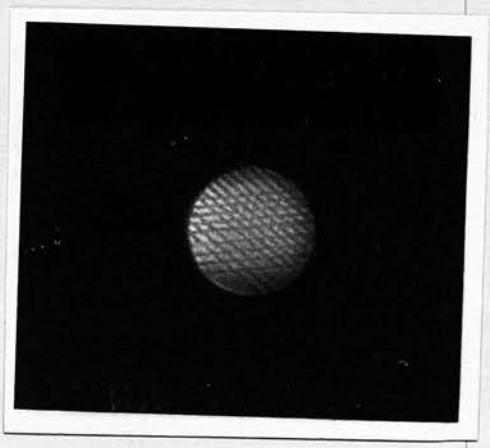

Plate XVI

Ilfex
E.O.M. : 7X
O.M. : 3X

Electron Micrographs of Various Objects.

(see page 60 for details).

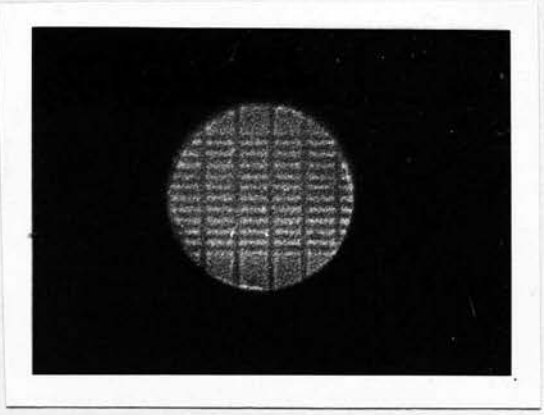

Plate XVII.

Industrial G
E.O.M. : 6X
O.M. : 4X

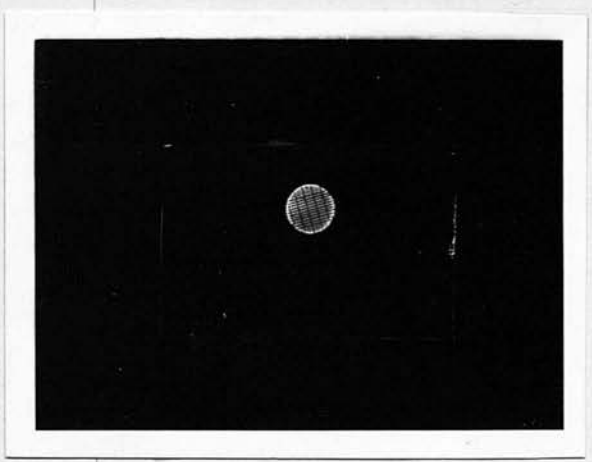

Plate XVIII(a)

Ilford G5
E.O.M. : 6X
O.M. : 1X

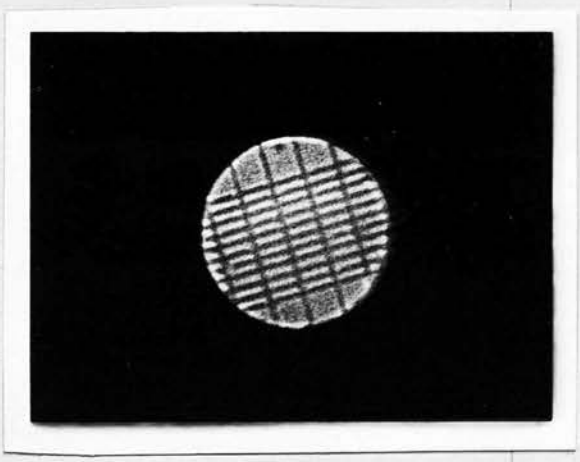

Plate XVIII(b)

Ilford G5
E.O.M. : 6X
O.M. : 4X

Comparison of Ilford G5 Emulsion and Ilford Industrial G X-Ray Film.

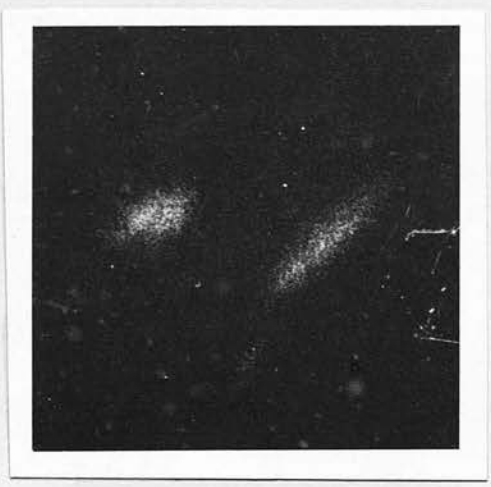

Plate XIX.

Diatoms Activated with ThB.

Ilford G5

E.O.M. : 6X

O.M. : 11X

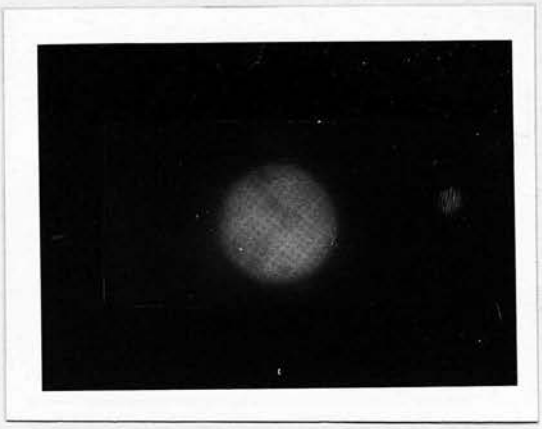

Plate XX

Silver Grid activated with I^{131}

Ilford Industrial G
E.O.M. : 7X
O.M. : 1X

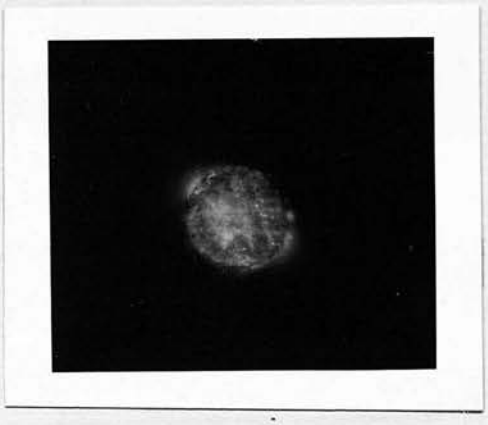

Plate XXI

Friction Tracks. (I^{131} as tracer). Copper, Lead and Silver on Aluminium.

Contact Autoradiograph.

Ilford Industrial G.

O.M. : 2X.

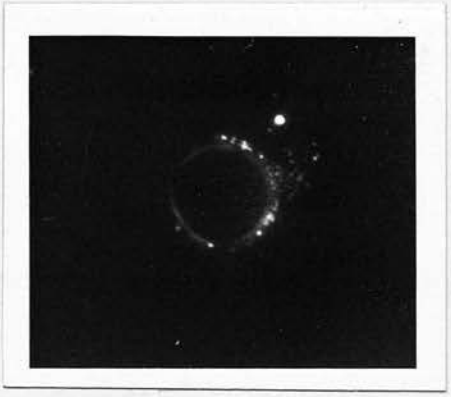

Plate XXII.

Electron Optical
Ilford Industrial G
E.O.M. : 6X
O.M. : 2X

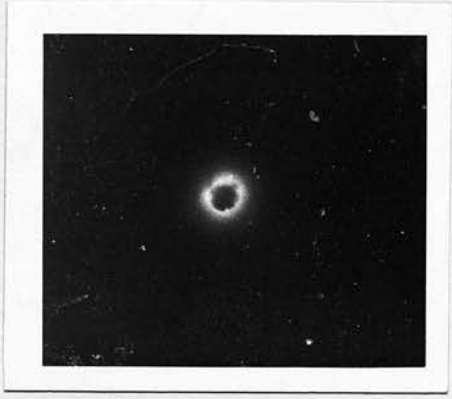

Plate XXIII

Contact Autoradiograph
Ilford Industrial G
O.M. : 5X

Micrographs of Aluminium Wire before Polishing.

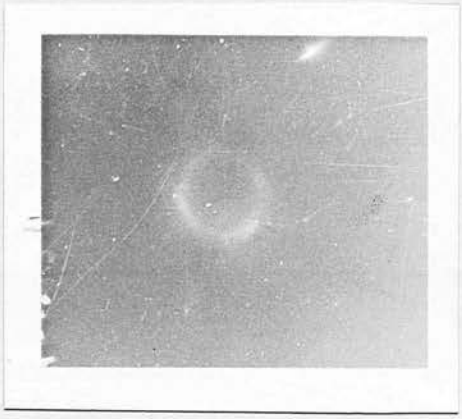

Plate XXIV.

Electron Optical
Ilford Industrial G
E.O.M. : 6X
O.M. : 2X

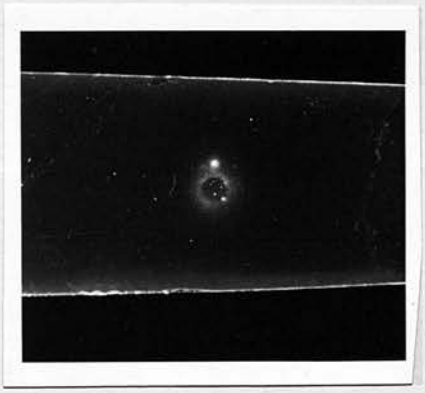

Plate XXV.

Contact Autoradiograph
Ilford Industrial G
O.M. : 5X

Micrographs of Aluminium Wire after Polishing.

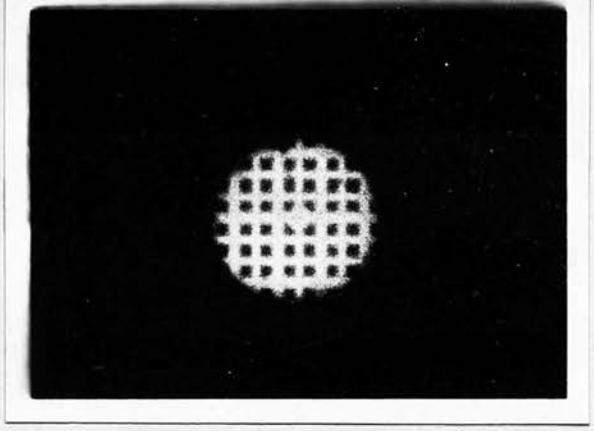

(a) Density : 1.0

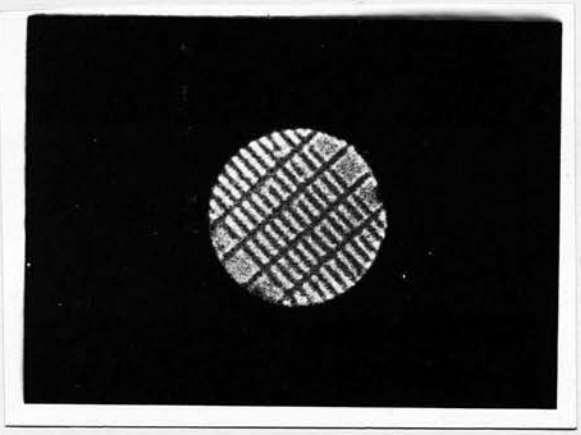

(b) Density : 0.5

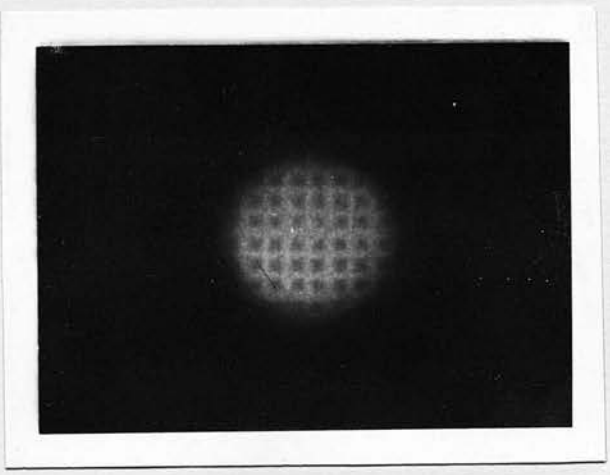

(c) Density : 0.14

Plate XXVI.

Images of Various Densities of Blackening.

Ilford G5
E.O.M. : 6X
O.M. : 3.5X